Northeast
Nuclear Energy

Rope Ferry Rd. (Route 156), Waterford, CT 06385

Millstone Nuclear Power Station
Northeast Nuclear Energy Company
P.O. Box 128
Waterford, CT 06385-0128
(860) 447-1791
Fax (860) 444-4277

The Northeast Utilities System

JAN - 4 2001

Docket No. 50-336
B18294

Re: 10 CFR 50.90

U.S. Nuclear Regulatory Commission
Attention: Document Control Desk
Washington, DC 20555

Millstone Nuclear Power Station, Unit No. 2
Response to a Request For Additional Information Regarding Proposed Revision to Final Safety Analysis Report
Fuel Centerline Melt Linear Heat Rate Limit (PLAR 2-00-2)

This letter provides Northeast Nuclear Energy Company (NNECO) response to a request for additional information regarding proposed changes to the Final Safety Analysis Report (FSAR) associated with Fuel Centerline Melt Linear Heat Rate (FCMLHR) limit (PLAR 2-00-2).

By a letter dated July 31, 2000,[1] NNECO requested that the Nuclear Regulatory Commission (NRC) review and approve changes to the FSAR through an amendment to Operating License DPR-65, pursuant to 10 CFR 50.90. The changes in the Millstone Unit No. 2 FSAR are due to changing the method used to determine the FCMLHR limit.

On November 9, 2000,[2] NNECO received a request for additional information from the NRC regarding the above mentioned license amendment request. This request for additional information contains four questions. The purpose of this letter is to transmit NNECO's responses to these four questions, which are contained in Attachment 1. Attachment 2 contains a markup of FSAR Section 14.1.5, including the associated

(1) Raymond P. Necci to the Nuclear Regulatory Commission, "Millstone Nuclear Power Station, Unit No. 2, License Amendment Request - Unreviewed Safety Question, Proposed Revision to Final Safety Analysis Report, Fuel Centerline Melt Linear Heat Rate Limit (PLAR 2-00-2)," dated July 31, 2000.

(2) J. I. Zimmerman to Ravi Joshi, "Draft Request for Additional Information Associated with July 31, 2000 Submittal on Fuel Centerline Melt Linear Heat Rate Limit FSAR USQ'S, Millstone Nuclear Power Station, Unit No. 2, TAC NO. MA9626," dated November 9, 2000.

A001

tables and figures. This markup includes two FSAR changes processed by NNECO under 10 CFR 50.59 as well as those proposed changes due to changing the method used to determine the FCMLHR limit transmitted in the July, 2000, letter. Attachment 3 contains a typed version of the text and tables contained in Attachment 2.

There are no regulatory commitments contained within this letter.

If you should have any questions on the above, please contact Mr. Ravi Joshi at (860) 440-2080.

Very truly yours,

NORTHEAST NUCLEAR ENERGY COMPANY

Raymond P. Necci
Vice President - Nuclear Technical Services

Sworn to and subscribed before me

this 4th day of January, 2001

Notary Public

My Commission expires

SANDRA J. ANTON
NOTARY PUBLIC
COMMISSION EXPIRES
MAY 31, 2005

Attachments (3)

cc: H. J. Miller, Region I Administrator
J. I. Zimmerman, NRC Project Manager, Millstone Unit No. 2
S. R. Jones, Senior Resident Inspector, Millstone Unit No. 2

Docket No. 50-336
B18294

Attachment 1

Millstone Nuclear Power Station, Unit No. 2

Proposed Revision to Final Safety Analysis Report
Fuel Centerline Melt Linear Heat Rate Limit (PLAR 2-00-2)

Response to a Request For Additional Information

**Response to a Request For Additional Information Regarding Proposed Revision to Final Safety Analysis Report
Fuel Centerline Melt Linear Heat Rate Limit (PLAR 2-00-2)**

Question No. 1:

Why have Hot Zero Power (HZP) outside containment post-trip scram Steamline Break (SLB) events become more limiting than the Hot Full Power (HFP) events?

Response:

The HZP SLB events became more limiting than the HFP SLB events as a result of the reanalysis of the post-scram SLB in support of the Cycle 14 reload design. For Cycle 14, the HZP cases became more limiting than the full power cases because of the incorporation of a revised neutronics methodology, and a reduction in the excess conservatism in the moderator reactivity feedback at reduced RCS temperatures.

For Cycle 14, Northeast Nuclear Energy Company updated FSAR Section 14.1.5 to reflect a revised Siemens Power Corporation (SPC) approved neutronics methodology. The change affects the SLB analysis by changing the analytical method used for determining the neutronics and axial and radial power distribution input parameters utilized in the ANF-RELAP and XCOBRA-IIIC calculations. For Cycle 13, the XTGPWR code was used to generate these input parameters. For Cycle 14, the PRISM code was used to generate these input parameters. For Cycle 14, the SPC methodology also utilizes PRISM to verify that the reactivity calculated by ANF RELAP is conservative. For Cycle 13, the XTGPWR code was used to verify that the reactivity calculated by ANF-RELAP was conservative. The PRISM calculations produce significantly increased axial and radial power distributions at the time of the post-scram return to power (all Control Element Assemblies (CEAs) inserted with the most reactive CEA stuck out).

To compensate for these increased power peaking factors, SPC refined their analysis to eliminate some of the excess conservatism in the moderator reactivity feedback at reduced temperatures. The moderator reactivity feedback utilized in the Cycle 14 analysis continues to bound the most negative moderator temperature coefficient specified in the core operating limits report of -2.8×10^{-4} $\Delta K/K/°F$ at rated thermal power.

The Table provided below summarizes the results of the limiting Cycle 13 and Cycle 14 SLB Cases with respect to maximizing linear heat rate:

Cycle	Initial Power	Limiting Case Peak Power MW(t)	Limiting Case Peak LHR kW/ft
13	HFP	**378.0 MW(t)**	**24.27 kW/ft**
	HZP	343.5 MW(t)	23.47 kW/ft
14	HFP	194.8MW(t)	21.0 kW/ft
	HZP	**271.6MW(t)**	**23.3 kW/ft**

A comparison of the Cycle 14 SLB analysis results with the Cycle 13 SLB analysis results shows that the peak power dropped a greater amount for the HFP cases than for the HZP cases. The excess conservatism in the moderator reactivity feedback was more effective in reducing the calculated peak average power of the HFP cases than those of the HZP cases. For Cycle 14, the peak linear heat rate is obtained by combining this larger peak average power of the HZP SLB cases with the more adverse axial and radial power distributions generated using PRISM. As such, for Cycle 14, the peak linear heat rate of the HZP SLB cases is more limiting than the HFP cases.

Question No. 2:

According to Table 14.1.5.2-6, HZP SLB outside containment with offsite power available results in a maximum linear heat generation rate (LHGR) of 23.3 kW/ft. Since this appears to be higher than the minimum power level required to produce centerline melt, why does insert 6 to page 14.1.23 state that no fuel failure is predicted to occur due to violation of the fuel centerline melt linear heat rate (FCMLHR) limit?

Response:

The HZP SLB for Cycle 14 predicts a maximum linear heat rate of 23.3 kW/ft. This is greater than the existing licensing basis limit of 21 kW/ft. For Cycle 14, the SPC calculated FCMLHR limit is $\leq$ 24.5 kW/ft. Utilizing the cycle specific FCMLHR limit results in a prediction of no fuel failure.

Question No. 3:

The third paragraph of 14.1.5.2.7 states that the highest calculated LHGR value of 24.27 kW/ft. is below the FCMLHR limit. This also appears to be higher than the

limit required to produce fuel centerline melt. Since Table 14.1.5.2-6 lists a value of 21.0 kW/ft., is the 24.27 kW/ft. value correct?

Response:

The 24.27 kW/ft limit was the Cycle 13 value for the HFP SLB. When reanalyzed for Cycle 14, the HFP SLB resulted in a peak LHR of 21.0 kW/ft, as shown in Table 14.1.5.2-6. An earlier separate FSAR change, processed under 10 CFR 50.59, deleted this value from the third paragraph of Section 14.1.5.2-7. This value was deleted in the earlier FSAR change because it duplicates the information contained in Table 14.1.5.2-6.

To provide more clarification, Attachment 2 provides a markup of the FSAR Section 14.1.5 in its entirety, including the associated tables and figures. This attachment includes the changes to FSAR Section 14.1.5 associated with the Cycle 14 SLB reanalyses that were processed under 10 CFR 50.59. These changes are identified by FSAR Change Numbers 00-MP2-23 and 00-MP2-39 in the attachment. The proposed changes associated with the change to a cycle specific linear heat rate limit are identified by FSAR Change Number 00-MP2-38 in the attachment. Attachment 3 includes a typed version of the text and tables contained in Attachment 2.

Question No. 4:

Section 14.1.5.2.6.2 refers to Figs. 14.1.5.2-10 through 14.1.5.2-16 and Table 14.1.5.2-8 as representative of the HZP SLB event outside containment. However, these figures and table previously referred to the HFP event. Should they be revised accordingly?

Response:

The cited figures and table have been updated by an earlier FSAR change associated with the Cycle 14 reload design change. To provide more clarification, Attachment 2 includes a markup of the FSAR Section 14.1.5, including the associated tables and figures. This attachment includes the changes to FSAR Section 14.1.5 associated with the Cycle 14 SLB reanalyses, and the proposed changes associated with the change to a cycle specific linear heat rate limit. The changes associated with the Cycle 14 SLB reanalyses are identified by FSAR Change Numbers 00-MP2-23 and 00-MP2-39 in the attachment. The proposed changes associated with the cycle specific linear heat rate limit are identified by FSAR Change Number 00-MP2-38 in the attachment.

Docket No. 50-336
B18294

Attachment 2

Millstone Nuclear Power Station, Unit No. 2

Proposed Revision to Final Safety Analysis Report
Fuel Centerline Melt Linear Heat Rate Limit (PLAR 2-00-2)

Markup of the FSAR Section 14.1.5, Including the Associated Tables and Figures

CHAPTER 14

TABLE OF CONTENTS

CHAPTER 14

TABLE OF CONTENTS

CHAPTER 14

LIST OF TABLES

FSAR CR 00-MP2-23

ATTACHMENT 2
Page 4 of 104

CHAPTER 14

LIST OF TABLES

ATTACHMENT 2
Page 5 of 104

CHAPTER 14

LIST OF FIGURES

CHAPTER 14

LIST OF FIGURES

CHAPTER 14

LIST OF FIGURES

14.1.4 Inadvertent Opening of a Steam Generator Relief or Safety Valve

14.1.4.1 Event Initiator

This event is initiated by an increase in steam flow caused by the inadvertent opening of a secondary side safety or relief valve.

14.1.4.2 Event Description

The resulting mismatch in energy generation and removal rates results in an overcooling of the primary system. If the MTC is negative, the reactor power will increase.

14.1.4.3 Reactor Protection

Reactor protection is provided by the variable overpower trip, LPD trip, TM/LP trip, low secondary pressure trip, and low steam generator water level trip. In Modes 1, 2, and 3, protection is also provided by the safety injection actuation signal (SIAS) on low pressurizer pressure. Reactor protection for the Inadvertent Opening of a Steam Generator Relief or Safety Valve event is summarized in Table 14.1.4-1.

14.1.4.4 Disposition and Justification

The inadvertent opening of a steam generator safety valve would result in an increased steam flow of approximately 6.75% of full rated steam flow. Each dump (relief) valve is sized for approximately 7.50% steam flow with the reactor at full rated power. As such, the consequences of any of these occurrences will be bounded by the events in Section 14.1.3. The disposition of events for the Inadvertent Opening of a Steam Generator Relief or Safety Valve event is summarized in Table 14.1.4-2.

14.1.5 Steam System Piping Failures Inside and Outside of Containment

Two separate analyses have been performed for the ~~Steam Line Break~~ SLB (SLB) event. Section 14.1.5.1 describes the pre-scram analysis performed to determine Departure from Nucleate Boiling Ratio (DNBR) and Linear Heat Generation Rate (LHGR) up to and including reactor trip. This time period represents the highest reactor power condition and the assumptions have been selected to minimize DNBR and maximize LHGR during this time frame. Section 14.1.5.2 describes the post-scram analyses performed to determine MDNBR and LHGR during the return to power caused by the overcooling. A different set of assumptions and single failure were determined to minimize MDNBR and maximize LHGR for the return to power time frame. 98-145

14.1.5.1 Pre-Scram Analysis

14.1.5.1.1 Event Initiator

The pre-scram SLB analysis is initiated by a rupture in the main steam piping which results in an uncontrolled steam release from the secondary system.

14.1.5.1.2 Event Description

The increase in energy removal through the secondary system results in a severe overcooling of the primary system. With a negative MTC, the primary system cooldown causes the reactor power level to increase. If the break is not large enough to trip the reactor on a Low Steam Generator Pressure signal, the cooldown will continue until the reactor is tripped on a Variable Overpower or TM/LP signal (for breaks outside containment) or a High Containment Pressure signal (for breaks inside containment) or until the reactor reaches a new steady-state condition at an elevated power level.

Although the SLB calculation is typically a cooldown event, for the pre-scram analysis the cooldown event is not significant for the limiting pre-scram case. The case with a loss of offsite power, also known as a "pumps off" case, credits the low reactor coolant flow trip for harsh conditions. In this case, the Reactor Coolant Pumps (RCPs) are tripped shortly after the initiation of the transient. The sharp reduction in reactor coolant flow causes the pre-scram pumps off calculation to become a heat up transient very similar to a Loss of Coolant Flow (LOCF). Therefore, the conditions for this case are biased as if it were a LOCF (i.e. BOC neutronics). This case becomes a combination of an MSLB and an LOCF event.

14.1.5.1.3 Reactor Protection

Reactor protection is provided by the low steam generator pressure and water level trips, variable overpower trip, LPD trip, TM/LP trip, high containment pressure trip, low reactor coolant flow, and SIAS. Reactor protection for the Steam System Piping Failures Inside and Outside of Containment event is summarized in Table 14.1.5.1-1. 98-145

14.1.5.1.4 Disposition and Justification

HFP initial conditions are limiting for the pre-scram SLB cases since this is the highest power condition.

The outside containment breaks do not cause harsh conditions inside containment, and therefore, do not cause the Low Reactor Coolant Flow trip to be degraded. If a loss of offsite power were concurrent with an outside containment break, the primary coolant flow rate would coastdown similar to an LOCF event, without the Low Reactor Coolant Flow trip being degraded. The outside containment break case with loss of offsite power is therefore bounded by the LOCF event.

The inside containment breaks do cause harsh conditions inside containment, and therefore, an increased allowance for instrument uncertainty was applied for the Low Reactor Coolant Flow trip. Therefore, only the inside containment breaks will be analyzed with a loss of offsite power.

The following pre-scram HFP Steam Line Break cases for break sizes ranging up to a double-ended guillotine break in a main steam line were analyzed, with the effects of power decalibration and harsh containment conditions (where applicable) included in the analysis:

1. Breaks outside containment and downstream of the check valves (symmetric cases)

2. Breaks outside containment and upstream of a check valve (asymmetric cases)

3. Breaks inside containment with RCPs on (asymmetric cases)

4. Breaks inside containment with RCPs off (asymmetric cases)

The event is analyzed to support the technical specification EOC MTC limit. This event must be analyzed both with and without a coincident loss-of-offsite power.

The single failure assumed in this analysis is the loss of one channel of Nuclear Instrumentation (NI) which provides power indication to the RPS. If one channel is out of service, the three remaining NI safety channels will be in a 2-out-of-3 coincidence mode. With the assumption of a failure in one of these channels, both of the remaining channels are required for a trip, relying on the lowest power indication for the safety function.

The disposition of events for the Steam System Piping Failures Inside and Outside of Containment event is summarized in Table 14.1.5.1-2.

14.1.5.1.5 Definition of Events Analyzed

The pre-scram SLB event is initiated by a rupture in the main steam piping. The break location is downstream of the steam generator integral flow restrictor and either : 98-145

1. outside containment and upstream of the main steam line check valves (asymmetric break), or

2. outside containment and downstream of the main steam line check valves (symmetric break), or

3. inside containment and upstream of the main steam check valves (asymmetric break).

Steam released through a break located downstream of the main steam line check valves flows to the break from both steam generators and, therefore, results in a symmetric transient. However, steam released through a break located upstream of one of the check valves flows to the break from the upstream steam generator only (because the check valve precludes backflow to the break from the other steam generator) and, therefore, results in an asymmetric transient.

Power decalibration is caused by density-induced changes in the reactor vessel downcomer shadowing of the power-range ex-core detectors during heatup or cooldown transients. The nuclear power levels indicated by those instruments are lower than the actual reactor power levels when the coolant entering the reactor vessel is cooler than the normal temperature for full-power operation (and higher when the vessel inlet coolant is warmer than the normal full-power temperature). This effect is included in the modeling of any power-dependent reactor trips credited in the analysis of full-power cooldown events and low-power events. The Variable Overpower trip, the Thermal Margin/Low Pressure

(TM/LP) trip function, and the Local Power Density (LPD) trip all depend on the indicated nuclear power level.

Harsh containment conditions can be caused by the release of steam within the reactor containment. Under such conditions, only those trips which have been qualified for harsh environments are credited, and increased uncertainties are included in the setpoints of all environmentally qualified trips which are credited.

As outlined in Reference 14.1-1, three computerized calculations are required prior to the final calculation of the Minimum Departure From Nucleate Boiling Ratio (MDNBR) values and the maximum Linear Heat Generation Rate (LHGR) values utilized in the determination of fuel failure. The NSSS response is computed using the Siemens Power Corporation (SPC) ANF-RELAP code (Reference 14.1-2), the detailed core and hot assembly power distributions and the reactivity at the time of peak post-scram power are calculated using the SPC ~~XTGPWR~~ PRISM code (Reference 14.1-3), and the detailed core and hot assembly flow and enthalpy distributions are calculated using the SPC XCOBRA-IIIC code (Reference 14.1-4). The SPC XNB correlation was utilized to calculate MDNBR.

14.1.5.1.5.1 Analysis of Results

The ANF-RELAP analysis provides the NSSS boundary conditions for the ~~XTGPWR~~ PRISM and the XCOBRA-IIIC calculations. This section presents a description of the treatment of factors which can have a significant impact on NSSS response and resultant MDNBR and LHGR values. The plant specific parameters used in this analysis are listed in Tables 14.1.5.1-3 to 14.1.5.1-5. Conservatisms are included in parameters or factors known to have significant effects on the NSSS performance and resulting MDNBR and LHGR values. 98-115

14.1.5.1.5.1.1 Break Location, Size, and Flow Model

The pre-scram SLB event analyzes breaks outside containment both downstream (symmetric cases) and upstream (asymmetric cases) of the main steam line check valves and breaks inside containment (asymmetric cases). A full range of break sizes, up to the double-ended guillotine break of a main steam line, were considered.

The ANF-RELAP break mass flow rate is computed using the Moody critical flow model modified such that only steam flows out the break.

14.1.5.1.5.1.2 Power Decalibration

Power decalibration is caused by density-induced changes in the reactor vessel downcomer shadowing of the power-range ex-core detectors during heatup or cooldown transients. The nuclear power levels indicated by those instruments are lower than the actual reactor power levels when the coolant entering the reactor vessel is cooler than the normal temperature for full-power operation (and higher when the vessel inlet coolant is warmer than the normal full-power temperature). This effect is included in the modeling of any power-dependent reactor trips credited in the analysis of full-power cooldown events and low-power events. The Variable Overpower trip, the Thermal Margin/Low Pressure (TM/LP) trip function, and the Local Power Density (LPD) trip all depend on the indicated nuclear power level.

14.1.5.1.5.1.3 Harsh Containment Conditions

Harsh containment conditions can be caused by the release of steam within the reactor containment. Under such conditions, only those trips which have been qualified for harsh environments are credited, and increased uncertainties are included in the setpoints of all environmentally qualified trips which are credited.

14.1.5.1.5.1.4 Boron Injection

Boron injection into the primary system acts to mitigate the return to power. Injection of boron is modeled from the HPSI system. The HPSI system is conservatively modeled to take suction from the Refueling Water Storage Tank (RWST) at 35°F with a boron concentration of 1720 ppm. Initially, the line volume between the check valves isolating the system pumps and the cold leg injection location is assumed to be filled with unborated water. The time required to flush this unborated water from the safety injection lines is included as an integral part of the ANF-RELAP NSSS calculation. In the pre-scram SLB event, the analysis is terminated shortly after reactor trip, therefore injection of borated water is not a factor in the analysis.

14.1.5.1.5.1.5 Single Failure Assumption

In order to simulate the asymmetric thermal-hydraulic and reactivity feedback effects that occur during the pre-scram SLB event, the core is divided into an affected sector (1/2 of the core) and an unaffected sector (1/2 of the core). The single failure assumed in this analysis is the loss of one channel of Nuclear Instrumentation (NI) which provides power indication to the Reactor Protection System (RPS). If one channel is out of service, the three remaining NI safety channels will be in a 2-out-of-3 coincidence mode to cause a reactor trip. The excore detectors are placed around the reactor vessel in positions that result in one detector seeing the flux only from the affected region, one seeing the flux only from the unaffected region, and two detectors seeing nearly equal flux from both regions. If one of these latter two is out of service, and the other is assumed to be a single failure, the remaining two channels will be required to cause an RPS trip (high power or TM/LP). Since the power in the affected region will always be higher than in the unaffected region, it is sufficient to model the NI channel reading the unaffected region only. 98-145

14.1.5.1.5.1.6 Feedwater

Normal MFW flow is assumed to be delivered to both SGs. The MFW flow increases as the secondary pressure decreases at the lowest possible fluid temperature until the feedwater regulator valve closes. Fluid temperature is determined by assuming heating of the feedwater ceases at the same time the break is initiated. The MFW flow is terminated 14 seconds after receiving the isolation signal.

14.1.5.1.5.1.7 Trips and Delays

Actuation signals and delays are given in Table 14.1.5.1-4. Biases to account for uncertainties are included in the trip setpoints as shown. In the pre-scram SLB event, the analysis is terminated shortly after reactor trip, therefore injection of borated water is not a factor in the analysis.

14.1.5.1.5.1.8 Neutronics

The core kinetics input for this calculation consisted of the minimum required control rod shutdown worth at EOC, and EOC values associated with the reactivity feedback curves, delayed neutron fraction, delayed neutron fraction distribution and related time constants, and prompt neutron generation time. The ANF-RELAP default fission product and actinide decay constants were utilized for this calculation.

The core reactivity is derived from input of several functions. These include effects from control rod worth, moderator density changes, boron concentration, and Doppler effects. The reactivity is weighted between the core sectors. The ANF-RELAP analyses for cases with offsite power available were performed with an MTC of -28 pcm/°F. The ANF-RELAP analyses for cases with a loss of offsite power were performed with an MTC of +4.0 pcm/°F. A summary of the nuclear input and assumptions is given in Table 14.1.5.1-5.

14.1.5.1.5.1.9 Decay Heat

The presence of radioisotope decay heat at the initiation of the SLB event will reduce the rate and the extent of cooldown of the primary system. The initial decay heat is calculated on the basis of infinite irradiation time at a power of 2754 MW prior to transient initiation. This treatment of decay heat serves to maximize the stored energy and provide limiting stored energy conditions for the SLB cases.

14.1.5.1.5.1.10 Nodalization

98-145

The NSSS transient calculations presented in this report utilized the nodalization model described in Reference 14.1-1. The nodalization treats all major NSSS components and subcomponents as discrete elements, with the exception of the secondary side of the steam generators. In addition, all components with long axial dimensions are divided into subcells adequate to minimize numerical diffusion and smearing of gradients.

In order to simulate the asymmetric thermal-hydraulic and reactivity feedback effects that occur during the pre-scram SLB event, the core is divided into an affected sector (1/2 of the core) and an unaffected sector (1/2 of the core).

14.1.5.1.5.1.11 Interloop Mixing

During an actual SLB transient, some mixing between the parallel channels within the reactor pressure vessel will occur in the downcomer, the lower plenum, the core, and the upper plenum due to lateral momentum imbalances, and turbulence or eddy mixing. The mixing will act to reduce the positive reactivity feedback effects due to a reduced rate and magnitude of cooldown of the affected loop and associated core sector.

In this analysis, no credit is taken for turbulent or eddy mixing of coolant between loops or the parallel flow channels within the reactor pressure vessel. However, interloop mixing is calculated to occur due to flow in interloop junctions in the upper and lower plenums. Mixing in the lower plenum was effectively reduced to zero by using an extremely high loss coefficient between the affected and intact sectors.

14.1.5.1.5.2 Minimum Departure From Nucleate Boiling and Linear Heat Generation Rate Analysis

The ~~XTGPWR~~ PRISM (Reference 14.1-3) core neutronics code is used to calculate the core radial power distributions for XCOBRA-IIIC (Reference 14.1-4) during the asymmetric transients with offsite power available only. The ~~XTGPWR~~ PRISM model is a three-dimensional representation of the entire core, with four radial nodes and 24 axial nodes for each fuel assembly.

Based on the overall core conditions calculated by ANF-RELAP for the symmetric cases (or ANF-RELAP and ~~XTGPWR~~ PRISM for the asymmetric cases with offsite power available) at the peak heat flux time-point, the XCOBRA-IIIC fuel assembly thermal-hydraulic code is used to calculate the flow and enthalpy distributions for the entire core and the DNB performance for the DNB-limiting assembly. The XCOBRA-IIIC model consists of a thermal-hydraulic model of the core (representing each assembly by a single "channel") linked to a detailed thermal-hydraulic model of the limiting assembly (representing each subchannel by a single "channel"). The limiting assembly DNBR calculations are performed using the XNB DNB correlation (Reference 14.1-4).

For the asymmetric transients, the radial power peaking is augmented above the Technical Specification limit to account for the increase in radial power peaking which occurs during the transient. The increase in peaking is determined by ~~XTGPWR~~ PRISM.

14.1.5.1.6 Analysis Results

A summary of calculated results important to this analysis is presented in Table 14.1.5.1-6 for the limiting MDNBR and LHGR cases. The MDNBR values are listed together with the corresponding core power values at the time of MDNBR which corresponds to the maximum power level. For cases where offsite power was available for operation of the primary coolant system pumps, the MDNBR and the maximum LHGR occurred at the time of the maximum power condition. For cases where offsite power is lost and the primary system pumps coast down, the maximum LHGR and the MDNBR occur when the worst combination of core power, flow, inlet temperature, and pressure are present. These conditions occurred at the time of peak power in this analysis. 98-195

The scenario which resulted in the highest power level and the largest LHGR is the HFP 3.50 ft^2 symmetric break outside containment with offsite power available for operation of the primary coolant pumps. This case is presented in detail.

The scenario which resulted in the limiting MDNBR is the HFP case with a loss of offsite power and is also presented in detail.

14.1.5.1.6.1 Hot Full Power 3.50 ft^2 Break Outside Containment and Downstream of a Check Valve with Offsite Power Available

The ANF-RELAP simulation of the NSSS during the HFP symmetric break transient with offsite power available is illustrated in Figures 14.1.5.1-1 through 14.1.5.1-6. A tabulation of the sequence of events is presented in Table 14.1.5.1-7. The ANF-RELAP computation was terminated 60 seconds after break initiation. This is well beyond the time of MDNBR or peak LHGR. The general response of the reactor was the same for all the symmetric break sizes but the occurrence of events was delayed as the break size decreased.

14.1.5.1.6.1.1 Secondary System Parameters

Upon break initiation the break flow increased sharply and then began to decline in response to falling secondary side pressure. When the turbine trip occurred, the break flow increased due to a local pressure increase. The main steam line flow rate from each generator initially increased (see Figure 14.1.5.1-6) in response to the break and the assumed instantaneous full opening of the turbine control valves. The increased steam flow creates a mismatch between the core heat generation rate and the steam generator heat removal rate. This power mismatch causes the primary-to-secondary heat transfer rate to increase, which in turn causes the primary system to cool down (see Figure 14.1.5.1-2). When the reactor scram occurred, the turbine valves closed and steam flow declined sharply. At this point, the MFW flow may exceed the steam flow as the control system attempts to restore steam generator mass. Both steam flow and MFW flow were terminated when the main steam isolation valves closed.

14.1.5.1.6.1.2 Primary System Parameters

Approximately five seconds after the break occurred, the core inlet temperature began to decline. With a negative MTC (see Figure 14.1.5.1-3), the primary system cooldown caused the reactor power level to increase. The core power continues to increase until reactor scram on low steam generator pressure occurs. This terminated the power excursion. The pressurizer pressure and level began to decline as the volume of water in the primary system shrank. The core inlet mass flow rate increased due to the increasing density of the primary system fluid while the reactor coolant pumps' speed remained constant.

98-145

14.1.5.1.6.1.3 Departure From Nucleate Boiling Ratio and Linear Heat Generation Rate Results

The MDNBR value for this scenario was calculated to be 1.29~~8~~9 which is above the 95/95 XNB correlation limit. Therefore, no fuel rods would be expected to fail during this transient scenario from an MDNBR stand point.

The peak LHR for the LHR-limiting case (3.50~~1~~20.8 ft² break outside containment and downstream of a check valve) is calculated to be ~~19.7~~8 kW/ft. Comparing this LHGR value with ~~a centerline melt criteria of 21 kW/ft~~, it is apparent that centerline melt is not predicted to occur. Thus, no fuel failures are predicted to occur due to violation of the centerline melt criteria.

00-MP2-38

the FCMLHR limit

14.1.5.1.6.2 Hot Full Power 3.51 ft² Inside Containment Asymmetric Break Concurrent with a Loss of Offsite Power

The ANF-RELAP NSSS simulation of the most limiting pre-scram SLB scenario from an MDNBR standpoint (i.e., HFP 3.51 ft² inside containment asymmetric break concurrent with a loss of offsite power) is illustrated in Figures 14.1.5.1-7 through 14.1.5.1-11. A tabulation of the sequence of events is presented in Table 14.1.5.1-8. The ANF-RELAP computation was terminated 60 seconds after break initiation. This is well beyond the time of MDNBR or peak LHGR.

The transient is initiated by the opening of the break. The RCPs tripped shortly after transient initiation. The sharp reduction in the reactor coolant flow causes this pre-trip pumps off calculation to become a heat up transient very similar to a Loss of Coolant Flow event. Typically, the Steam Line Break calculation is a cooldown event. Because this case is a heat up event the most positive BOC neutronics conditions are used, and the maximum inside containment asymmetric break size is used. The maximum break size causes the biggest decrease in primary pressure. Maximizing the primary system pressure decrease causes the maximum decrease in moderator density and the maximum positive moderator feedback. The RCP trip causes the RCS flow to decrease rapidly throughout this transient. The decreasing RCS flow causes the transient time of the fluid in the core to increase and the fluid temperature begins to rise. The increasing fluid temperature causes positive moderator feedback, which in turn causes an increase in core power. However, the decreasing RCS flow causes the heat transfer to the fluid to decrease. The increase in core power is offset by the decrease in heat transfer from the fuel rods, such that, the fuel rod heat flux decreases slightly until reactor scram. The reactor scrams on the low reactor coolant flow trip signal.

00-MP2-39

14.1.5.1.6.2.β1 Departure From Nucleate Boiling Ratio and Linear Heat Generation Rate Results

The MDNBR value for the pre-scram 3.51 ft² asymmetric break inside containment with a loss of offsite power was calculated to be 0.88 which is below the 95/95 XNB correlation limit. The number of failed assemblies is determined by comparing the core power distribution to the assembly power where DNB occurs. This results in a predicted failure of 3.7% of the fuel rods in the core. 98-145

00-MP2-38

The peak LHR for this case is bounded by the 3.50 ft² outside containment symmetric break. Therefore, the LHGR for this case is below the ~~criteria of 21.0 kW/ft~~ and no fuel failures are predicted to occur due to violation of the centerline melt criteria.

FCMLHR limit

14.1.5.1.7 Conclusions

00-MP2-39

20.8 ~~20.6~~

00-MP2-38

The HFP 3.50 ft² break outside containment and downstream of a check valve (symmetric break) with offsite power available was determined to be the most limiting in this analysis from an LHGR standpoint (~~19.7~~ kW/ft). In no scenario evaluated, however, was fuel failure calculated to occur as a result of violating the ~~21 kW/ft fuel centerline melt criteria~~.

FCMLHR limit.

The HFP 3.51 ft² asymmetric break inside containment coincident with a loss of offsite power was determined to be the most limiting in this analysis from the standpoint of MDNBR. The MDNBR was calculated to be 0.88 which is below the 95/95 XNB correlation limit. This results in a predicted failure of 3.7% of the fuel rods in the core.

14.1.5.2 Post-Scram Analysis

14.1.5.2.1 Event Initiator

This event is initiated by a rupture in the main steam piping downstream of the integral steam generator flow restrictors and upstream of the MSIVs which results in an uncontrolled steam release from the secondary system.

14.1.5.2.2 Event Description

The increase in energy removal through the secondary system results in a severe over-cooling of the primary system. In the presence of a negative MTC, this cooldown causes a decrease in the shutdown margin (following reactor scram) such that a return to power might be possible following a steam line rupture. This is a potential problem because of the high power peaking factors which exist, assuming the most reactive control rod to be stuck in its fully withdrawn position.

14.1.5.2.3 Reactor Protection

Reactor protection is provided by the low steam generator pressure and water level trips, ~~variable overpower trip~~, LPD trip, TM/LP trip, high containment pressure trip, and SIAS. Reactor protection for the Steam System Piping Failures Inside and Outside of Containment event is summarized in Table 14.1.5.2-1.

14.1.5.2.4 Disposition and Justification

At rated power conditions, the stored energy in the primary coolant is maximized, the available thermal margin is minimized, and the pre-trip power level is maximized. These conditions result in the greatest potential for cooldown and provide the greatest challenge to the SAFDLS. Initiating this event from rated power also results in the highest post-trip power since it maximizes the concentration of delayed neutrons providing for the greatest power rise for a given positive reactivity insertion. ~~Additional thermal margin is also provided at lower power levels by the automatically decreasing setpoint of the variable overpower trip.~~ Thus, this event initiated from rated power conditions will bound all other cases initiated from at power operation modes. 98-145

For the zero power and subcritical plant states (Modes 2-6), there is a potential for a return-to-power at reduced pressure conditions. The most limiting steam line break (SLB) event at zero power is one which is initiated at the highest temperature, thereby providing the greatest capacity for cooldown. This occurs in Modes 2 and 3. Thus, the event initiated from Modes 2 and 3 will bound those initiated from Modes 4-6. Further, the limiting initial conditions will occur when the core is just critical. These conditions will maximize the available positive reactivity and produce the quickest and largest return to power. Thus, the SLB initiated from critical conditions in Mode 2 will bound the results of the event initiated form subcritical Mode 3 conditions.

The technical specifications only require a minimum of one RCP to be operating in Mode 3. One pump operation provides the limiting minimum initial core flow case. Minimizing core flow minimizes the clad to coolant heat transfer coefficient and degrades the ability to remove heat generated within the fuel pins. Conversely, however, a maximum loop flow will maximize the primary to secondary heat transfer coefficient, thus providing for the greatest cooldown. Higher loop flow will sweep the cooler fluid into the core faster, maximizing the rate of positive reactivity addition and the peak power level.

The worst combination of conditions is achieved for the four pump loss of offsite power case. In this situation, the initial loop flow is maximized resulting in the greatest initial cooldown, while the final loop flow is minimized providing the greatest challenge to the DNB SAFDL. Since the natural circulation flow which is established at the end of the

transient will be the same regardless of whether one or four pumps were initially operating the results of the four pump loss of offsite power case will bound those of the one pump case. Thus, only four pump operation need be analyzed for the Mode 2 case.

The event is analyzed to support the technical specification EOC MTC limit. This event must be analyzed both with and without a coincident loss-of-offsite power. Typically there are two single failures which are considered for the offsite power available case. The first is failure of a High Pressure Safety Injection (HPSI) pump to start. The second is failure of an MSIV to close, resulting in a continued uncontrolled cooldown. However, Millstone 2 has combination MSIV/swing disc check valves. A double valve failure would thus be required for steam from the intact steam generator to reach the break. This is not deemed credible. Thus, the single failure to be considered with offsite power available is failure of a HPSI pump to start. For the loss-of-offsite power case, the limiting single failure is the failure of a diesel generator to start. This is assumed to result in the loss of one HPSI pump. The disposition of events for the Steam System Piping Failures Inside and Outside of Containment event is summarized in Table 14.1.5.2-2.

14.1.5.2.5 Definition of Events Analyzed

The post-scram SLB is initiated by a rupture in the main steam piping downstream of the integral steam generator flow restrictors and upstream of the MSIVs which results in an uncontrolled steam release from the secondary system. The effects of harsh containment conditions (where applicable) are included in the following analyses: 98-145

1. HFP and HZP breaks outside containment with offsite power available

2. HFP and HZP breaks outside containment with a loss of offsite power

3. HFP and HZP breaks inside containment with offsite power available

4. HFP and HZP breaks inside containment with a loss of offsite power

The event is analyzed to support the technical specification EOC MTC limit. This event must be analyzed both with and without a coincident loss-of-offsite power.

The single failure assumed in this analysis results in the disabling of one of the two HPSI pumps required to be in service during normal operation. In addition to the single failure, there is no credit taken for the charging pump system. This assumption results in an additional delay in the time required for boron to reach the core. The delay is amplified when combined with the assumption of a stagnant upper head which serves to maintain the primary system pressure due to flashing of the hot fluid in the upper head.

The increase in energy removal through the secondary system results in a severe over-cooling of the primary system. In the presence of a negative MTC, this cooldown results in a large decrease in the shutdown margin and a return to power. This return to power is exacerbated because of the high power peaking factors which exist, with the most reactive control rod stuck in its full withdrawn position.

As outlined in Reference 14.1-1, three computerized calculations are required prior to the final calculation of the Minimum Departure From Nucleate Boiling Ratio (MDNBR) values

and the maximum Linear Heat Generation Rate (LHGR) values utilized in the determination of fuel failure. The NSSS response is computed using the Siemens Power Corporation (SPC) ANF-RELAP code (Reference 14.1-2), the detailed core and hot assembly power distributions and the reactivity at the time of peak post-scram power are calculated using the SPC ~~XTGPWR~~ PRISM code (Reference 14.1-3), and the detailed core and hot assembly flow and enthalpy distributions are calculated using the SPC XCOBRA-IIIC code (Reference 14.1-4). The modified Barnett correlation was utilized to calculate MDNBR due to the reduced pressures occurring during the SLB event.

14.1.5.2.5.1 Analysis of Results

The ANF-RELAP analysis provides the NSSS boundary conditions for the ~~XTGPWR~~ PRISM and the XCOBRA-IIIC calculations. This section presents a description of the treatment of factors which can have a significant impact on NSSS response and resultant MDNBR and LHGR values. The plant specific parameters used in this analysis are listed in Tables 14.1.5.2-3 to 14.1.5.2-5. Conservatisms are included in parameters or factors known to have significant effects on the NSSS performance and resulting MDNBR and LHGR values.

14.1.5.2.5.1.1 Break Location, Size, and Flow Model

98-145

The post-scram SLB event is initiated by a double ended guillotine break of a main steam line downstream of the integral steam generator flow restrictors and upstream of the MSIVs. The flow is choked at the integral steam generator flow restrictor, which has an area of 3.51 ft^2. On the steam generator side of the break, steam flows out of the break throughout the entire transient. On the MSIV side of the break, break flow terminates after the MSIVs are fully closed. As an added conservatism, the main steam check valves are not credited in the analysis. The event occurs concurrent with the most reactive control rod stuck out of the core. The break flow areas for the affected and intact steam generators are listed in Table 14.1.5.2-3. ~~These areas correspond to the locations in the flow path where choked flow will occur~~.

The ANF-RELAP break mass flow rate is computed using the Moody critical flow model modified such that only steam flows out the break.

14.1.5.2.5.1.2 Boron Injection

Boron injection into the primary system acts to mitigate the return to power. Injection of boron is modeled from the HPSI system. The HPSI system is conservatively modeled to take suction from the Refueling Water Storage Tank (RWST) at 35°F with a boron concentration of 1720 ppm. Initially, the line volume between the check valves isolating the system pumps and the cold leg injection location is assumed to be filled with unborated water. The time required to flush this unborated water from the safety injection lines is included as an integral part of the ANF-RELAP NSSS calculation. The characteristics of the HPSI system are listed in Table 14.1.5.2-3. The delivery curve for the HPSI system used in this analysis is given in Figure 14.1.5.2-1.

14.1.5.2.5.1.3 Single Failure Assumption

The single failure assumed in the engineered safeguards system results in the disabling of one of the two HPSI pumps required to be in service during normal operation. In addition

to the single failure, there is no credit taken for the charging pump system. This assumption results in an additional delay in the time required for boron to reach the reactor core. The delay is further amplified when combined with the assumption of a stagnant upper head which serves to maintain the primary system pressure due to flashing of the hot fluid in the upper head.

14.1.5.2.5.1.4 Feedwater

For the HFP scenarios, normal MFW flow is assumed to be delivered to both ~~SGs~~ steam generators. The MFW flow increases as the secondary pressure decreases at the lowest possible fluid temperature until the feedwater regulating valve closes. Fluid temperature is determined by assuming heating of the feedwater ceases at the same time the break is initiated. The MFW flow is terminated 14 seconds after receiving the isolation signal.

For the HFP scenarios, the AFW flow is assumed to be zero at break initiation. After 180 seconds, AFW is delivered at the maximum capacity of the AFW system with flow restrictors installed on the AFW delivery lines. For the HZP scenarios, the AFW flow is increased to the maximum capacity immediately at break initiation. For all scenarios, all of the AFW flow is directed to the affected steam generator to maximize the cooldown rate. The operator is assumed to terminate the AFW flow to the affected steam generator at 600 seconds.

14.1.5.2.5.1.5 Trips and Delays

98-145

Trips for the HPSI, main feedwater valves, and MSIVs are given in Table 14.1.5.2-4. Biases to account for uncertainties are included in the trip setpoints as shown. For the steam and feedwater valves, the delay times given are between the time the trip setpoint is reached and the time full valve closure is reached. For the HPSI system, the delay time given is from the time the setpoint is reached until the pumps have accelerated to rated speed. Additional delay time required to sweep the lines of unborated water is accounted for by setting the boron concentration of the injected flow to zero until the volume of the injection lines has been cleared.

14.1.5.2.5.1.6 Neutronics

The core kinetics input for this calculation consisted of the minimum required control rod shutdown worth at the EOC, and EOC values associated with the reactivity feedback curves, delayed neutron fraction, delayed neutron fraction distribution and related time constants, and prompt neutron generation time. The ANF-RELAP default fission product and actinide decay constants were utilized for this calculation.

The core reactivity is derived from input of several functions. These include effects from control rod worth, moderator density changes, boron concentration, and Doppler effects. The reactivity is weighted between the core sectors. Different reactivity functions were utilized where necessary for the HZP and the HFP cases. The ANF-RELAP analyses were performed with an MTC of -28 pcm/°F. A summary of the nuclear input and assumptions is given in Table 14.1.5.2-5.

14.1.5.2.5.1.7 Decay Heat

The presence of radioisotope decay heat at the initiation of the SLB event will reduce the rate and the extent of cooldown of the primary system. For the HFP scenarios, the initial decay heat is calculated on the basis of infinite irradiation time at a power of 2700 MW prior to transient initiation. For the HZP scenarios, the initial decay heat is calculated on the basis of infinite irradiation time at a power of 1 W prior to transient initiation. For both scenarios, decay heat generated from return to power is calculated. This treatment of decay heat serves to maximize the stored energy in the HFP cases and to minimize it in the HZP cases. This treatment provides limiting stored energy conditions for the SLB cases.

14.1.5.2.5.1.8 Nodalization

The NSSS transient calculations utilized the nodalization model described in Reference 14.1-1. The nodalization treats all major NSSS components and subcomponents as discrete elements, with the exception of the secondary side of the steam generators. In addition, all components with long axial dimensions are divided into subcells adequate to minimize numerical diffusion and smearing of gradients.

In order to simulate the asymmetric thermal hydraulic and reactivity feedback effects that occur during an SLB transient, the core is nodalized into three radial sectors. One sector corresponds to the region immediately surrounding the assembly where the most reactive control rod is assumed stuck out of the core. This sector is termed the 'stuck rod' sector. The remainder of the region of the core which is directly affected by the loop containing the break is the second sector and is termed the 'affected' sector. The remainder of the core and the other loop is termed either the 'unaffected' or the 'intact' sector or loop. 98-145

14.1.5.2.5.1.9 Interloop Mixing

During an actual SLB transient, some mixing between the parallel channels within the reactor pressure vessel will occur in the downcomer, the lower plenum, the core, and the upper plenum due to lateral momentum imbalances, and turbulence or eddy mixing. The mixing will act to reduce the positive reactivity feedback effects due to a reduced rate and magnitude of cooldown of the affected loop and associated core sector.

In this analysis, no credit is taken for turbulent or eddy mixing of coolant between loops or the parallel flow channels within the reactor pressure vessel (RPV). However, interloop mixing is calculated to occur due to flow in interloop junctions in the upper and lower plenums. Mixing in the lower plenum was reduced to a minimum by using an extremely high loss coefficient between the affected and intact sectors.

14.1.5.2.5.1.10 Harsh Containment Conditions

Harsh containment conditions can be caused by the release of steam within the reactor containment. Under such conditions, only those trips which have been qualified for harsh environments are credited, and increased uncertainties are included in the setpoints of all environmentally qualified trips which are credited.

14.1.5.2.5.2 Minimum Departure From Nucleate Boiling and Linear Heat Generation Rate Analysis

MDNBR calculations require determination of the power, enthalpy, and flow distributions within the highest power assembly of the stuck rod core sector. Similarly, determination of the maximum LHGR also requires characterization of the power distribution. The power distribution within the core, including the highest powered assembly within the stuck rod core sector, is calculated with ~~XTGPWR~~ PRISM (Reference 14.1-3). Flow and enthalpy distributions within the core, including the highest powered assembly within the stuck rod core sector, are calculated with XCOBRA-IIIC (Reference 14.1-4). In order to obtain compatible flows, moderator densities, and powers within the high power assemblies, iteration between ~~XTGPWR~~ PRISM and XCOBRA-IIIC is conducted.

For this calculation, the modified Barnett correlation was found to be suitable for the MDNBR calculation. The modified Barnett correlation is based upon closed channels and primarily uniform power distribution data. The correlation is based on assembly inlet (or upstream) fluid conditions rather than on local fluid conditions as is the case with subchannel based correlations. ~~Use of the correlation is limited to the range of the data base unless conservative extrapolations can be made.~~

14.1.5.2.6 Analysis Results

A summary of calculated results important to this analysis is presented in Table 14.1.5.2-6 for the limiting MDNBR and LHGR scenarios. The MDNBR values are listed together with the corresponding core power values at the time of MDNBR which corresponds to the maximum post-scram power level. The outside containment cases, regardless of whether or not offsite power was or was not available, were found to be the most limiting. For cases where offsite power was available for operation of the primary coolant system pumps, the MDNBR and the maximum LHGR occurred at the time of the maximum power condition. For cases where offsite power is lost and the primary system pumps coast down, the maximum LHGR and the MDNBR occur when the worst combination of core power, flow, inlet temperature, and pressure are present. These conditions occurred at the time of peak power in this analysis. 98-145

The scenario which resulted in the highest post-scram power level and the largest LHGR is that initiated from ~~HFP~~ HZP with the break occurring outside containment and with offsite power available for operation of the primary coolant pumps. This case is presented in detail.

The NSSS responses for the scenarios with loss of offsite power for operation of the primary system coolant pumps are different from those scenarios where offsite power is available throughout the transient due to the pump coastdown and subsequent natural circulation of the primary coolant. Post-scram maximum power levels attained during the transient are significantly lower. Lower power levels result from lower positive moderator feedback. The positive moderator feedback is reduced due to the coolant density reductions that occur axially upwards in the core at low core flow rates, even for low core power levels. Lower power levels cause MDNBR values to increase, but lowering flow rates cause MDNBR values to decrease. Overall, the combination of factors results in lower MDNBR values for the reduced flow condition than for the full flow condition.

Of the two loss of offsite power scenarios analyzed, the ~~HFP~~ HZP break occurring outside containment case resulted in lower MDNBR values. The general response of the HFP and HZP cases with loss of offsite power is comparable. Because the two scenarios are quite similar in terms of their general response, only the limiting MDNBR case (i.e., ~~HFP~~ HZP break outside containment and without offsite power) is presented in detail.

14.1.5.2.6.1 Hot ~~Full~~ ZERO Power Outside Containment with Offsite Power Available

The ANF-RELAP simulation of the NSSS during the ~~HFP~~ HZP transient with offsite power available is illustrated in Figures 14.1.5.2-2 through 14.1.5.2-9. A tabulation of the sequence of events is presented in Table 14.1.5.2-7. The ANF-RELAP computation was terminated 600 seconds after break initiation. This is well beyond the time of MDNBR or peak LHGR. ~~AFW termination of the AFW by manual operator action was assumed to occur 600 seconds after initiation of the break.~~

14.1.5.2.6.1.1 Secondary System Thermal Hydraulic Parameters

Insert O

Steam flow out the break is the source of the NSSS cooldown. Break flow for the steam generators is plotted in Figure 14.1.5.2-2. Secondary pressure for the steam generators is plotted in Figure 14.1.5.2-3. After break initiation, the pressure in the affected steam generator decreased immediately and then stabilized around 180 seconds. The mass inventory in both steam generators decreased throughout the transient. The relatively high reactor power level caused the affected steam generator to dry out by 490 seconds. The affected steam generator drying out caused the primary-to-secondary heat transfer to deteriorate. As a result, the primary system temperature rose, the secondary side pressure decreased, and, since the break flow is determined by the secondary system pressure, the break flow also declined. The heatup of the primary coolant reduced the reactivity present and power dropped rapidly.

98-145

The intact steam generator blows down for a short period until the MSIVs completely close approximately ~~17~~ 15 seconds after the break is initiated. The pressure recovers as the intact steam generator equilibrates with the primary system, ~~and then slowly increases as the primary system begins to heat up~~.

14.1.5.2.6.1.2 Primary System Thermal Hydraulic Parameters

The primary system coolant temperature and pressurizer pressure and level responses resulting from the break flow are illustrated in Figures 14.1.5.2-4 through 14.1.5.2-6. The primary system pressure decays rapidly as the coolant contracts due to cooldown and the pressurizer empties. The MSIVs close at ~~17~~ 15 seconds, ending the blowdown of the intact steam generators and reducing the rate of energy removal from the primary fluid. The pressurizer emptied at approximately ~~60~~ 40 seconds and system pressure (which increased slowly for the duration of the transient) was thereafter established by the saturation temperature of the primary coolant in the upper head of the reactor vessel.

14.1.5.2.6.1.3 Reactivity and Core Power

The reactivity transient calculated by ANF-RELAP is illustrated in Figure 14.1.5.2-8. Initially, the core is assumed to be at ~~full~~ ZERO power. All control rods, except the most reactive one, are assumed to be inserted into the core following the reactor trip signal. The

INSERT G to Page 14.1-21

INSERT G ①

The mass inventory in the affected steam generator decreased throughout the first 450 seconds of the transient and began increasing slowly thereafter. With the exception of a slight decrease at the beginning of the transient, the unaffected steam generator mass inventory remained essentially constant throughout the transient.

Insert 2

reactivity transient then proceeds. The total core reactivity, initially at 0.00$, decreased instantly due to the scram worth at reactor trip, but then steadily increased due to moderator and Doppler feedback associated with the primary system cooldown. Shortly thereafter, power begins to rise steadily due to the dominating positive reactivity feedback from the moderator. The reactor soon achieves a quasi-steady-state power level where the Doppler and the moderator reactivities balance the scram reactivity.

Fifty-five seconds after break initiation, the RCS pressure dropped below the shutoff head of the HPSI system and HPSI flow to the RCS began. But, the elevated primary pressure limited the delivery of boron into the core due to the pressure versus flow characteristics of the HPSI system and unborated water never cleared the safety injection lines during the transient.

Figure 14.1.5.2-9 shows the transient reactor power. The reactor power initially declined due to insertion of the control rods. The severe cooldown resulted in power increasing after 52 seconds. A quasi steady-state reactor power level was established by 260 seconds and a maximum power level of 378 MW or 14% of rated power occurred at 462 seconds.

85 A 272 10 300

PRISM

14.1.5.2.6.1.4 XTGPWR and XCOBRA-IIIC Results

PRISM

PRISM

The XTGPWR calculation is made initially on the basis of ANF-RELAP input. Each assembly within the three channels is assumed to have a uniform flow corresponding to the sector flows calculated with ANF-RELAP. Due to high power peaking in the region of the stuck control rod, large moderator density reductions are calculated to occur in the top portions of several assemblies in this region of the core in the XTGPWR calculation. This moderator density decrease is a major factor in the flattening of the axial and radial profiles, and the significant reduction in reactivity observed when XTGPWR is compared to ANF-RELAP. An XCOBRA-IIIC analysis is also conducted to define the flow and enthalpy distribution within the high power assembly.

CORE RESPONSIBLE FOR

98-145

PRISM

from the event initiation to the time of maximum LHGR

The ANF-RELAP reactivity and power calculation has considerable inherent conservatism. To demonstrate this, a comparison of the change in reactivity at the maximum LHGR time is made. A comparison of the overall change in reactivity between ANF-RELAP and XTGPWR shows that ANF-RELAP conservatively underestimates the negative reactivity by 1.01$ at the time of maximum LHGR thus indicating that the ANF-RELAP power calculation is conservative.

PRISM

14.1.5.2.6.1.5 Departure From Nucleate Boiling Ratio and Linear Heat Generation Rate Results

For the MDNBR portion of the calculation, the radial power distribution was modified to conservatively account for local rod power distribution affects within the hot assembly. This was done by raising the power of the hot assembly to bound the peak rod power.

On the bases of these conservative assumptions, the MDNBR value was calculated to be 2.28. This compares to a 95/95 DNBR limit of 1.135 for the modified Barnett correlation. Therefore, no fuel rods would be expected to fail during this transient scenario from an MDNBR stand point.

2.44

FSARCR 00-MP2-23

ATTACHMENT 2
Page 26 of 104

~~Insert to Page 14.1-22~~

INSERT 2 ②

The total core reactivity, initially at 0.00$ decreased initially due to reactor scram worth, then steadily increased due to moderator and Doppler feedback associated with the primary system cooldown. The reactor was approaching a quasi steady-state, with the Doppler and the moderator reactivities balancing the scram reactivity, when boron began entering the core, causing the power to decrease.

HPSI flow to the RCS began 42 seconds after break initiation and 25 seconds after the HPSI actuation signal. Twenty-five seconds was the assumed time for the HPSI pumps to reach rated speed.

The analysis of the peak LHGR also comes from the ~~XTGPWR~~ PRISM and XCOBRA-IIIC analysis. The peak LHGR is calculated from the ANF-RELAP total core power and the ~~XTGPWR~~ PRISM radial and axial peaking. The peak LHGR ~~24.27 kW/ft~~ was calculated for the ~~HFP~~ outside HZP containment break with offsite power available event. ~~When compared to a centerline melt criteria of 21.0 kW/ft, four assembly quadrants (one full assembly) or 0.46% of the core, are predicted to fail due to violation of the centerline melt criteria.~~ INSERT 6

00-MP2-38

14.1.5.2.6.2 Hot ~~Full~~ Zero Power Outside Containment with Loss of Offsite Power

The ANF-RELAP NSSS simulation of the most limiting SLB scenario from an MDNBR standpoint (i.e., ~~HFP~~ HZP outside containment break with a loss of offsite power) is illustrated in Figures 14.1.5.2-10 through 14.1.5.2-16. A tabulation of the sequence of events is presented in Table 14.1.5.2-8. Termination of the AFW by manual operator action was assumed to occur 600 seconds after initiation of the break. This is well beyond the time of MDNBR and maximum LHGR. ~~Termination of AFW would cause the affected SG to dry out and an increase in the primary system temperature. The increase in primary temperature, will drive the reactor suberitical and restore shutdown.~~

14.1.5.2.6.2.1 Secondary System Thermal Hydraulic Parameters

Steam flow out the break is the source of the NSSS cooldown. Steam flow for the affected steam generator is plotted in Figure 14.1.5.2-10. Secondary pressure for the steam generators is plotted in Figure 14.1.5.2-11. The affected steam generator blows down through the break throughout the transient. The pressure and mass flow rate dropped rapidly at first and then proceeded downward at a slower decay rate until natural circulation flow was established by approximately ~~250~~ 220 seconds. 98-145

The intact steam generators blow down for a short period until the MSIVs completely close approximately ~~10~~ 14 seconds after the break is initiated. The pressure recovers as the intact steam generator equilibrates with the primary system. Subsequently, the intact steam generator pressure remains essentially constant as the primary intact coolant loop approaches natural circulation conditions.

14.1.5.2.6.2.2 Primary System Thermal Hydraulic Parameters

The primary system core coolant temperature and pressurizer pressure and level responses resulting from the break flow are illustrated in Figures 14.1.5.2-12 through 14.1.5.2-14. The primary system pressure decays rapidly as the coolant contracts due to the cooldown and the pressurizer empties. Continued pressure reduction in the primary system causes the relatively hot stagnant liquid in the head of the RPV vessel to flash. The flashing in the upper head, coupled with near equilibration of other NSSS parameters, retards the pressure decay from that point forward.

A comparison of intact and affected core sector inlet temperatures throughout the transient indicates significant differences due to the limited cross flow allowed between loops. The core sector flows all show the same trend due to the coastdown of the primary coolant pumps. That is, all flows decrease rapidly until natural circulation conditions are achieved in the two flow loops.

00-MP2-38

Insert 6

No fuel failure is predicted to occur due to the violation of the FCMLHR limit. However, one full assembly, or 0.46% of the core, is assumed to fail when determining the radiological consequences of a main steam line break.

14.1.5.2.6.2.3 Reactivity and Core Power

Insert 3

The reactivity transient calculated by ANF-RELAP is illustrated in Figure 14.1.5.2-15. Initially, the core is assumed to be at ~~full~~ power. All control rods, except the most reactive ~~one~~, are assumed to be inserted into the core following the reactor trip signal. The ~~reactivity~~ transient then proceeds. The total core reactivity, initially at 0.00$, decreased instantly due to the scram worth at reactor trip, but then steadily increased due to moderator and Doppler feedback associated with the primary system cooldown. Shortly thereafter, power begins to rise steadily due to the dominating positive reactivity feedback from the moderator. The reactor soon achieves a quasi-steady-state power level where the Doppler and the moderator reactivities balance the scram reactivity.

Ninety seconds after break initiation, the RCS pressure dropped below the shutoff head of the HPSI system and HPSI flow to the RCS began. But, the elevated primary pressure limited the delivery of boron into the core due to the pressure versus flow characteristics of the HPSI system and unborated water never cleared the safety injection lines during the transient.

Insert 4

The transient experienced by the core power is illustrated in Figure 14.1.5.2-16. ~~The reactor power declined to a decay heat level during the first 150 seconds of the transient. The maximum peak power level of 207 MW or 7.7% of rated power occurred at 488 seconds.~~

14.1.5.2.6.2.4 ~~XTGPWR~~ and XCOBRA-IIIC Results

The ~~XTGPWR~~ calculation is initially made on the basis of ANF-RELAP predicted core power, flow, pressure, and inlet temperatures. The ~~XTGPWR~~ calculations provide the radial and axial power distributions for use in the XCOBRA-IIIC code. Due to the high power peaking in the region of the stuck control rod, and the low core average natural circulation flow rates, large moderator density decreases are calculated in several assemblies in this region in the ~~XTGPWR~~ calculation. ~~This is a major factor in the flattening of the axial and radial profiles, and~~ the significant reduction in reactivity observed when ~~XTGPWR~~ is compared to ANF-RELAP. An XCOBRA-IIIC analysis is also conducted to define the flow and enthalpy distribution within the high power assembly.

A comparison of the overall change in reactivity between ANF-RELAP and ~~XTGPWR~~ shows ~~that ANF-RELAP conservatively underestimates the negative reactivity by 1.00$ at the time of MDNBR thus indicating that~~ the ANF-RELAP power calculation is conservative.

14.1.5.2.6.2.5 Departure From Nucleate Boiling Ratio and Linear Heat Generation Rate Results

The MDNBR of the hot fuel assembly is calculated to be ~~1.71~~ 1.74 which is above the modified Barnett 95/95 DNBR correlation limit. Therefore, no fuel rods are expected to fail from an MDNBR standpoint.

00-MP2-38

As before, the analysis of the peak LHGR comes from the ~~XTGPWR~~ and the XCOBRA-IIIC analysis. The peak LHGR was ~~17.96~~ 16.6 kW/ft. Comparing this LHGR with ~~a centerline melt criteria of 21 kW/ft~~ the FCM LHR limit, it is apparent that centerline melt is not predicted to occur. Thus, no fuel failures are predicted to occur due to violation of the centerline melt criteria.

FSARCR 00-MP2-23

INSERTS TO page 14.1-24

INSERT 3

③

The total core reactivity, initially at 0.00$ decreased initially due to reactor scram worth, then steadily increased due to moderator and Doppler feedback associated with the primary system cooldown. The rise in reactor power was arrested when boron began entering the core at 320 seconds. Power then declined slowly due to an increasing boron concentration in the primary system.

The HPSI actuation signal was received at 22 seconds. After a 25 second delay, during which the HPSI pumps reached rated speed, HPSI flow to the RCS began, at 47 seconds.

INSERT 4

④

The core power, initially at 1 Watt, increased rapidly at 130 seconds and reached a peak power level of 5.6% of rated power (152 MW) at 320 seconds.

14.1.5.2.7 Conclusions — the scenarios with offsite power available

The HFP and HZP scenarios, with offsite power maintained for operation of the primary coolant pumps resulted in a return to higher power levels than the scenarios where offsite power is lost. However, these scenarios provide substantially greater margin to the MDNBR limit because of the higher coolant flow rate. In no scenario evaluated, however, was fuel failure calculated to occur as a result of penetration of the MDNBR safety limit. ~~The HFP and HZP scenarios with offsite power maintained for operation of the primary coolant pumps returned to higher power levels than the scenarios where offsite power is lost.~~ Even though ~~these scenarios~~ have substantially greater margin to the MDNBR limit because of a higher coolant flow rate, the higher power levels in combination with the highly skewed power distribution due to the assumed stuck rod cluster resulted in them having the least margin to the fuel centerline melt limit.

The ~~HFP~~ HZP outside containment break scenario concurrent with a loss of offsite power was determined to be the most limiting in this analysis from an MDNBR standpoint. The MDNBR of the hot fuel assembly is calculated to be ~~1.71 which is~~ above the modified Barnett 95/95 DNBR correlation limit. Therefore, no fuel rods are expected to fail from an MDNBR standpoint.

The ~~HFP~~ HZP outside containment break scenario with offsite power available was determined to be the most limiting in this analysis from the standpoint of centerline melt. This scenario results in the highest return to power and highest calculated LHGR ~~of 24.27 kW/ft. When compared to a centerline melt criteria of 21.0 kW/ft, four assembly quadrants (one full assembly) or 0.46% of the core, are predicted to fail due to violation of the centerline melt criteria.~~ assumed which is below the FCMLHR limit

00-MP2-38

98-145

14.1.5.3 Radiological Consequences of a Main Steam Line Break

The main steam line break is postulated to occur in a main steam line outside the containment. The radiological consequences of a main steam line break inside containment is bounded by the main steam line break outside containment. The plant is assumed to be operating with Technical Specification coolant concentrations and primary to secondary leakage. A 0.035 gpm primary to secondary leak is assumed to occur in both steam generators.

00-MP2-38

Two separate main steam line break cases are analyzed. In the first case, associated with this accident is that 1 fuel assembly is assumed to experiences melting and releases the melted fuel into the RCS at the onset of the accident. One fuel assembly is equivalent to 0.46% melt. The activity associated with the melt condition is therefore available for release to the atmosphere via primary to secondary leakage. In the second case a pre-accident iodine spike is assumed to occur. In this case the primary coolant iodine concentrations are 60 times the plant technical specification activity level of 1 uCi/gm DE I-131. In addition, the noble gas activity in the primary coolant is assumed to be at technical specification levels.

The noble gases and iodines in the primary coolant that leak into the faulted steam generator during the transient are released directly to the environment without holdup or decontamination. An iodine partition factor of 0.01 is used for the releases from the unaffected steam generator. Off-site power is assumed to be lost, thus making the condenser unavailable. The steam releases from the main steam line break are from the

turbine building blowout panels as the atmospheric dispersion factor is greater for this release point than the enclosure building blowout panels. The steam releases from the intact steam generator are from the MSSVs/ADVs.

The radiological consequences of a main steam line break (assuming one fuel assembly melted) to the EAB, LPZ and Millstone 2 Control Room are reported in Tables 14.1.5.3-2 and 14.1.5.3-3. The assumptions used to perform this evaluation are summarized in Table 14.1.5.3-1. 98-145

The resulting doses to the EAB and LPZ do not exceed the limits specified in 10CFR100. The resulting doses to the Control Room do not exceed the limits specified in GDC19.

FSARCR 00-MP2-23

ATTACHMENT 2
Page 33 of 104

REFERENCES

(A)

14.1-1 "Steam Line Break Methodology for PWRS," EMF-84-093(P) Revision 1, Siemens Power Corporation, Richland, WA, ~~June 1998~~ February 1999.

14.1-2 "ANF-RELAP Methodology for Pressurized Water Reactors: Analysis of Non-LOCA Chapter 15 Events," ANF-89-151(P)(A), Advanced Nuclear Fuels Corporation, May 1992.

14.1-3 ~~"XTG- A Two-Group Three-Dimensional Reactor Simulator Utilizing Coarse Mesh Spacing (PWR Version)," XN-CC-28, Volume 1, Revision 5, Exxon Nuclear Company, Richland, WA 99352, July 1979.~~ a

14.1-4 "XCOBRA-IIIC: A Computer Code to Determine the Distribution of Coolant During Steady-State and Transient Core Operation," XN-NF-75-21(A), Revision 2, Exxon Nuclear Company, January 1986.

98-145

INSERT 5

FSARCR 00-MP2-23

ATTACHMENT 2
Page 34 of 104

INSERT for page 14.1-27

INSERT 5

⑤ 14.1-3 "Reactor Analysis Systems for PWRs, Volume 1 – Methodology Description, Volume 2 – Benchmarking Results," EMF-96-029(P)(A), Siemens Power Corporation, January 1997.

ATTACHMENT 2
Page 35 of 104

TABLE 14.1.5.1-1

AVAILABLE REACTOR PROTECTION FOR STEAM SYSTEM PIPING FAILURES INSIDE AND OUTSIDE OF CONTAINMENT

PRE-SCRAM ANALYSIS

Reactor Operating Conditions	Reactor Protection
1	Low Steam Generator Pressure Trip
	Low Steam Generator Water Level Trip
	Low Reactor Coolant Flow
	Variable Overpower Trip
	Local Power Density Trip
	Thermal Margin/Low Pressure Trip
	High Containment Pressure Trip
	Safety Injection Actuation Signal
2	Low Steam Generator Pressure Trip
	Low Steam Generator Water Level Trip
	Low Reactor Coolant Flow
	Variable Overpower Trip
	High Containment Pressure Trip
	Safety Injection Actuation Signal
3-6	Technical Specification Requirements on Shutdown Margin, Inherent Negative Doppler Feedback

98-145

TABLE 14.1.5.1-2

DISPOSITION OF EVENTS FOR STEAM SYSTEM
PIPING FAILURES INSIDE AND OUTSIDE OF CONTAINMENT

PRE-SCRAM ANALYSIS

Reactor Operating Conditions	Disposition
1	Analyze
2	Analyze
3-6	Bounded by the above

98-145

ATTACHMENT 2
Page 37 of 104

TABLE 14.1.5.1-3

ANF-RELAP THERMAL-HYDRAULIC INPUT (PRE-SCRAM STEAM LINE BREAK)

Initial Condition Thermal-Hydraulic Input	HFP
Reactor Power (MW)	2754
Pressurizer Pressure (psia)	2250
Pressurizer Level (%)	65
Cold Leg Coolant Temperature (°F)	549
Total Primary Flow Rate (lbm/sec)	37,640
Secondary Pressure (psia)	881
Core Bypass Flow Rate (lbm/sec) per Loop	753
Main Feedwater Temperature (°F)	432
Steam Generator Mass Inventory (lbm)	167,237

98-145

TABLE 14.1.5.1-4

ACTUATION SIGNALS AND DELAYS (PRE-SCRAM STEAM LINE BREAK)

Reactor Trip	Non-Harsh Containment Condition Setpoint	Harsh Containment Condition Setpoint	Delay
Variable Overpower (ceiling)	111.6% of rated	Not credited	0.9 s
Low Reactor Coolant Flow	Credited	85% flow	0.65 s
High Containment Pressure	Not applicable	5.83 psig	0.9 s
Low Steam Generator Pressure	658	550	0.9 s
TM/LP (floor)	1728 psia	1700 psia	0.9 s
TM/LP (function)	Evaluated from function given in Technical Specification	Not credited	0.9 s

98-145

TABLE 14.1.5.1-5

ANF-RELAP NEUTRONICS INPUT AND ASSUMPTIONS (PRE-SCRAM STEAM LINE BREAK)

Point Kinetics Input	Value
Effective Delayed Neutron Fraction	0.0054
Moderator Temperature Coefficient (pcm/°F)	
Offsite Power Available (Technical Specification most negative limit)	-28
Loss of Offsite Power (Technical Specification most positive limit above 70% RTP)	+1
HFP Scram Worth (pcm)	6628
Shutdown Margin Requirement (pcm)	3600
Doppler Coefficient	
Offsite Power Available	1.20 x most-negative value at EOC
Loss of Offsite Power	0.80 x least-negative value at BOC
Fission Product and Actinide Decay Constants	
Default values in ANF-RELAP utilized	

98-145

TABLE 14.1.5.1-6

MDNBR AND PEAK REACTOR POWER LEVEL SUMMARY (PRE-SCRAM STEAM LINE BREAK)

Location of Break	Type of Cooldown	Size of Break	MDNBR	Peak Reactor Power (% of rated)
Outside containment, downstream of check valves	Symmetric	2.40 ft²	1.332	126.90%
		3.00 ft²	1.310	130.01%
		3.50 ft²	1.298 9	130.97 7 %*
Outside containment, upstream of check valve	Asymmetric	1.20 ft²	1.254 49	124.42 69 %
		1.40 ft²	1.244 0	126.06 29 %
		1.60 ft²	1.302	124.87%
		1.80 ft²	1.334	124.92%
Inside containment, upstream of check valve	Asymmetric	0.40 ft²	1.299	117.85%
		0.60 ft²	1.258	121.53%
		0.80 ft²	1.262	122.26%
		1.80 ft²	1.318	125.51%
Inside containment, upstream of check valve with loss of offsite power	Asymmetric	3.51 ft²	0.88**	106.86%

*The peak LHRs for all pre-scram breaks are bounded by the peak LHR for the 3.50 ft² break outside containment and downstream of a check valve.

**The MDNBRs for all pre-scram breaks are bounded by the MDNBR for the 3.51 ft² break inside containment and upstream of a check valve with the loss of offsite power.

TABLE 14.1.5.1-7

LHGR-LIMITING PRE-SCRAM STEAM LINE BREAK SEQUENCE OF EVENTS: HFP 3.50 ft^2 SYMMETRIC BREAK OUTSIDE CONTAINMENT WITH OFFSITE POWER AVAILABLE

Time (sec)	Event
0	Break downstream of main steam line check valves opens
0	Turbine control valves open fully
7	Low steam generator pressure trip setpoint reached
8	Turbine trips on reactor scram signal
9	Scram CEA insertion begins
9	Reactor power reaches maximum value
10	MDNBR occurs

98-145

TABLE 14.1.5.1-8

MDNBR-LIMITING PRE-SCRAM STEAM LINE BREAK SEQUENCE OF EVENTS: HFP 3.51 ft^2 ASYMMETRIC BREAK INSIDE CONTAINMENT WITH LOSS OF OFFSITE POWER

Time (sec)	Event
0	Break occurs
0	RCPs trip
0	Peak LHGR (kW/ft)
2	Scram signal on low flow trip
3	Scram CEA Insertion begins
3	Max Power (Fraction of RTP)
4	MDNBR

98-145

FSAR CR 00-MP2-23

ATTACHMENT 2
page 43 of 164

TABLE 14.1.5.2-1

AVAILABLE REACTOR PROTECTION FOR STEAM SYSTEM PIPING FAILURES INSIDE AND OUTSIDE OF CONTAINMENT

POST-SCRAM ANALYSIS

Reactor Operating Conditions	Reactor Protection
1	Low Steam Generator Pressure Trip
	Low Steam Generator Water Level Trip
	~~Variable Overpower Trip~~
	Local Power Density Trip
	Thermal Margin/Low Pressure Trip
	High Containment Pressure Trip
	Safety Injection Actuation Signal
2	Low Steam Generator Pressure Trip
	Low Steam Generator Water Level Trip
	~~Variable Overpower Trip~~
	High Containment Pressure Trip
	Safety Injection Actuation Signal
3-6	Technical Specification Requirements on Shutdown Margin, Inherent Negative Doppler Feedback

98-145

ATTACHMENT 2
page 44 of 104

TABLE 14.1.5.2-2

DISPOSITION OF EVENTS FOR STEAM SYSTEM
PIPING FAILURES INSIDE AND OUTSIDE OF CONTAINMENT

POST-SCRAM ANALYSIS

Reactor Operating Conditions	Disposition
1	Analyze
2	Analyze
3-6	Bounded by the above

98-145

TABLE 14.1.5.2-3

ANF-RELAP THERMAL-HYDRAULIC INPUT (POST-SCRAM STEAM LINE BREAK)

Initial Condition Thermal-Hydraulic Input	HFP	HZP
Core Power (MW)	2700	1E-6
Primary Pressure (psia)	2250	2250
Pressurizer Level (%)	65	40
Cold Leg Temperature (°F)	549	532
Primary Flow Rate per Loop (lbm/sec)	18,820	19,241
Secondary Pressure (psia)	880	892
Steam Generator Mass Inventory (lbm)	167,237	253,989
Total Steam Flow (lbm/sec) per Steam Generator	1634	4
~~Total MFW Flow (lbm/sec) per Steam Generator~~	~~1634~~	~~4~~
~~MFW Temperature (°F)~~	~~432~~	~~432~~
~~Total AF Flow (lbm/sec)~~	~~184~~	~~184~~
~~RWST Boron Concentration (ppm)~~	~~1720~~	~~1720~~
~~AF Temperature (°F)~~	~~32~~	~~32~~

98-145

Break Characteristics	
Minimum Flow Area	
Affected Steam Generator (ft^2)	3.51
Unaffected Steam Generator (ft^2)	3.51
Location of Pipe Break	Downstream of steam generator integral flow restrictor and upstream of MSIV

FSAR CR 00-MP2-23

ATTACHMENT 2
page 46 of 104

TABLE 14.1.5.2-3

ANF-RELAP THERMAL-HYDRAULIC INPUT (POST-SCRAM STEAM LINE BREAK)

Injection Systems	HFP	HZP
Total HPSI Pumps	3	3
Active HPSI Pumps	2	2
Single Failure (No credit for mounted spare)	1 HPSI pump	1 HPSI pump
Active Charging Pumps	0	0
Refueling Water Storage Tank Boron Concentration (ppm)	1720	1720
HPSI Delivery Curve	Fig. 14.1.5.2-1	Fig. 14.1.5.2-1
Feedwater		
Auxiliary		
Flow, maximum (lbm/sec)	184 ~~183.6~~	184 ~~183.6~~
Temperature (°F)	32 ~~32.1~~	32 ~~32.1~~
Main		
Initial Flow per Steam Generator (lbm/sec)	1634 ~~1634.1~~	4 ~~0.0~~
Initial Temperature (°F)	~~432.4~~ 432	~~N/A~~ 432

98-145

ATTACHMENT 2
page 47 of 104

TABLE 14.1.5.2-4

ACTUATION SIGNALS AND DELAYS (POST-SCRAM STEAM LINE BREAK)

Parameter Setpoints	Inside Containment	Outside Containment
1. Low Steam Generator Pressure Trip	550 psia	658 psia
2. Low Pressurizer Pressure SIAS	1500 psia	1578 psia
3. Low Steam Generator Pressure MSI	370 psia	478 psia

MSIV Closure

Required Actuation Signal
(3) Above

Delay - 6.9 seconds

98-145

HPSI Actuation

Required Actuation Signal
(2) Above

Delay - 25.0 seconds

Main Feedwater Valve Closure

Required Actuation Signal
(3) Above

Delay - 14.0 seconds

Reactor Scram

Required Actuation Signal
(1) Above

Delay - 0.9 second instrument delay
3.0 second insertion time

TABLE 14.1.5.2-5

ANF-RELAP NEUTRONICS INPUT AND ASSUMPTIONS (POST-SCRAM STEAM LINE BREAK)

Point Kinetics Input	Value
Effective Delayed Neutron Fraction	~~0.0054~~ 0.00525
Moderator Temperature Coefficient (pcm/°F)	-28.0
HFP Scram Worth (pcm)	~~6438.0~~ 6619.0
Shutdown Margin Requirement (pcm)	3600.0

98-145

Stuck Rod Location

Within half-core section cooled by affected loop

Fission Product and Actinide Decay Constants

Default values in ANF-RELAP utilized

FSARCR 00-MP2-23

ATTACHMENT 2
Page 49 of 104

TABLE 14.1.5.2-6

POST-SCRAM STEAM LINE BREAK ANALYSIS SUMMARY

FSAR CR 00-MP2-38

Initial Power Level	Offsite Power Available	Break Location	Maximum Post-Scram Return to Power (MW)	MDNBR	Maximum LHGR (kW/ft)	Fuel Failure (% of Core)
HFP	No	outside containment	~~207.5~~ 109.3	~~1.71~~ 2.62	~~17.96~~ 10.3	0.0
HFP	Yes	outside containment	~~378.0~~ 194.8	~~2.28~~ 2.75	~~24.27~~ 21.0	0.0 ~~0.5~~ ~~0.003~~
HZP	No	outside containment	~~182.9~~ 152.1	~~1.89~~ 1.74	~~15.76~~ 16.76	0.0
HZP	Yes	outside containment	~~343.5~~ 271.6	~~2.37~~ 2.44	~~23.47~~ 23.3	0.0 ~~0.3~~ ~~0.22~~

98-

Initial Power Level	Offsite Power Availability	Break Location	ANF-RELAP Reactivity Change ($)	XTGPWR Reactivity Change ($)	Conservatisms in Input Parameters (MTC, Doppler, and Scram Worth Bias) ($)	Net Conservatism in ANF-RELAP model ($)
HFP	No	outside containment	+0.00	-6.30	+5.30	+1.00
HFP	Yes	outside containment	+0.00	-5.87	+4.86	+1.01
HZP	No	outside containment	+6.69	+3.00	+2.72	+0.97
HZP	Yes	outside containment	+6.68	+3.43	+2.34	+0.91

FSARCR 00-MP2-23

ATTACHMENT 2
page 50 of 104

TABLE 14.1.5.2-7

LHGR-LIMITING POST-SCRAM STEAM LINE BREAK SEQUENCE OF EVENTS:
HFP OUTSIDE CONTAINMENT BREAK WITH OFFSITE POWER AVAILABLE

Time (sec)	Event
0.	Reactor at HFP
0.+	Double-ended guillotine break
4	Low steam generator pressure trip, Reactor trip
11	MSIV and MFW valves closure trip signal
16	SI signal
17	MSIVs closed
25	MFW valves closed
41	SI pumps at rated speed (25 s delay)
180	AFW starts
462	Peak post-scram power reached (378.03 MW)
N/A	SI lines cleared; boron begins to enter primary system
490	Steam generator dry out
600	Calculation terminated; power decreasing

98-145

~~SEE ATTACHMENT (NEXT PAGE)~~
Replace with Table 7

Table 14.1.5.2-7
LHGR-Limiting Sequence of Events - HZP Offsite Power Available

Time(s)	Event
0.	Reactor at HZP
0.+	Double ended guillotine break. Shutdown reactivity inserted. AFW increased to maximum flow, all directed to affected steam generator.
7.6	MSIV closure trip signal
14.5	MSIVs closed
17.1	SI signal
42.1	SI pumps at rated speed (25 s delay)
298.2	SI Lines cleared. Boron begins to enter primary system
300.	Peak post-scram power reached (271.6 MW)
600.	Calculation terminated. Power decreasing.

FSARCR 00-MP2-23

ATTACHMENT 2
Page 52 of 104

TABLE 14.1.5.2-8

MDNBR-LIMITING POST-SCRAM STEAM LINE BREAK SEQUENCE OF EVENTS: HFP OUTSIDE CONTAINMENT BREAK WITH LOSS OF OFFSITE POWER

Time (sec)	Event
0.	Reactor at HFP
0.+	Double-ended guillotine break; loss of offsite power
4	Low steam generator pressure trip, Reactor trip
9	MSIV and MFW valves closure trip signal
16	MSIVs closed
18	SI signal
23	MFW valves closed
43	SI pumps at rated speed (25 s delay)
180	AFW starts
488	Peak post-scram power reached (207.47 MW)
N/A	SI lines cleared; boron begins to enter primary system
600	Calculation terminated; power decreasing

98-145

SEE ATTATCHMENT (NEXT PAGE)

Replace with Table 8

Table 14.1.5.2-8
MDNBR-Limiting Post-Scram Steam Line Break Analysis Summary

Time(s)	Event
0.	Reactor at HZP
0.+	Double ended guillotine break. Loss of offsite power. Shutdown reactivity inserted. Full AFW flow started, all directed to the affected steam generator.
7.3	MSIV closure trip signal
14.2	MSIVs closed
21.6	SI signal
46.7	SI pumps at rated speed (25 s delay)
300.5	SI lines cleared. Boron begins to enter primary system
320.	Peak post-scram power reached (152.1 MW)
600.	Calculation terminated. Power decreasing.

TABLE 14.1.5.3-1

98-145

ASSUMPTIONS USED IN MAIN STEAM LINE BREAK ANALYSIS

Core Power Level (MW_t)	2754
Primary to Secondary Leak Rate per Steam Generator	0.035 gpm
Primary Coolant Iodine Concentration	1 uCi/gpm DE I-131
Secondary Coolant Iodine Concentration	0.1 uCi/gm DE I-131
Primary Coolant Noble Gas Concentration	$100/E_{bar}$
Pre-accident Spike Iodine Concentration	60 uCi/gm DE I-131
Melted Fuel Percentage (assumed)	0.46%
Peaking Factor	1.45
Reactor Coolant Mass	430,000 lbs
Intact Steam Generator Minimum Mass	100,000 lbs
Safety Injection Signal Response	85 seconds
Site Boundary Breathing Rate (m^3/sec)	
0 - 8 hr	3.47E-04
8 - 24 hr	1.75E-04
24 - 720 hr	2.32E-04
Site Boundary Dispersion Factors (sec/m^3)	
EAB: 0 - 2 hr	3.66E-04
LPZ: 0 - 4 hr	4.80E-05
4 - 8 hr	2.31E-05
8 - 24 hr	1.60E-05
24 - 96 hr	7.25E-06
96 - 720 hr	2.32E-06
Control Room Breathing Rate	3.47E-04 m^3/sec
Control Room Damper Closure Time	5 seconds
Control Room Intake Prior to Isolation	800 cfm
Control Room Inleakage During Isolation	130 cfm
Control Room Emergency Filtered Recirculation Rate (t=10 min)	2,250 cfm
Control Room Intake Dispersion Factors (sec/m^3)	
PORVs/ADVs: 0 - 8 hr	3.19 E-03
8 - 24 hr	2.05E-03
24 - 96 hr	7.61E-04
96 - 720 hr	2.13E-04
Turbine Building Blowout Panels:	
0 - 8 hr	4.23E-03
8 - 24 hr	2.85E-03
24 - 96 hr	1.12E-03
96 - 720 hr	3.63E-04
Control Room Free Volume	35,650 ft^3
Control Room Filter Efficiency (all iodines)	90%
Thyroid Dose Conversion Factors	ICRP 30

FSARCR 00-MP2-38

ATTACHMENT 2
page 58 of 104

TABLE 14.1.5.3-2

SUMMARY OF MILLSTONE 2 MSLB ACCIDENT DOSES
(0.46% Melted Fuel)
Assuming

Location	Thyroid (rem)	Whole Body (rem)	Beta (rem)
EAB	4.8	0.06	N/A
LPZ	2.3	0.02	N/A
Control Room	29	0.03	0.5

98-145

ATTACHMENT 2
Page 56 of 104

TABLE 14.1.5.3-3

SUMMARY OF MILLSTONE 2 MSLB ACCIDENT DOSES
(Pre-accident Iodine Spike)

Location	Thyroid (rem)	Whole Body (rem)	Beta (rem)
EAB	0.935	0.010	N/A
LPZ	0.176	0.002	N/A
Control Room	5.314	0.003	0.039

98-145

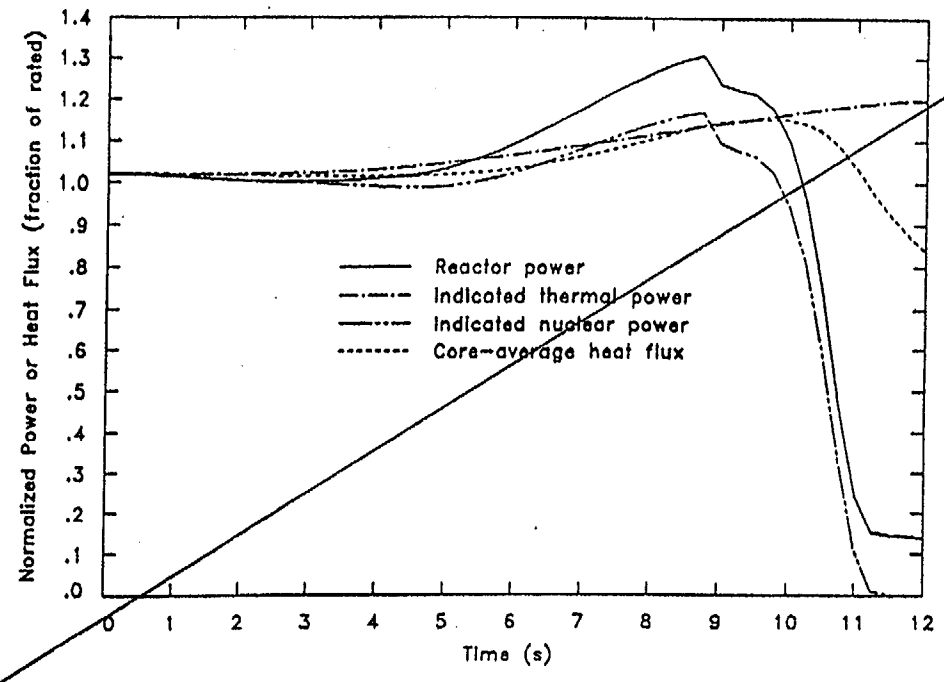

Replaced

FIGURE 14.1.5.1-1
NORMALIZED CORE POWER (SYMMETRIC 3.50 FT^2 BREAK OUTSIDE CONTAINMENT WITH OFFSITE POWER AVAILABLE)

Attachment 2
Page 57 of 104

FSAR CRM2-MP2-39

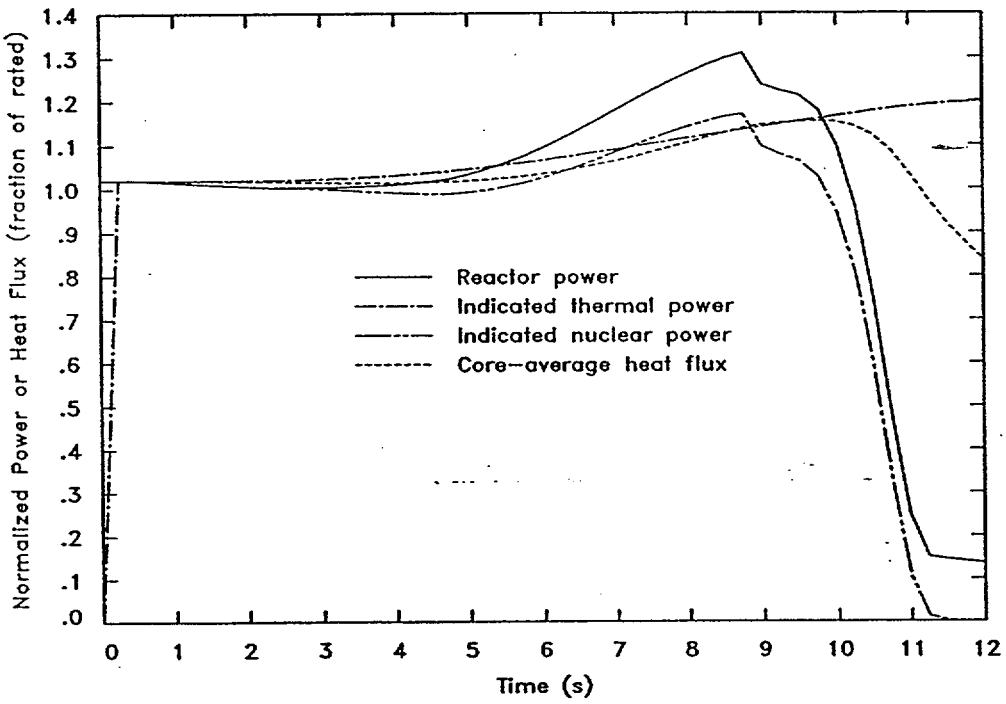

Figure 14.1.5.1-1 Normalized Core Power (Symmetric 3.50 ft^2 Break Outside Containment with Offsite Power Available)

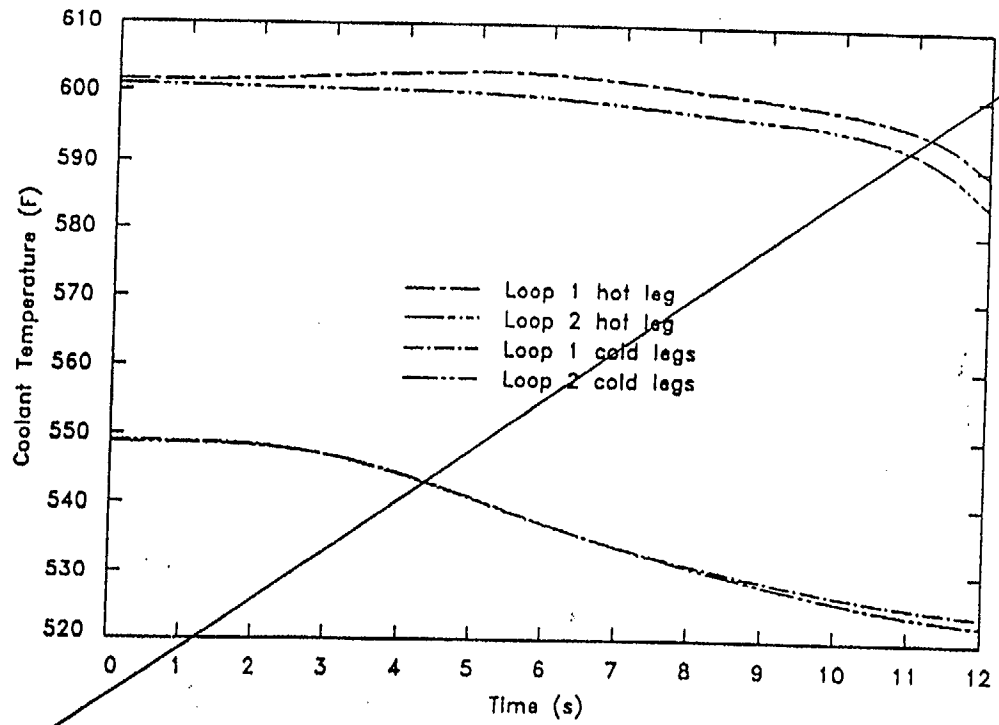

Replaced

FIGURE 14.1.5.1-2
CORE INLET TEMPERATURES (SYMMETRIC 3.50 FT^2 BREAK OUTSIDE CONTAINMENT WITH OFFSITE POWER AVAILABLE)

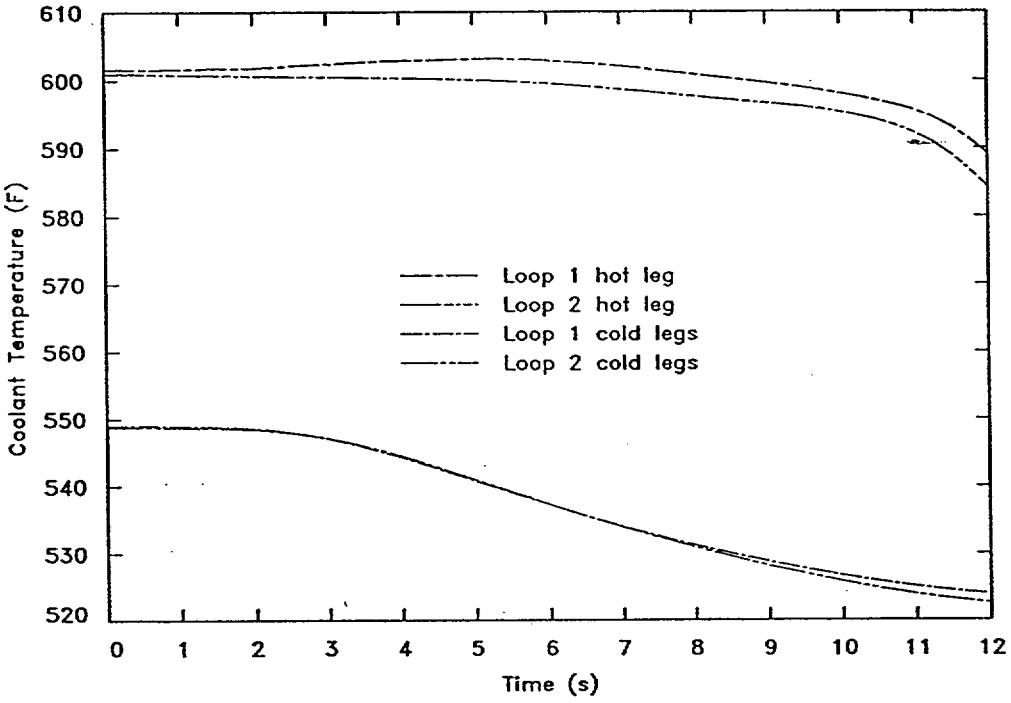

Figure 14.1.5.1-2 Core Inlet Temperatures (Symmetric 3.50 ft^2 Break Outside Containment with Offsite Power Available)

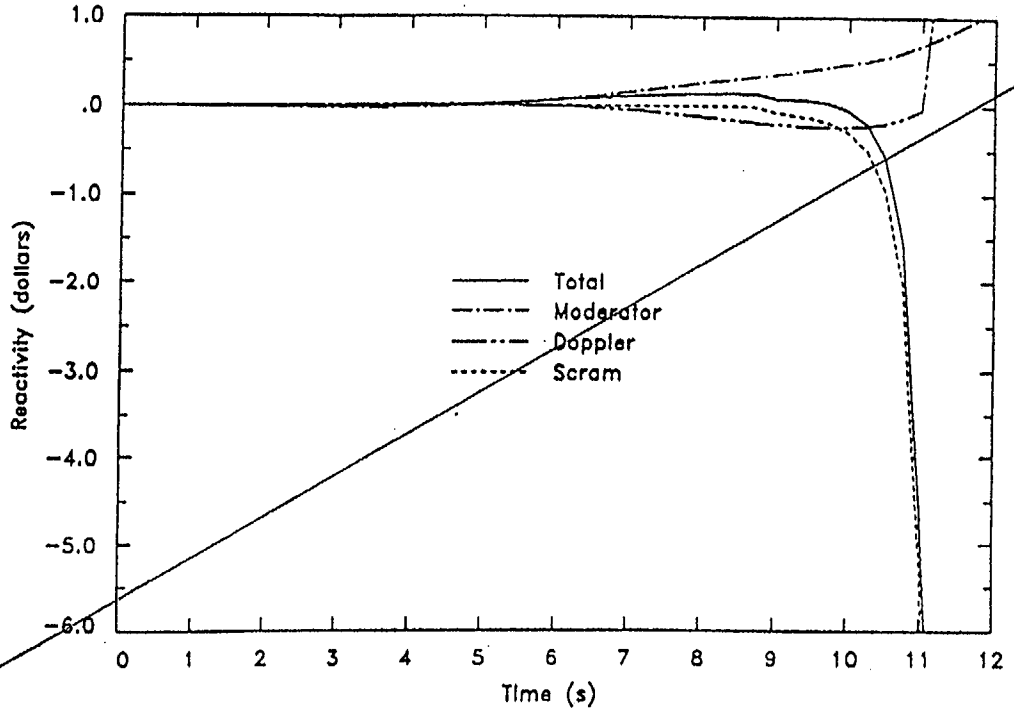

Replaced

FIGURE 14.1.5.1-3
REACTIVITY FEEDBACK (SYMMETRIC 3.50 FT^2 BREAK OUTSIDE CONTAINMENT WITH OFFSITE POWER AVAILABLE)

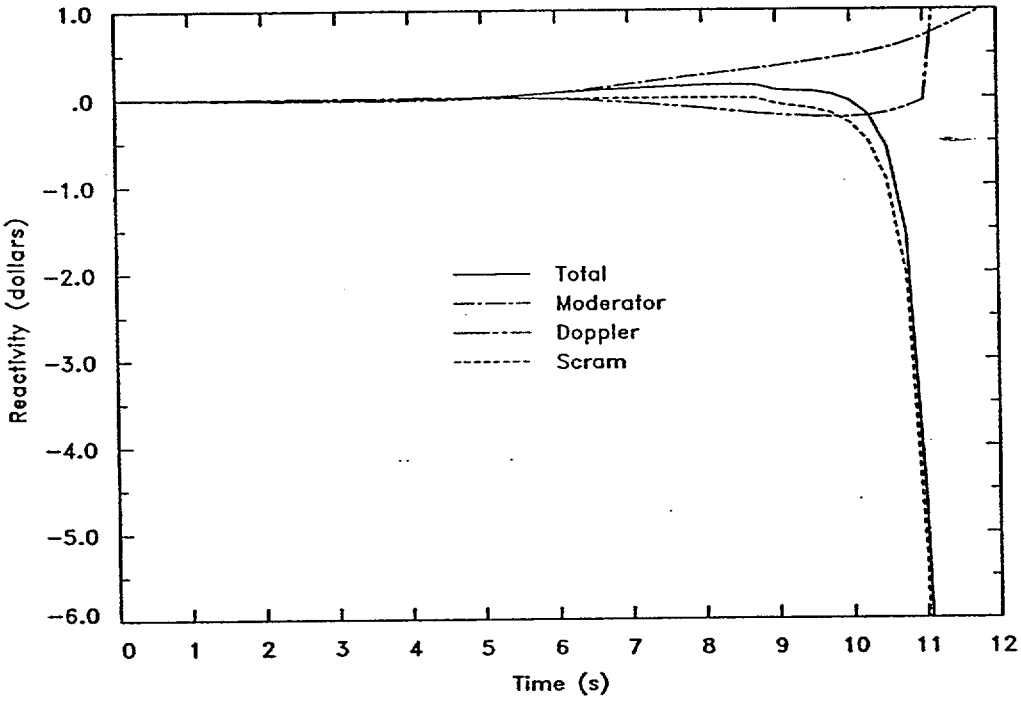

Figure 14.1.5.1-3 Reactivity Feedback (Symmetric 3.50 ft^2 Break Outside Containment with Offsite Power Available)

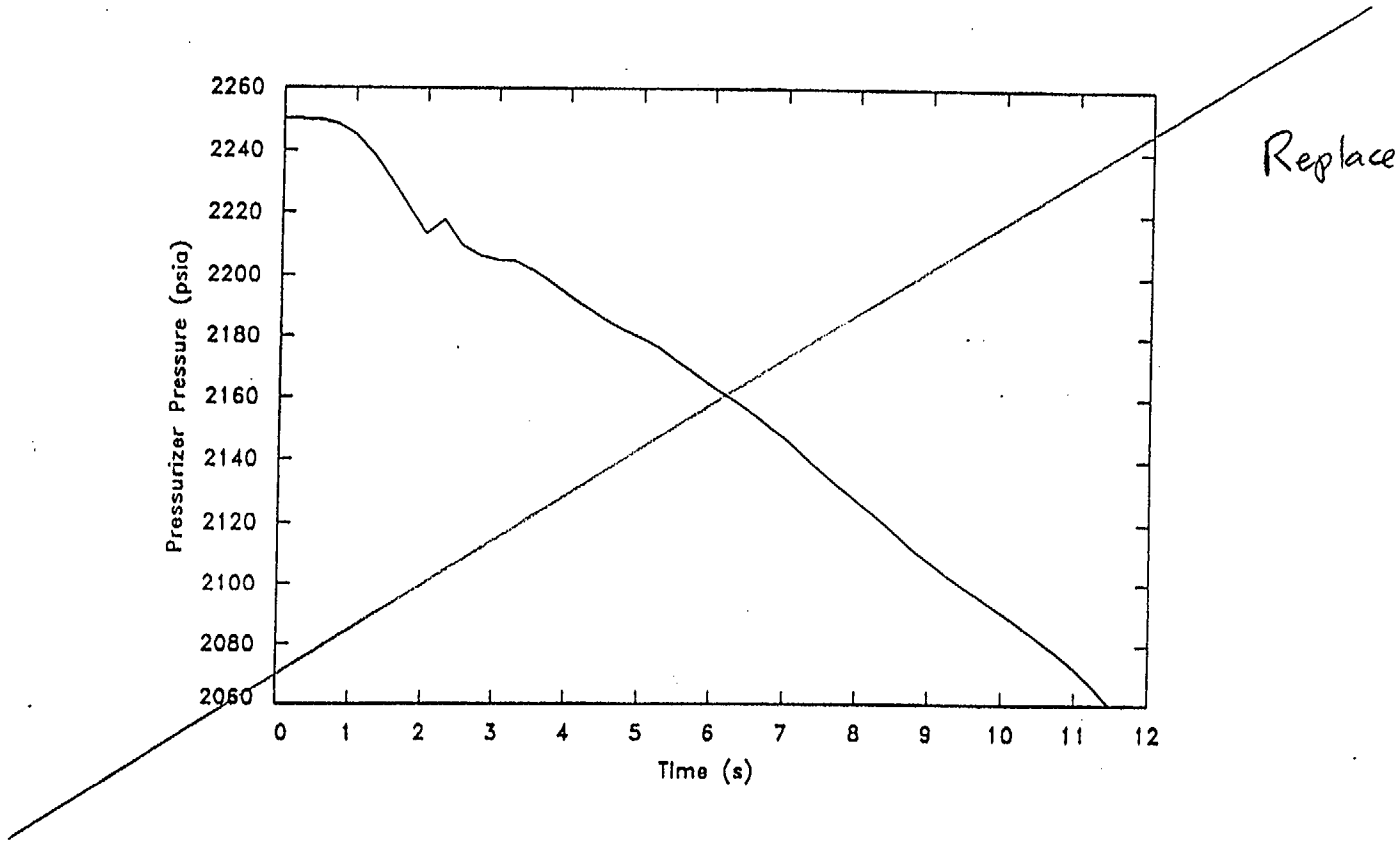

Replaced

FIGURE 14.1.5.1-4
PRESSURIZER PRESSURE (SYMMETRIC 3.50 FT^2 BREAK OUTSIDE CONTAINMENT WITH OFFSITE POWER AVAILABLE)

Attachment 2
Page 63 of 104

FSAR CR M2-MP2-39

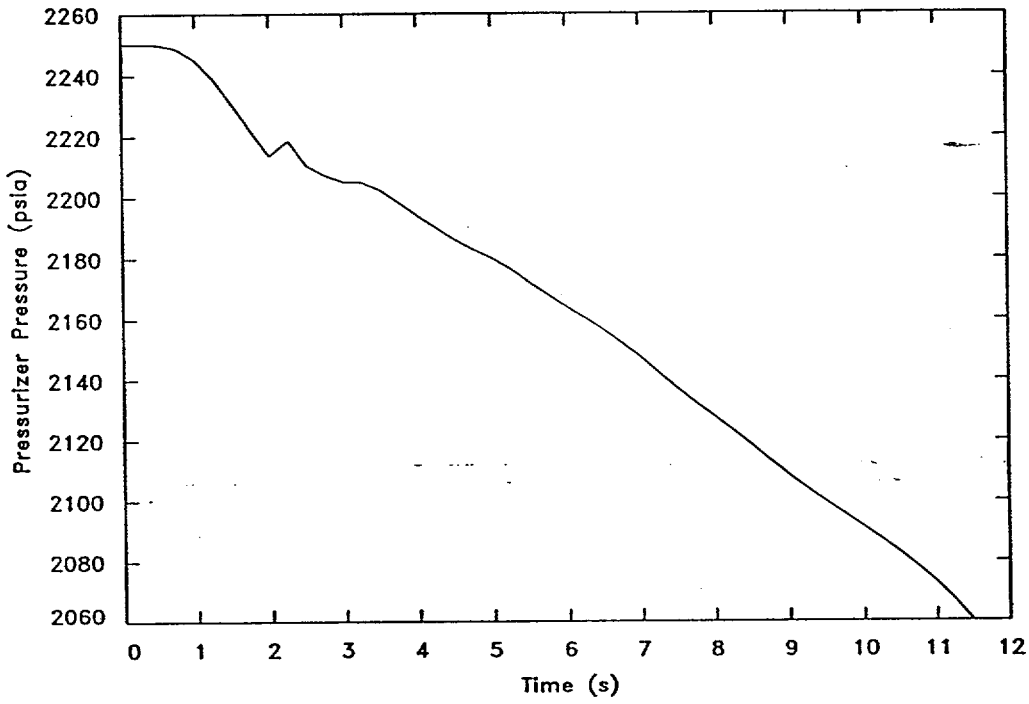

Figure 14.1.5.1-4 Pressurizer Pressure (Symmetric 3.50 ft^2 Break Outside Containment with Offsite Power Available)

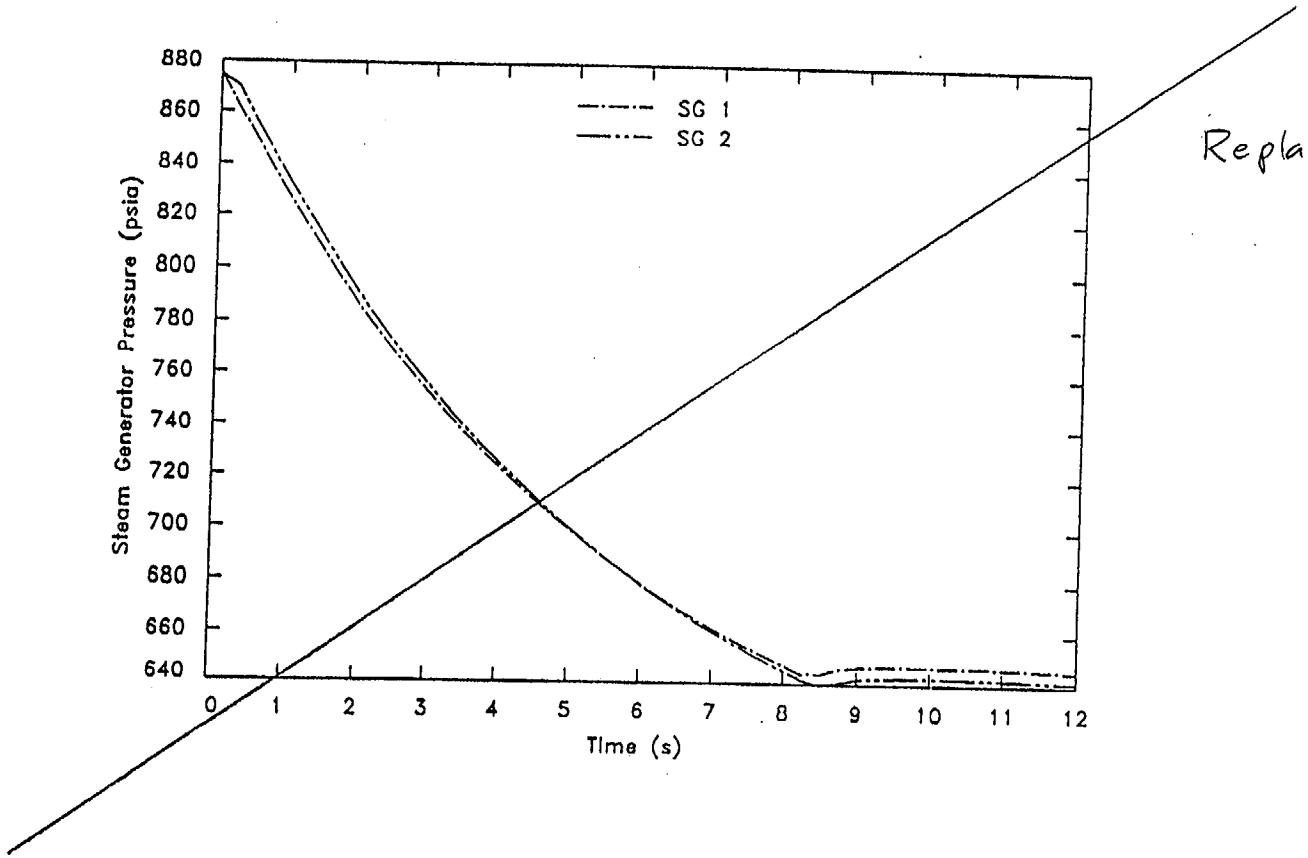

Replaced

Attachment 2
Page 65 of 104

FSAR CRM2-MP2-39

FIGURE 14.1.5.1-5
STEAM GENERATOR PRESSURES (SYMMETRIC 3.50 FT^2 BREAK OUTSIDE CONTAINMENT WITH OFFSITE POWER AVAILABLE)

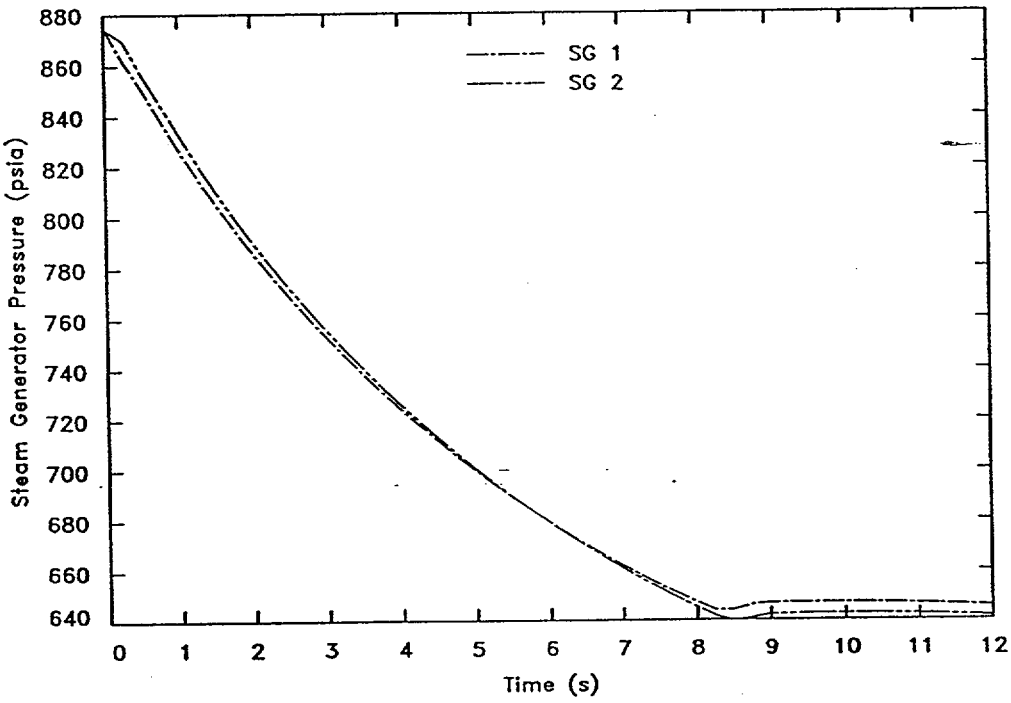

Figure 14.1.5.1-5 Steam Generator Pressures (Symmetric 3.50 ft^2 Break Outside Containment with Offsite Power Available)

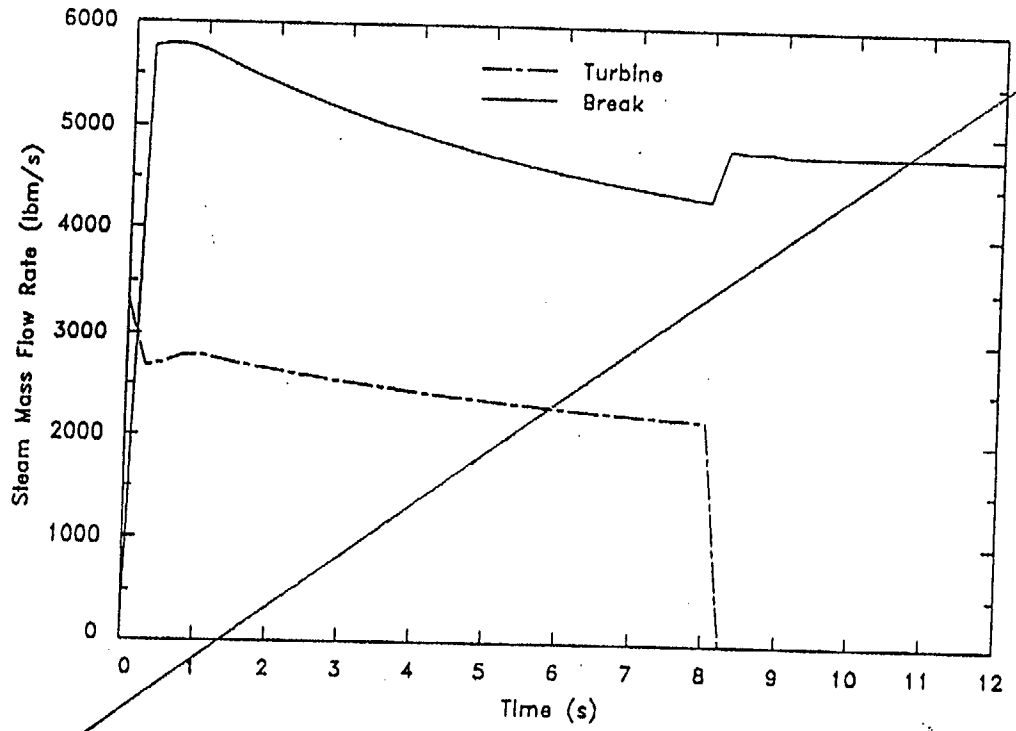

Replaced

FIGURE 14.1.5.1-6
MAIN STEAM LINE FLOW (SYMMETRIC 3.50 FT^2 BREAK OUTSIDE CONTAINMENT WITH OFFSITE POWER AVAILABLE)

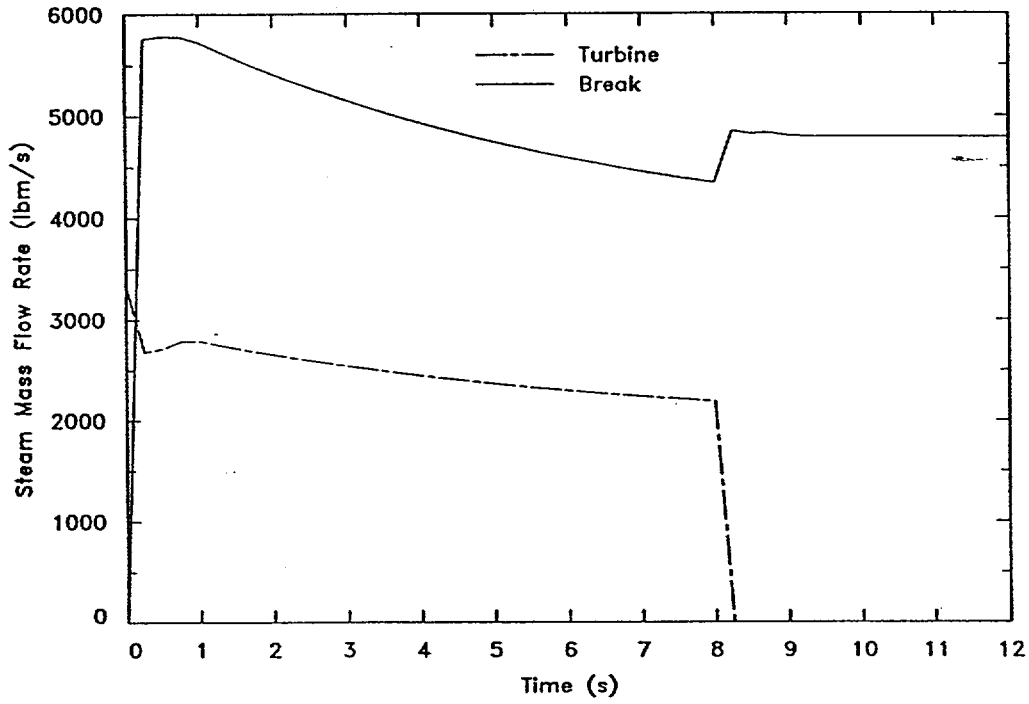

Figure 14.1.5.1-6 Main Steam Line Flow (Symmetric 3.50 ft^2 Break Outside Containment with Offsite Power Available)

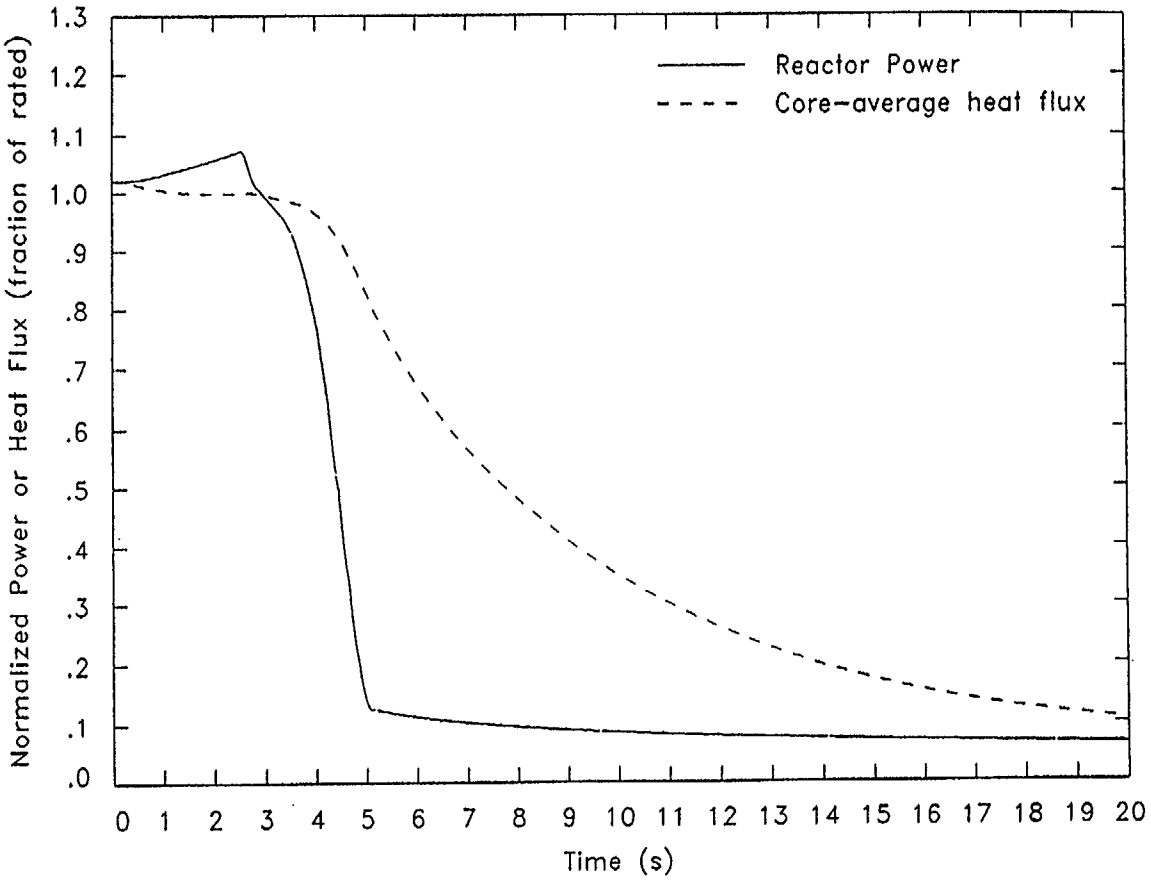

FIGURE 14.1.5.1-7
NORMALIZED POWER AND HEAT FLUX (ASYMMETRIC 3.51 FT² BREAK INSIDE CONTAINMENT WITH LOSS OF OFFSITE POWER)

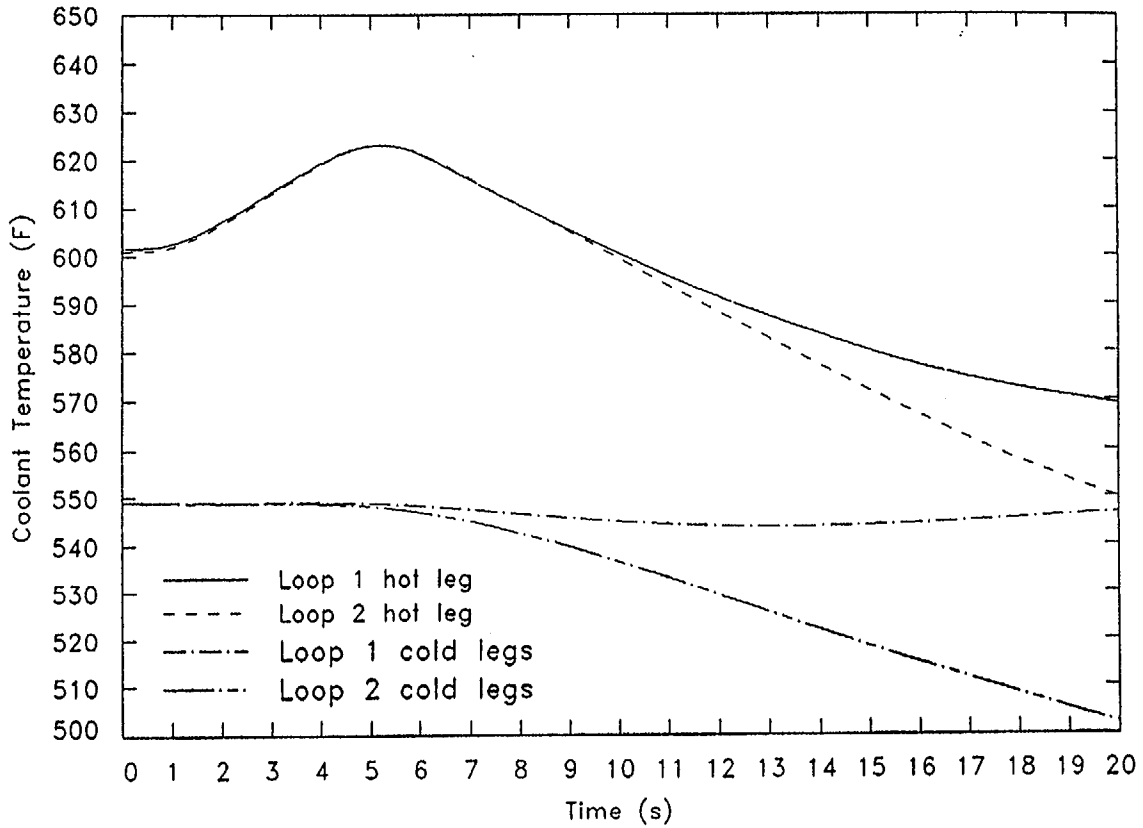

FIGURE 14.1.5.1-8
REACTOR COOLANT TEMPERATURES (ASYMMETRIC 3.51 FT² BREAK INSIDE CONTAINMENT WITH LOSS OF OFFSITE POWER)

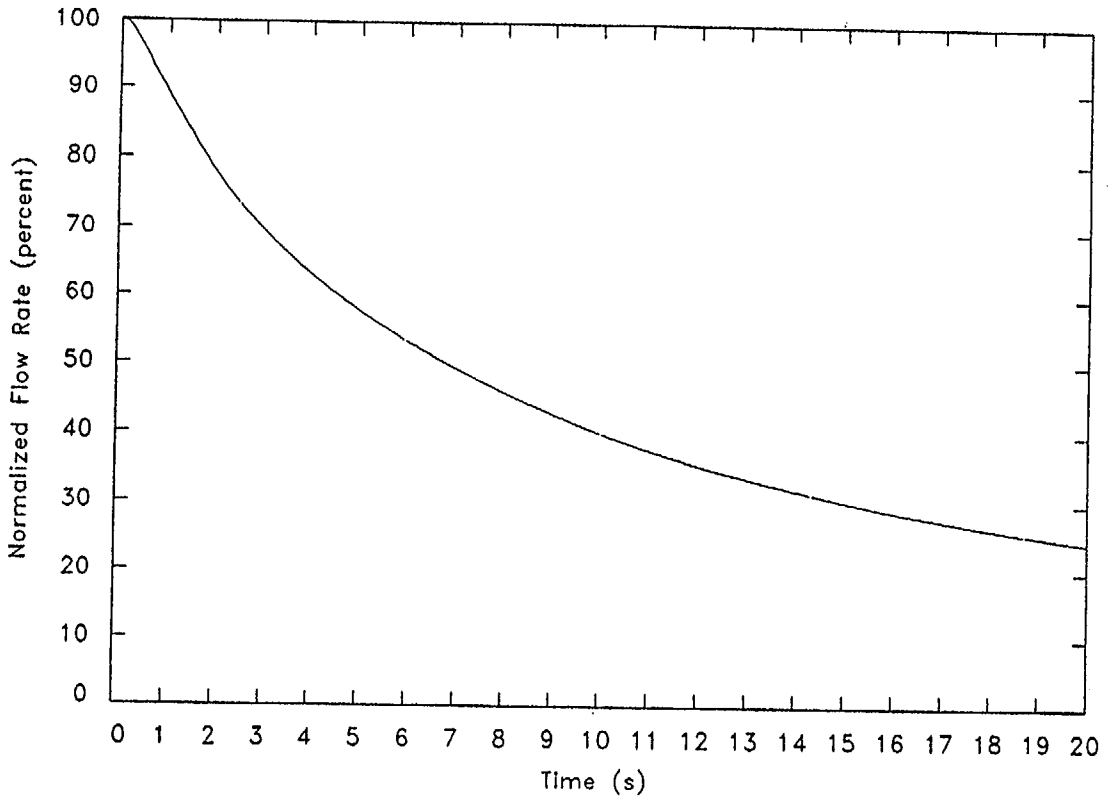

FIGURE 14.1.5.1-9
NORMALIZED REACTOR COOLANT SYSTEM FLOW RATE (ASYMMETRIC 3.51 FT^2 BREAK INSIDE CONTAINMENT WITH LOSS OF OFFSITE POWER)

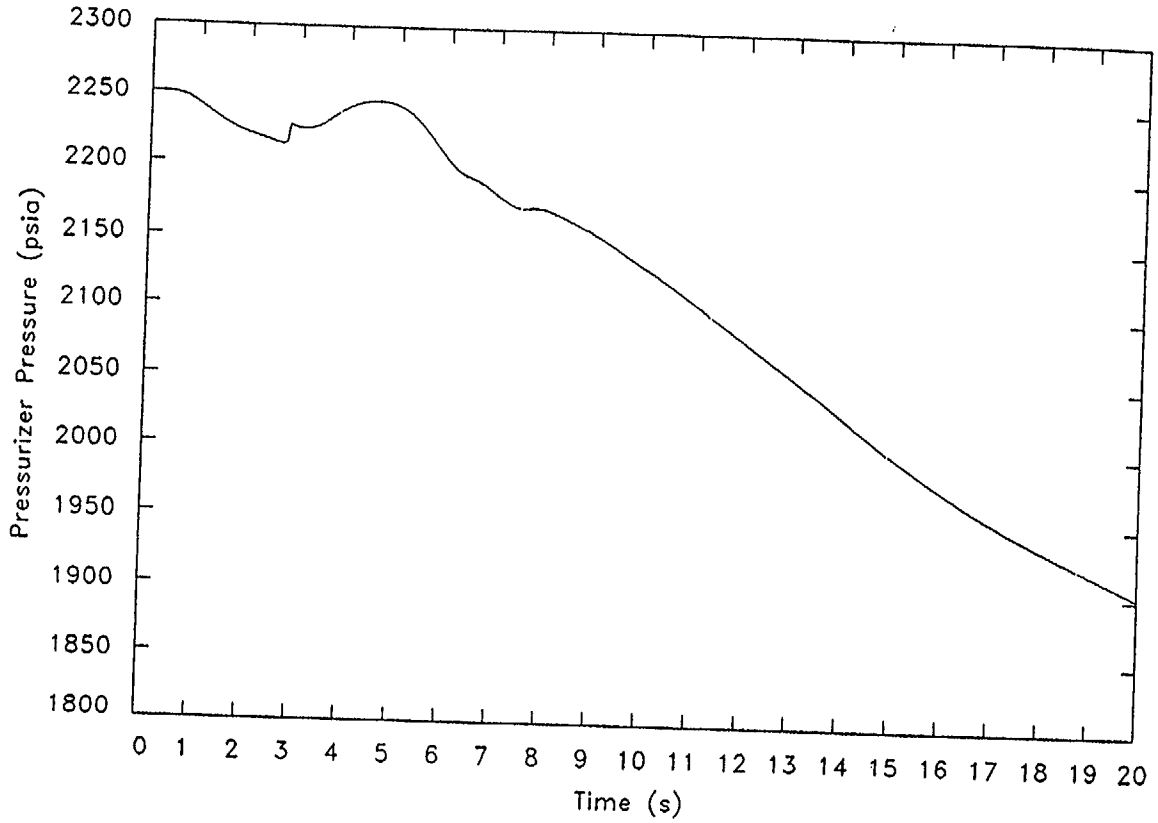

FIGURE 14.1.5.1-10
PRESSURIZER PRESSURE (ASYMMETRIC 3.51 FT^2 BREAK INSIDE CONTAINMENT WITH LOSS OF OFFSITE POWER)

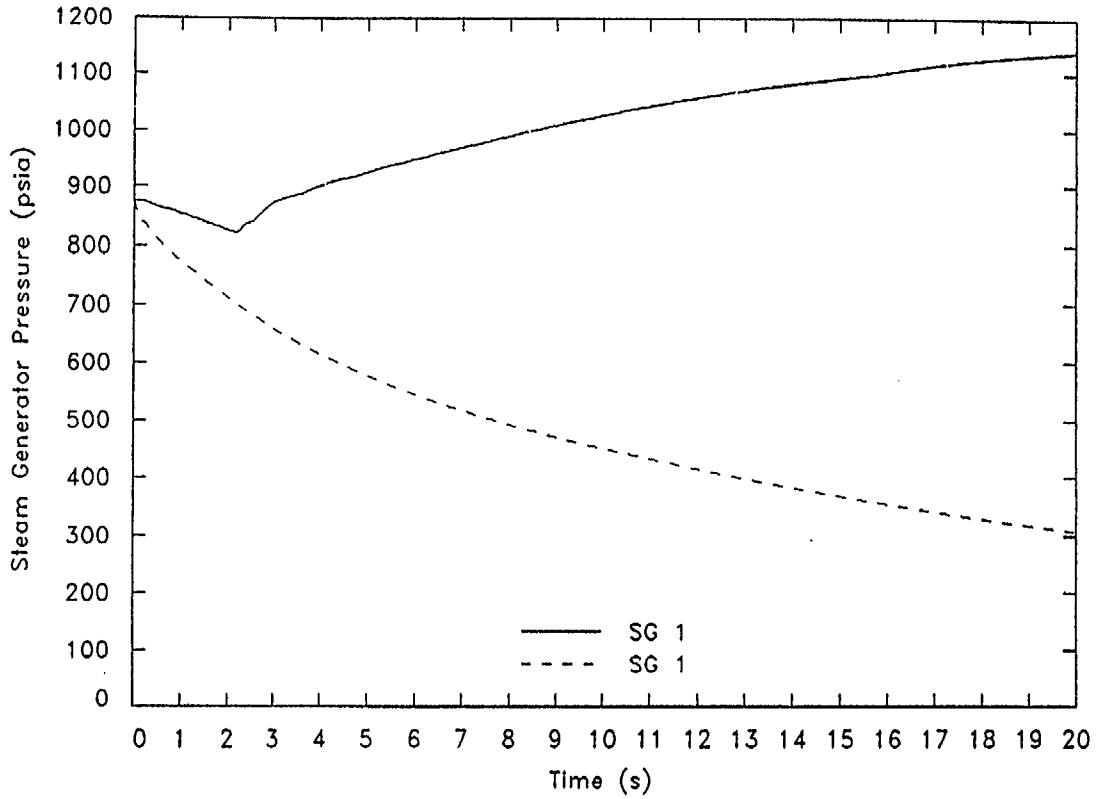

FIGURE 14.1.5.1-11
STEAM GENERATOR PRESSURES (ASYMMETRIC 3.51 FT^2 BREAK INSIDE CONTAINMENT WITH LOSS OF OFFSITE POWER)

MARCH 1999

ATTACHMENT 2
Page 73 of 104

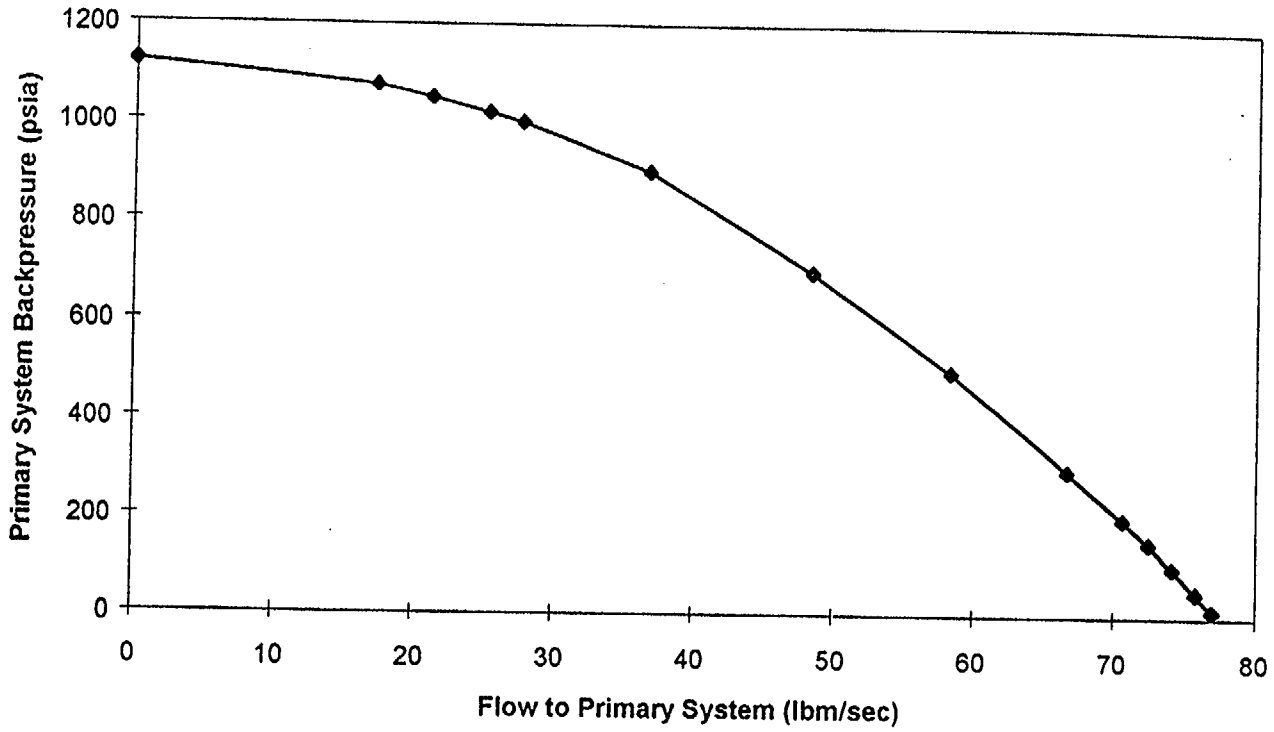

ATTACHMENT 2
Page 74 of 104

FIGURE 14.1.5.2-1
ONE PUMP HIGH PRESSURE SAFETY INJECTION SYSTEM DELIVERY VS. PRIMARY PRESSURE
(POST-SCRAM STEAM LINE BREAK)

MARCH 1999

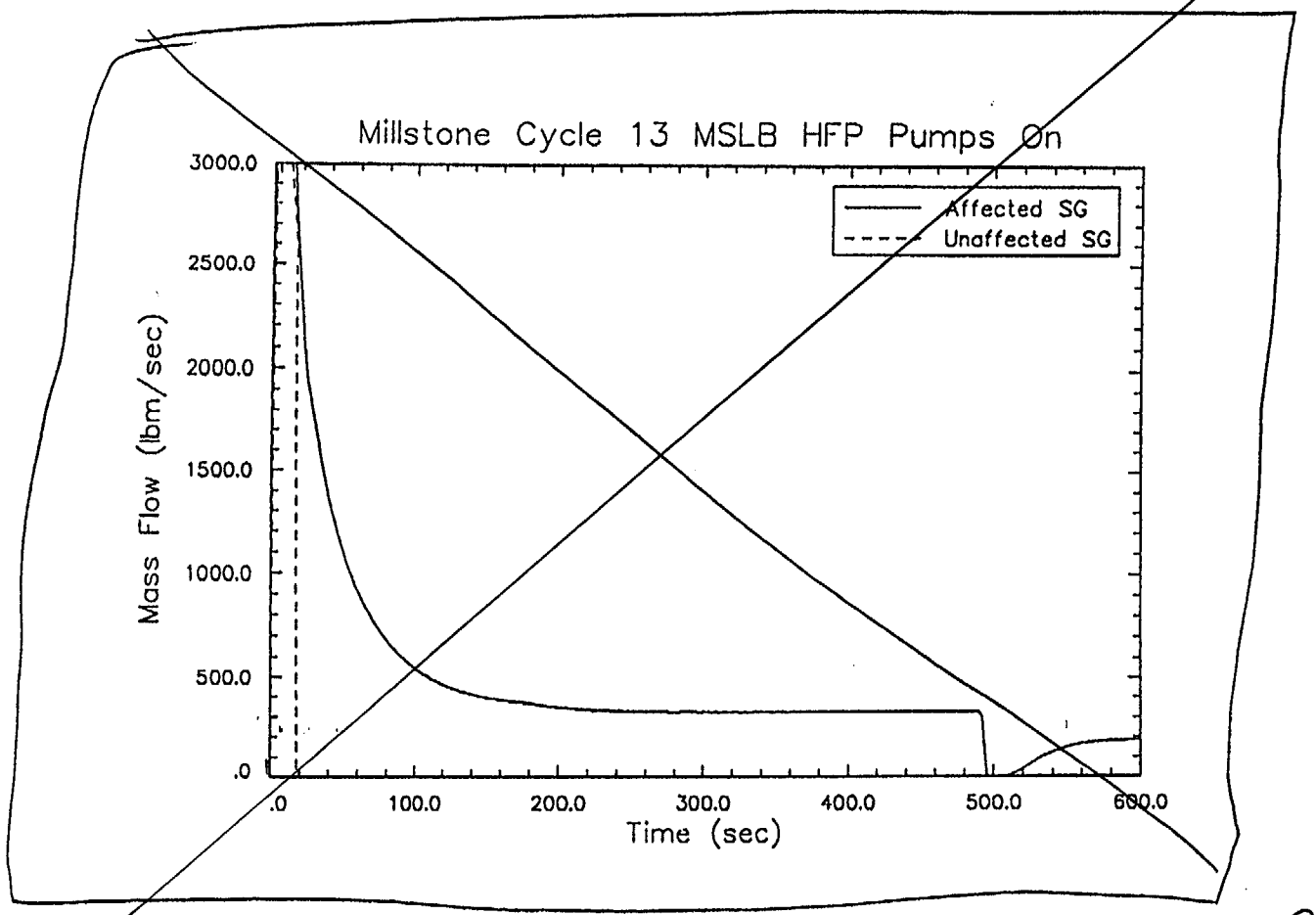

SEE ATTACHMENT (NEXT PAGE)

Replace with Figure 2

FSARCR MP2-00-MP2-23

ATTACHMENT 2
Page 75 of 104

FIGURE 14.1.5.2-2
STEAM GENERATOR BREAK FLOW (HFP POST-SCRAM STEAM LINE OUTSIDE CONTAINMENT BREAK WITH OFFSITE POWER AVAILABLE)

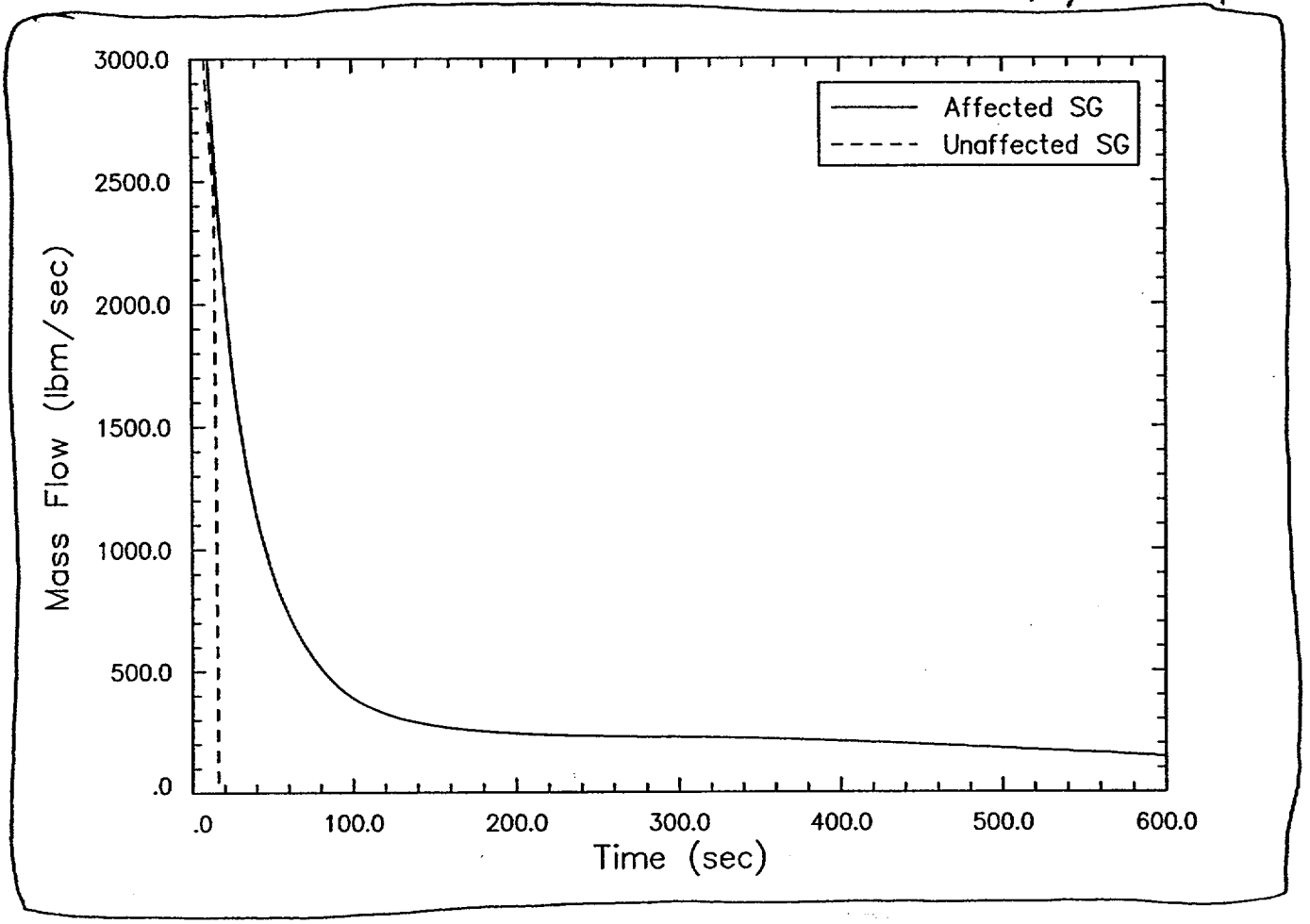

~~Figure 14.1.5.2-2 HZP Offsite Power Available (Break Flows)~~

Figure 2

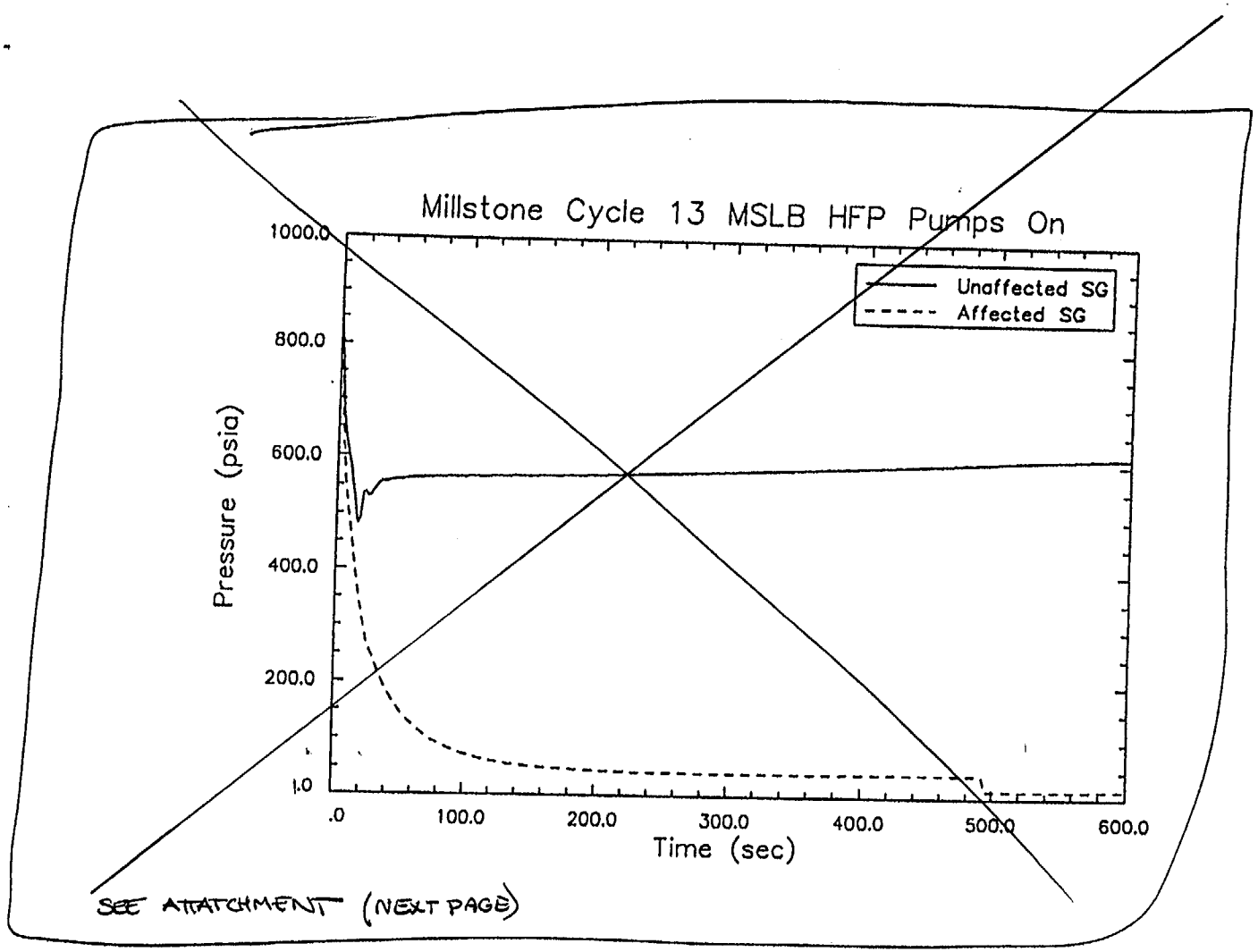

Replace with figure 3

FIGURE 14.1.5.2-3
STEAM GENERATORS' SECONDARY PRESSURES (HFP POST-SCRAM STEAM LINE OUTSIDE CONTAINMENT BREAK WITH OFFSITE POWER AVAILABLE)

MARCH 1999

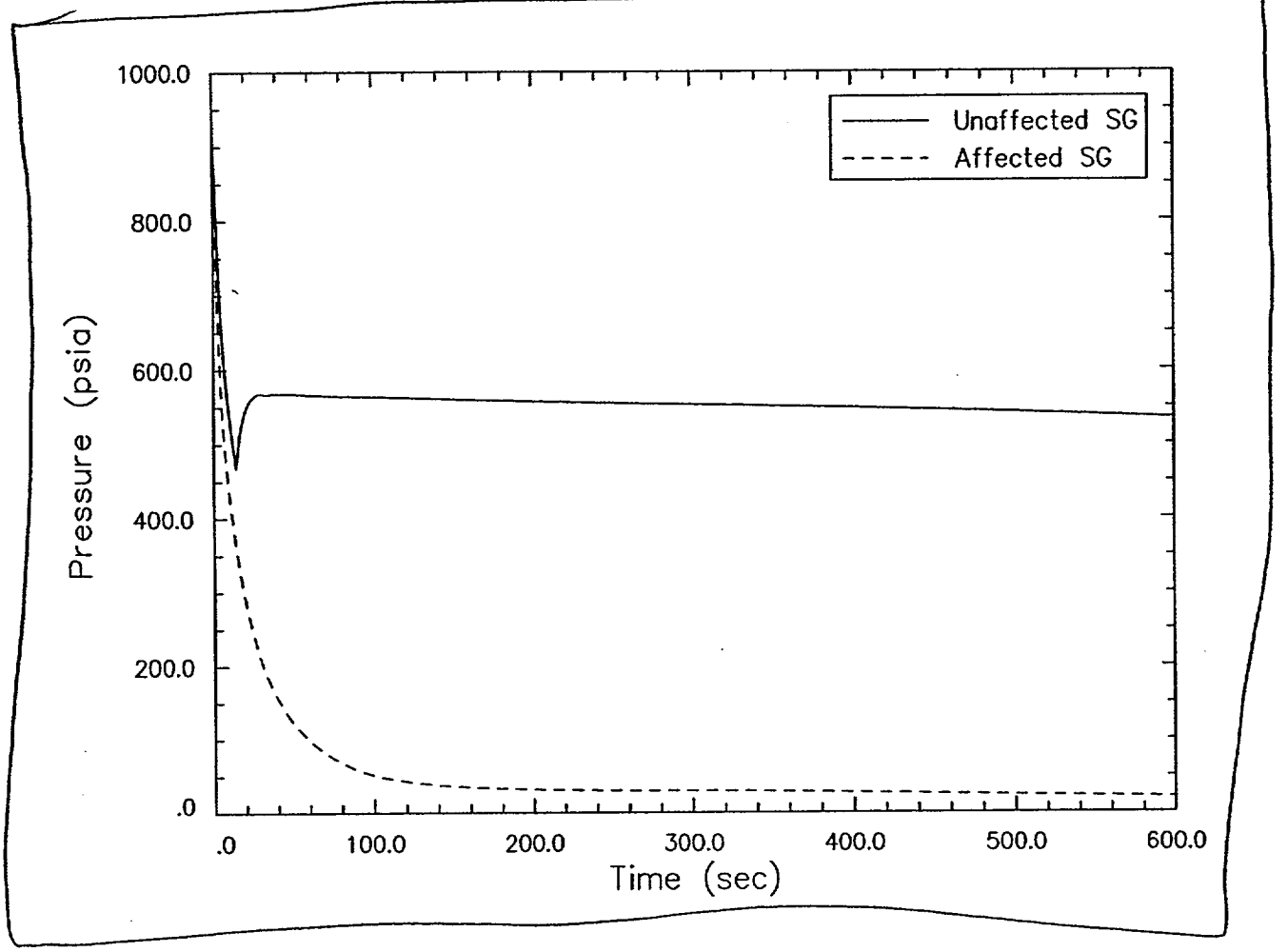

~~Figure 14.1.5.2-3 HZP Offsite Power Available~~
~~(Steam Generators' Secondary Pressures)~~

Figure 3

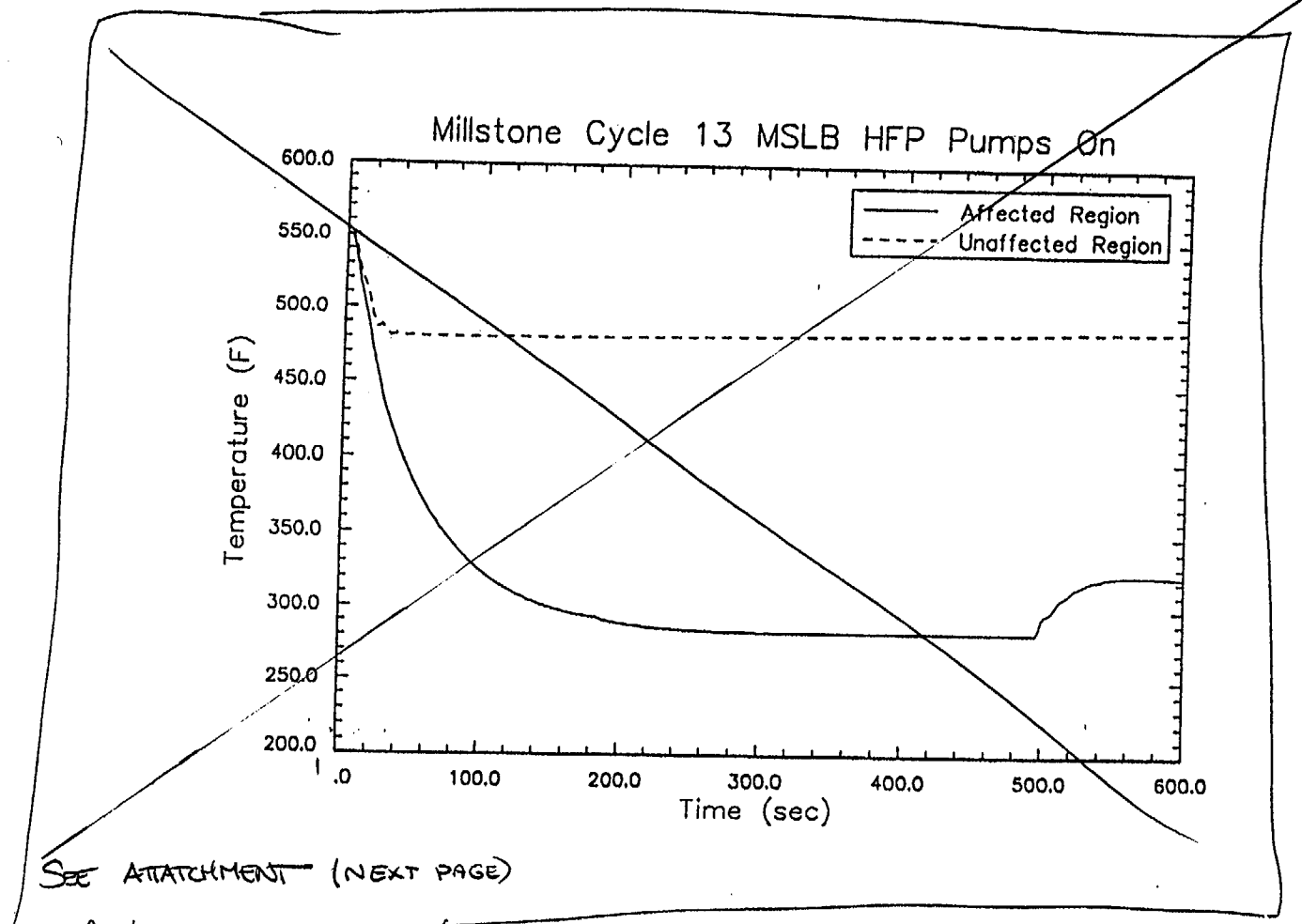

See ATTACHMENT (NEXT PAGE)

Replace with figure 4

FIGURE 14.1.5.2-4
CORE INLET TEMPERATURES (~~HFP~~ 2 POST-SCRAM STEAM LINE OUTSIDE CONTAINMENT BREAK WITH OFFSITE POWER AVAILABLE)

MARCH 1999

FSARCR 00-MP2-23

ATTACHMENT 2
Page 79 of 104

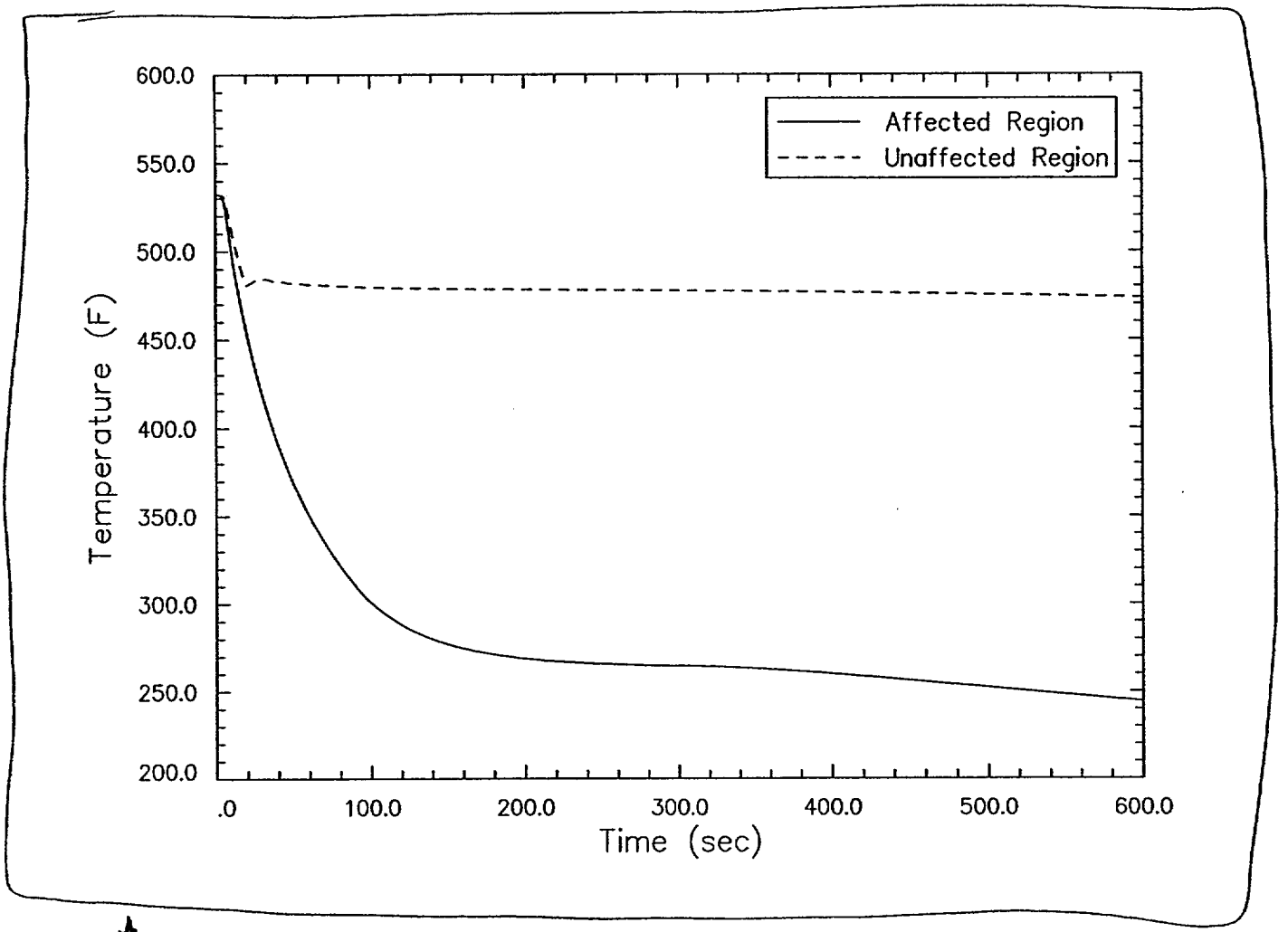

figure 4

~~Figure 14.1.5.2-4 HZP Offsite Power Available (Core Inlet Temperatures)~~

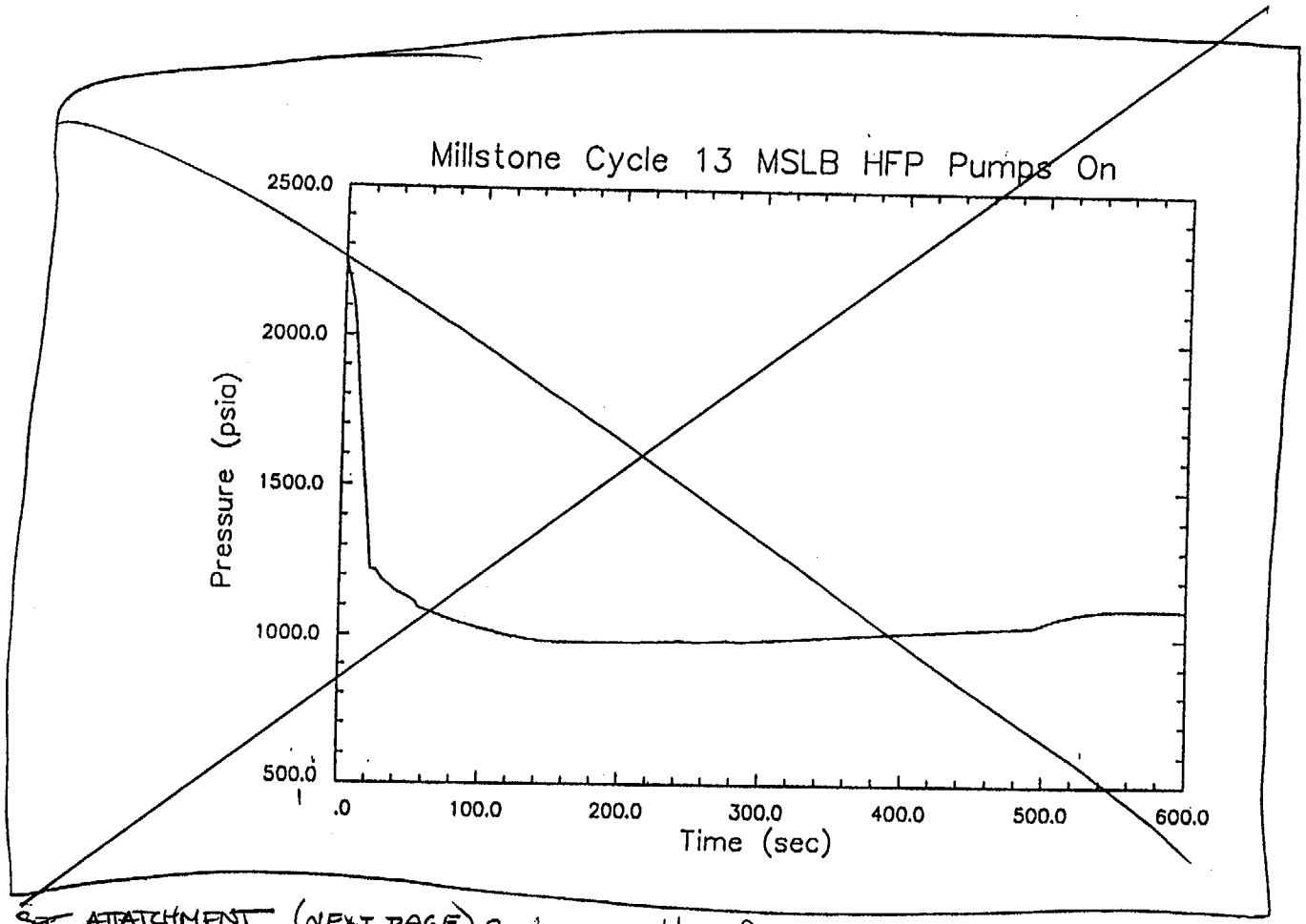

See ATTATCHMENT (NEXT PAGE) Replace with figure 5

FIGURE 14.1.5.2-5
PRESSURIZER PRESSURE (HFP POST-SCRAM STEAM LINE OUTSIDE CONTAINMENT BREAK WITH OFFSITE POWER AVAILABLE)

MARCH 1999

FSARCR 00-MP2-23

ATTACHMENT 2
Page 81 of 104

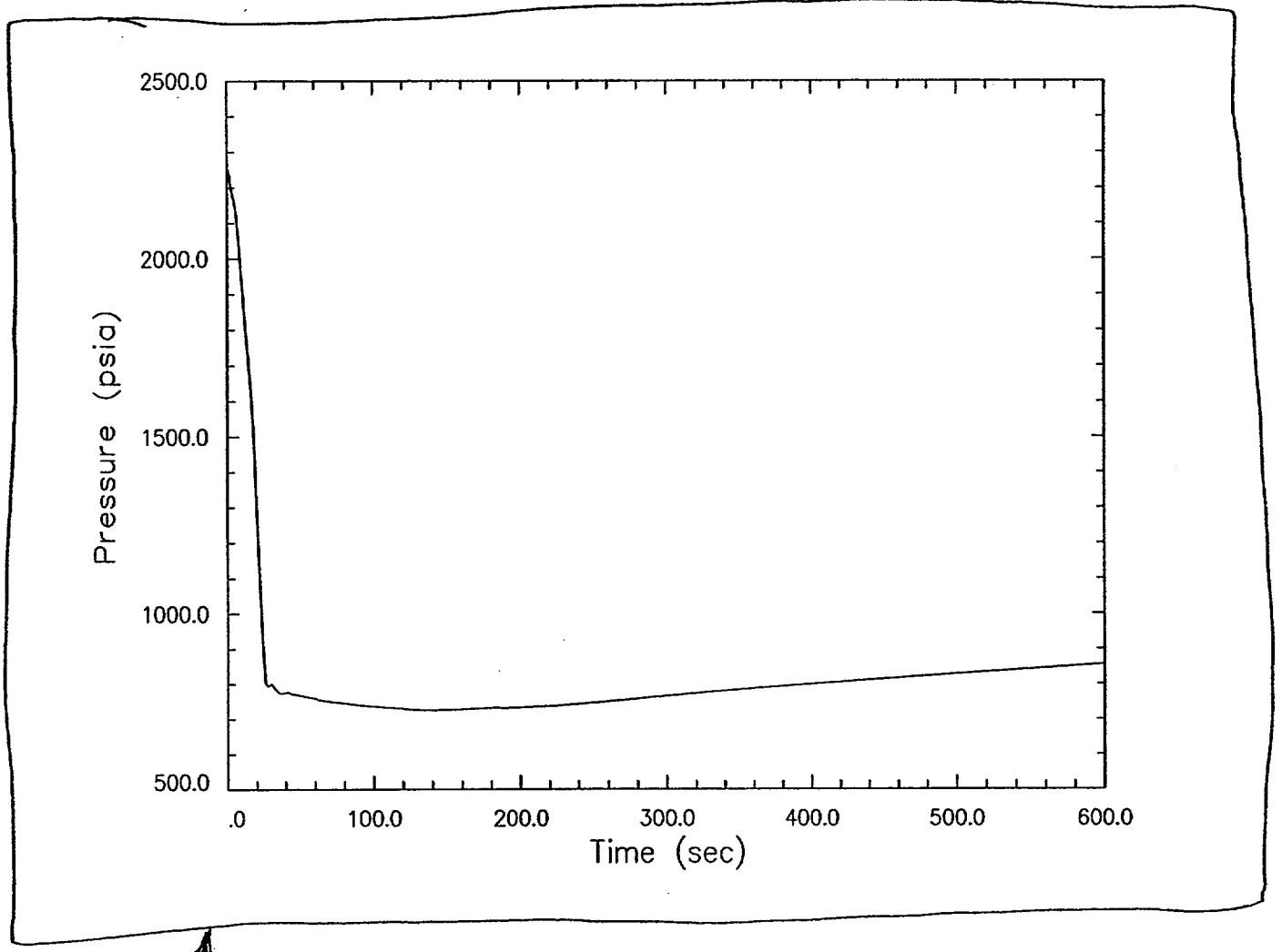

figure 5

~~**Figure 14.1.5.2-5 HZP Offsite Power Available (Pressurizer Pressure)**~~

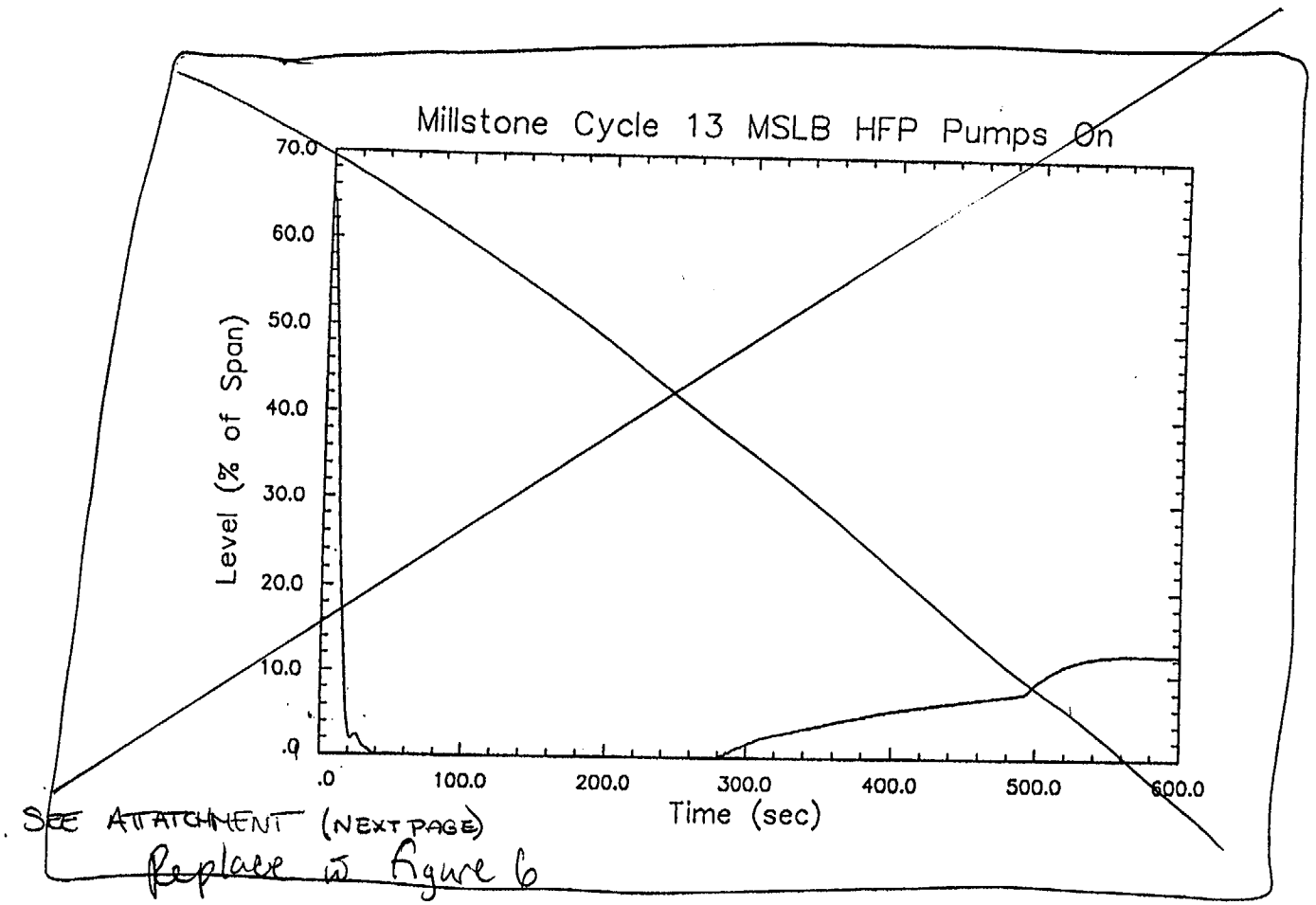

SEE ATTATCHMENT (NEXT PAGE)
Replace w figure 6

FSAR CR 00-MP2-23

ATTACHMENT 2
Page 83 of 104

FIGURE 14.1.5.2-6
PRESSURIZER LEVEL (HFP POST-SCRAM STEAM LINE OUTSIDE CONTAINMENT BREAK WITH OFFSITE POWER AVAILABLE)

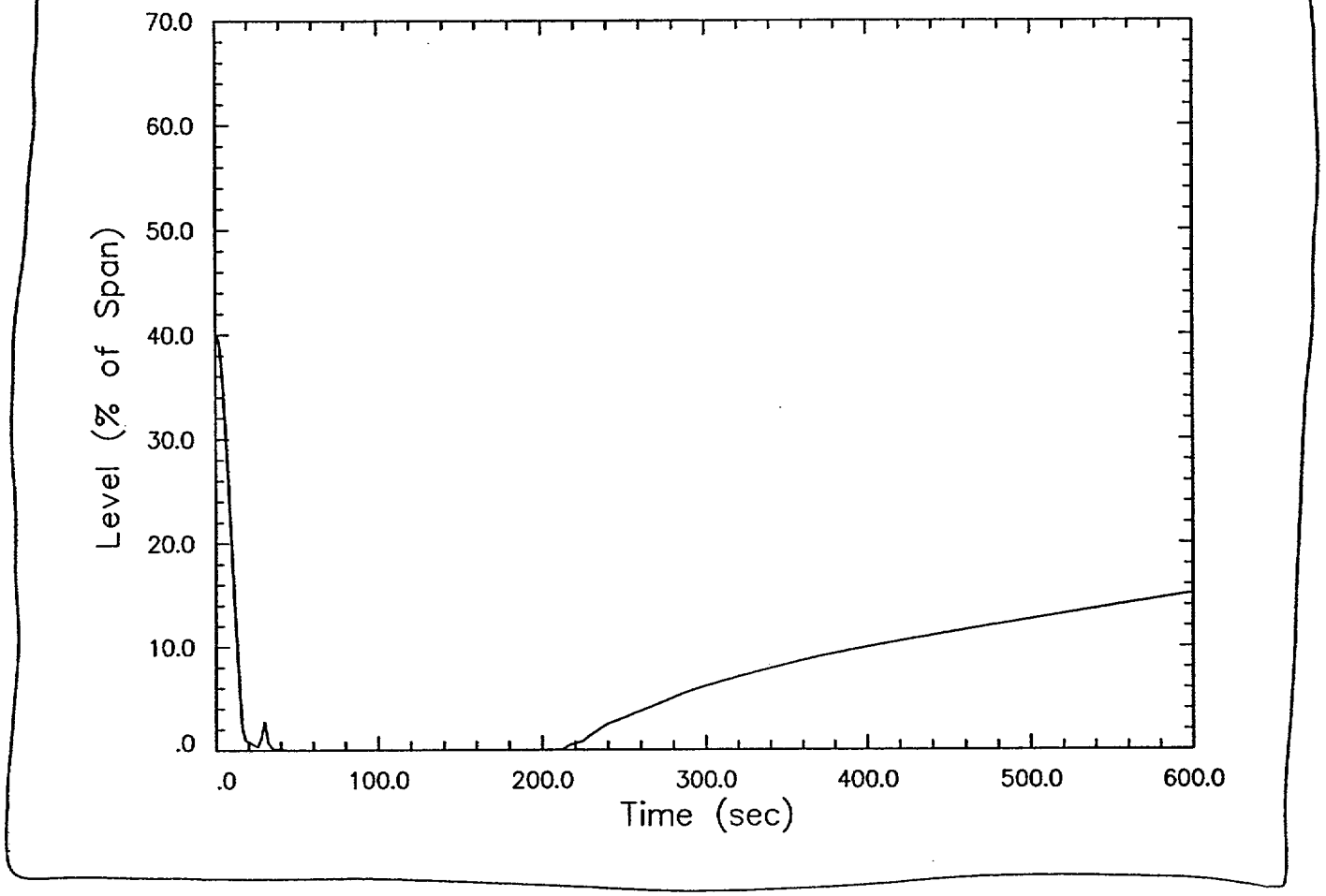

1
Figure 6

~~Figure 14.1.5.2-6 HZP Offsite Power Available (Pressurizer Level)~~

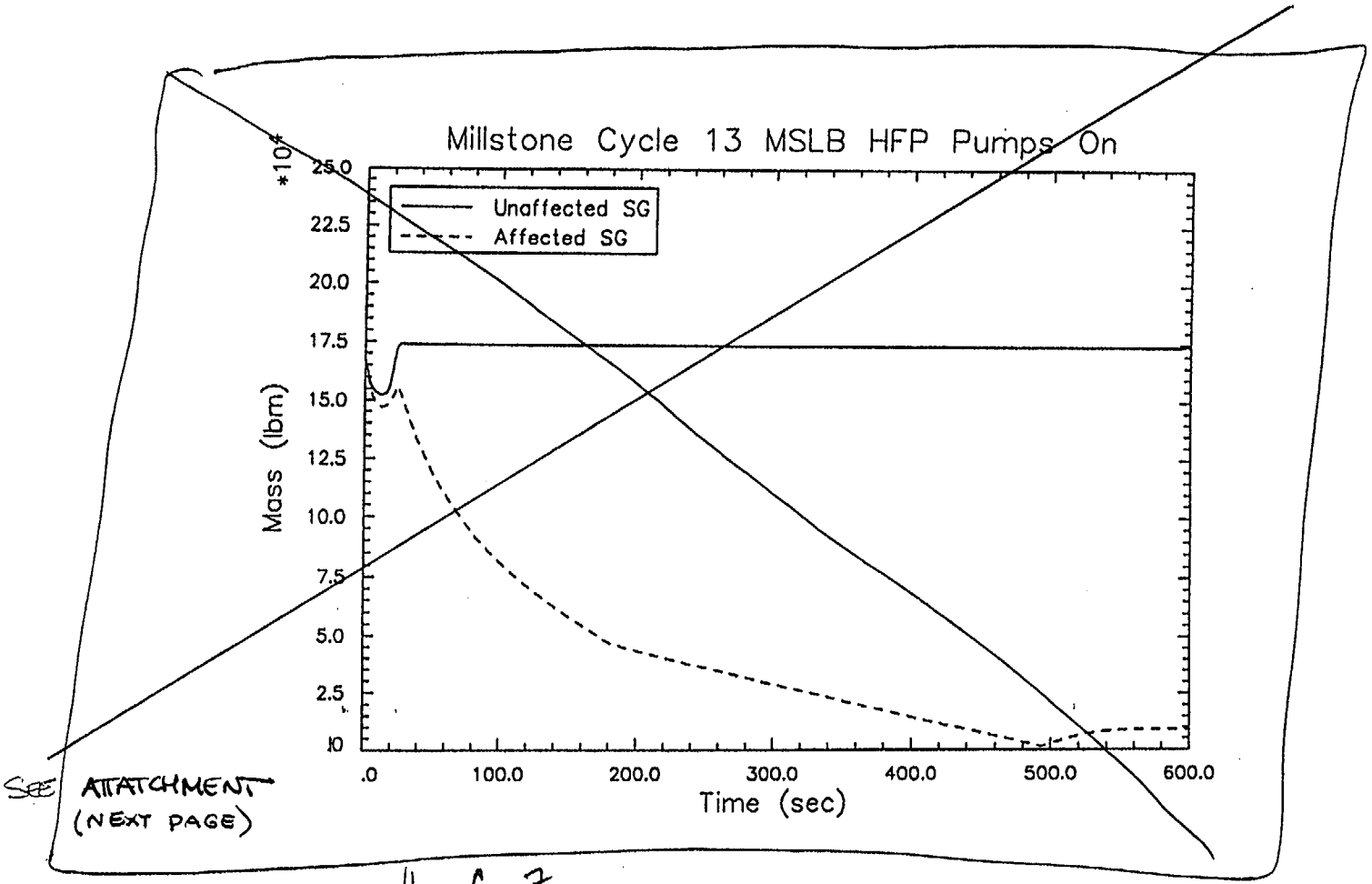

SEE ATTATCHMENT (NEXT PAGE)

Replace with fig 7

HZP

FIGURE 14.1.5.2-7

STEAM GENERATORS' SECONDARY MASS (~~HFP~~ POST-SCRAM STEAM LINE OUTSIDE CONTAINMENT BREAK WITH OFFSITE POWER AVAILABLE)

MARCH 1999

FSARCR 00-MP2-23

ATTACHMENT 2
Page 85 of 104

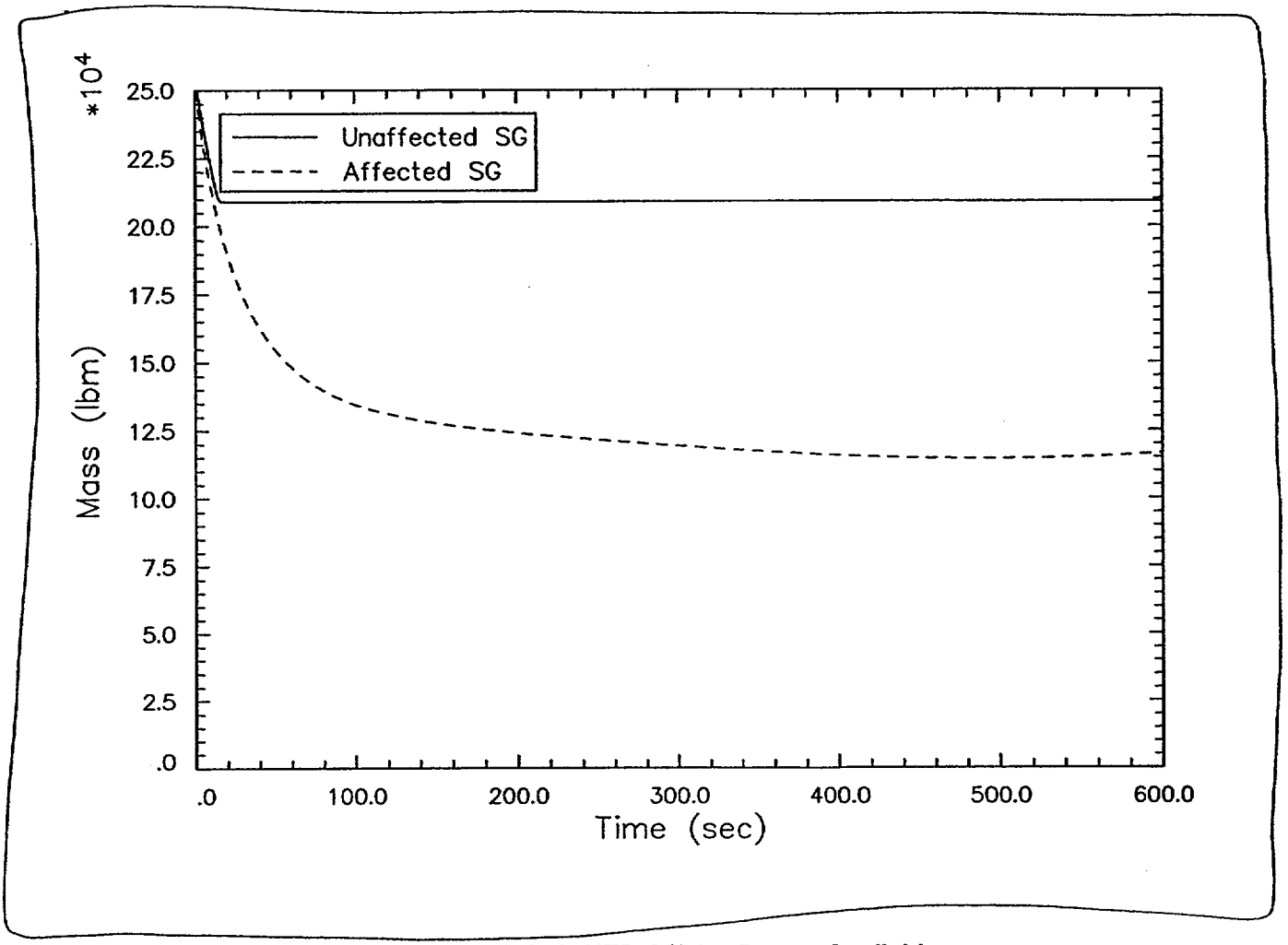

~~Figure 14.1.5.2-7 HZP Offsite Power Available (Steam Generators' Secondary Mass)~~

Figure 7

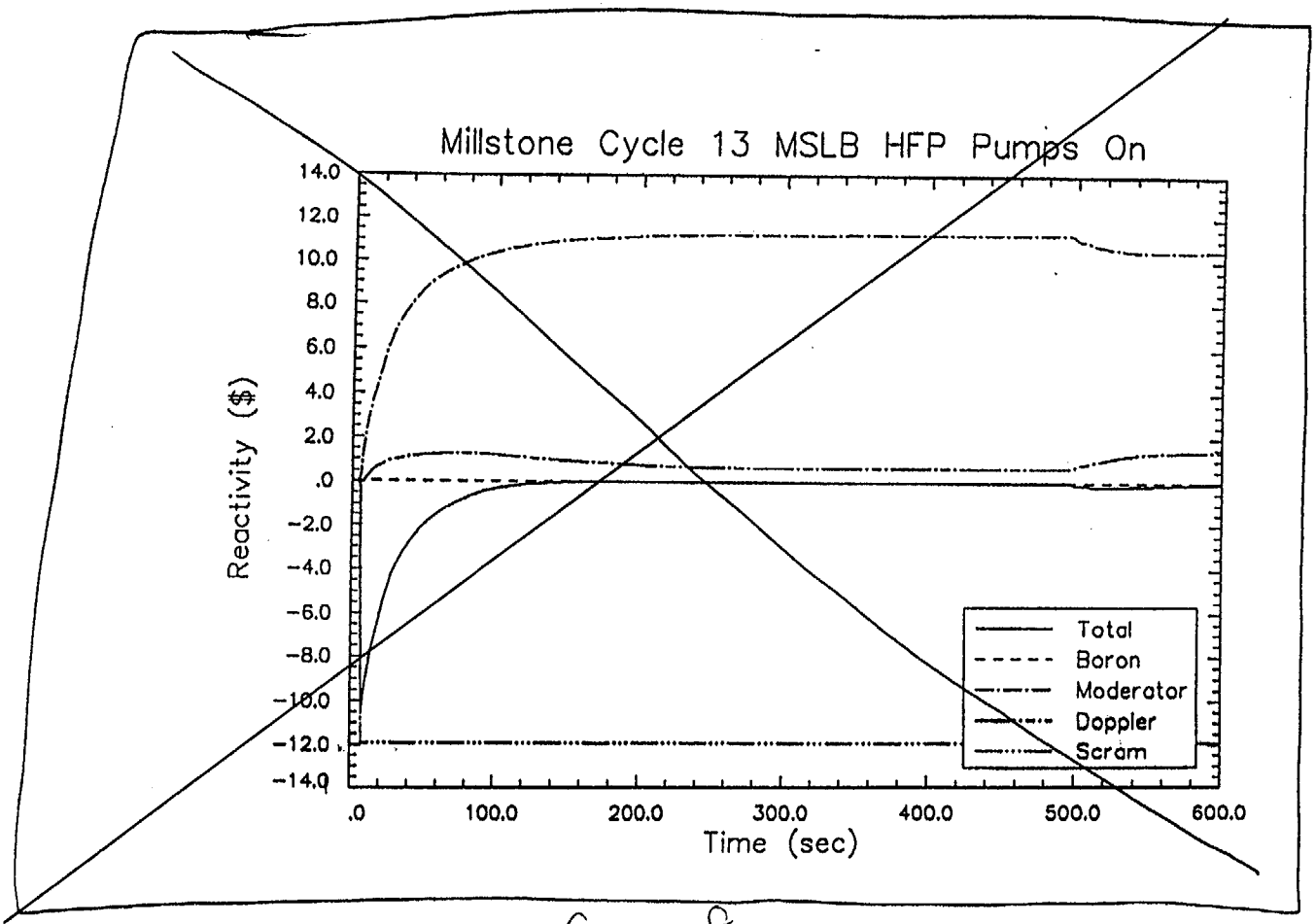

SEE ATTATCHMENT (NEXT PAGE)

Replace w figure 8

FIGURE 14.1.5.2-8

REACTIVITY COMPONENTS (~~HFP~~ HZP POST-SCRAM STEAM LINE OUTSIDE CONTAINMENT BREAK WITH OFFSITE POWER AVAILABLE)

MARCH 1999

FSARCR 00-MP2-23

ATTACHMENT 2
Page 87 of 104

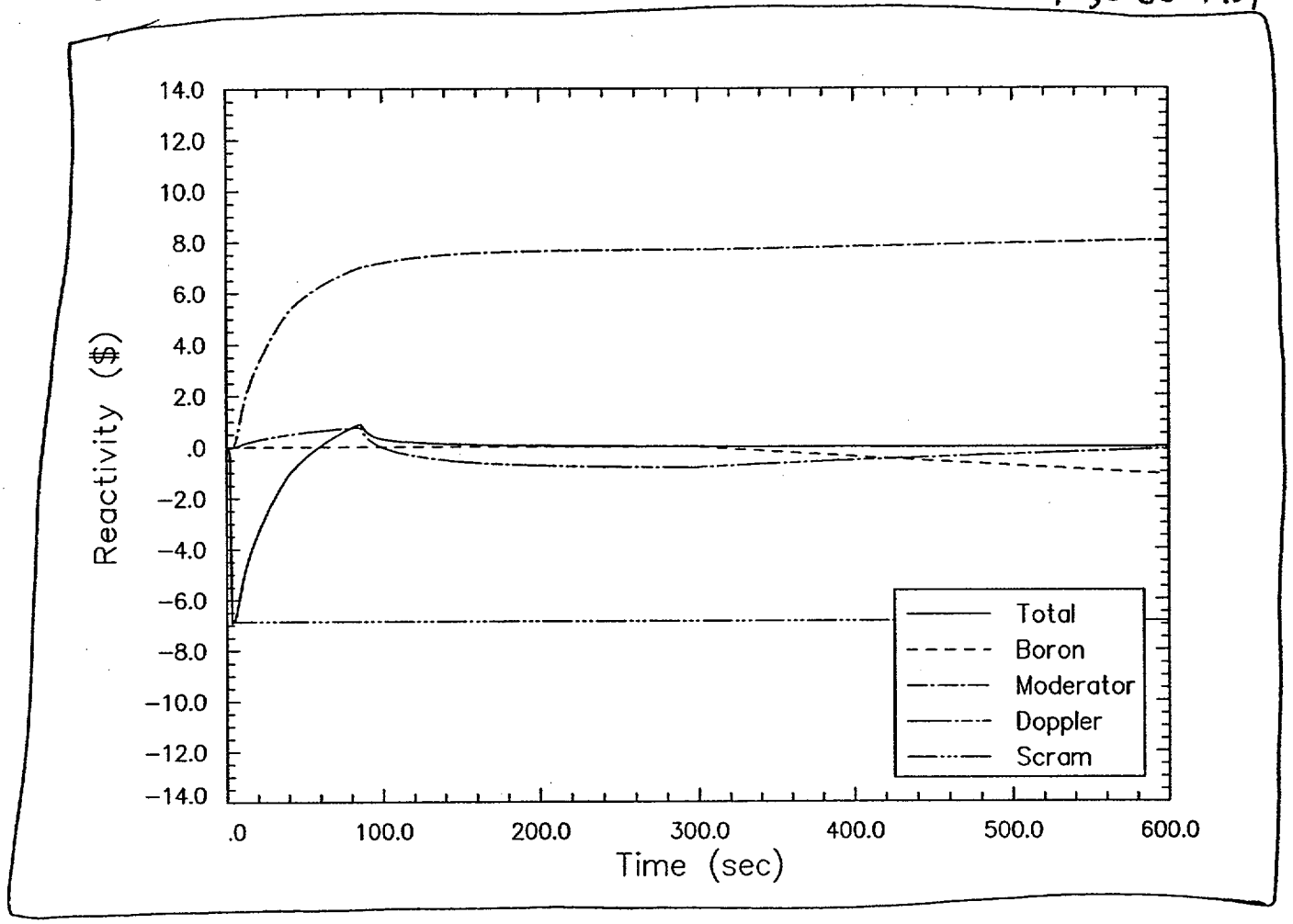

figure 8

~~Figure 14.1.5.2-8 HZP Offsite Power Available (Reactivity Components)~~

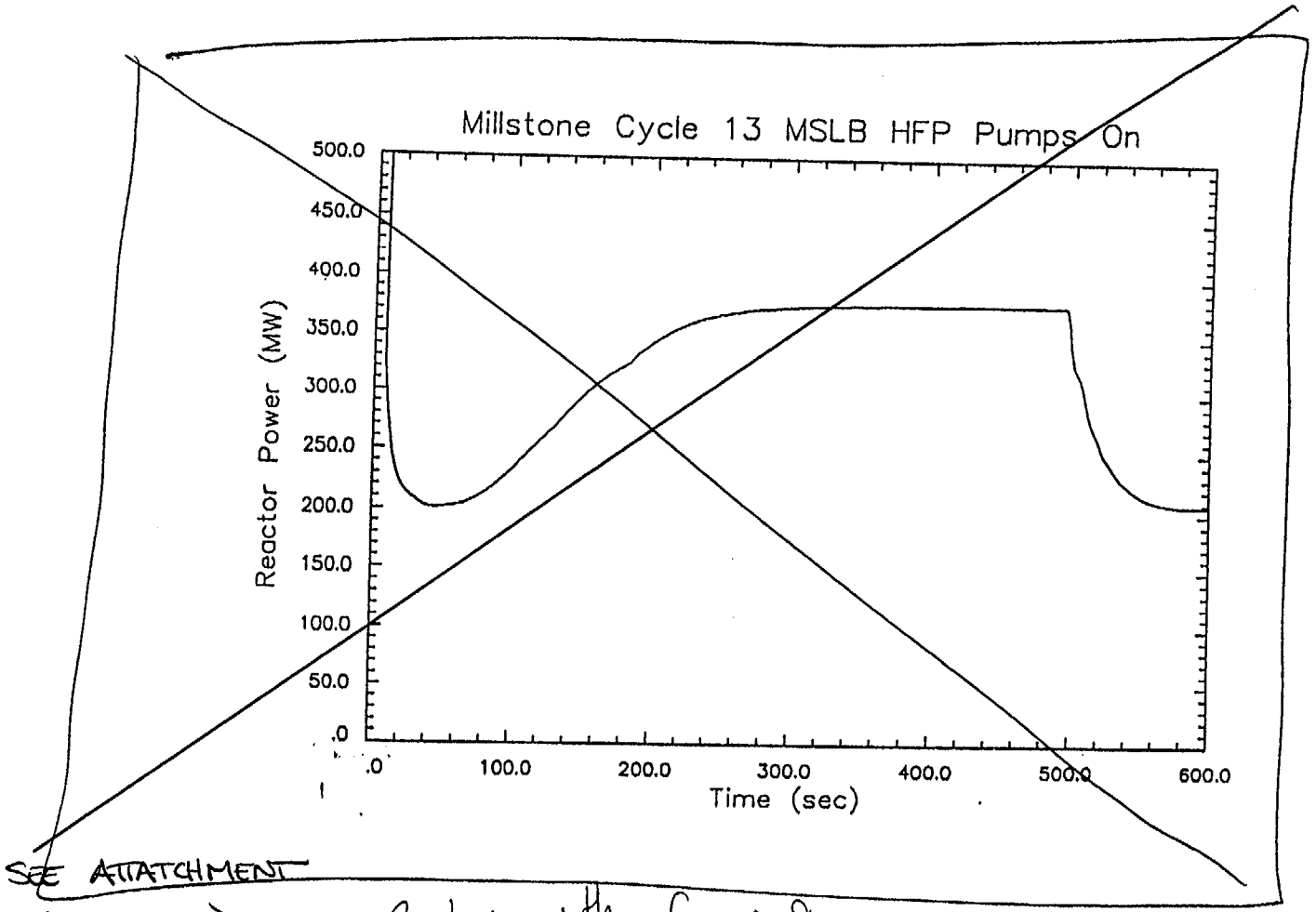

SEE ATTACHMENT (NEXT PAGE)

Replace with figure 9

HZP FIGURE 14.1.5.2-9
REACTOR POWER (~~HFP~~ POST-SCRAM STEAM LINE OUTSIDE CONTAINMENT BREAK WITH OFFSITE POWER AVAILABLE)

MARCH 1999

FSAR CR 00-MP2-23

ATTACHMENT 2
Page 89 of 104

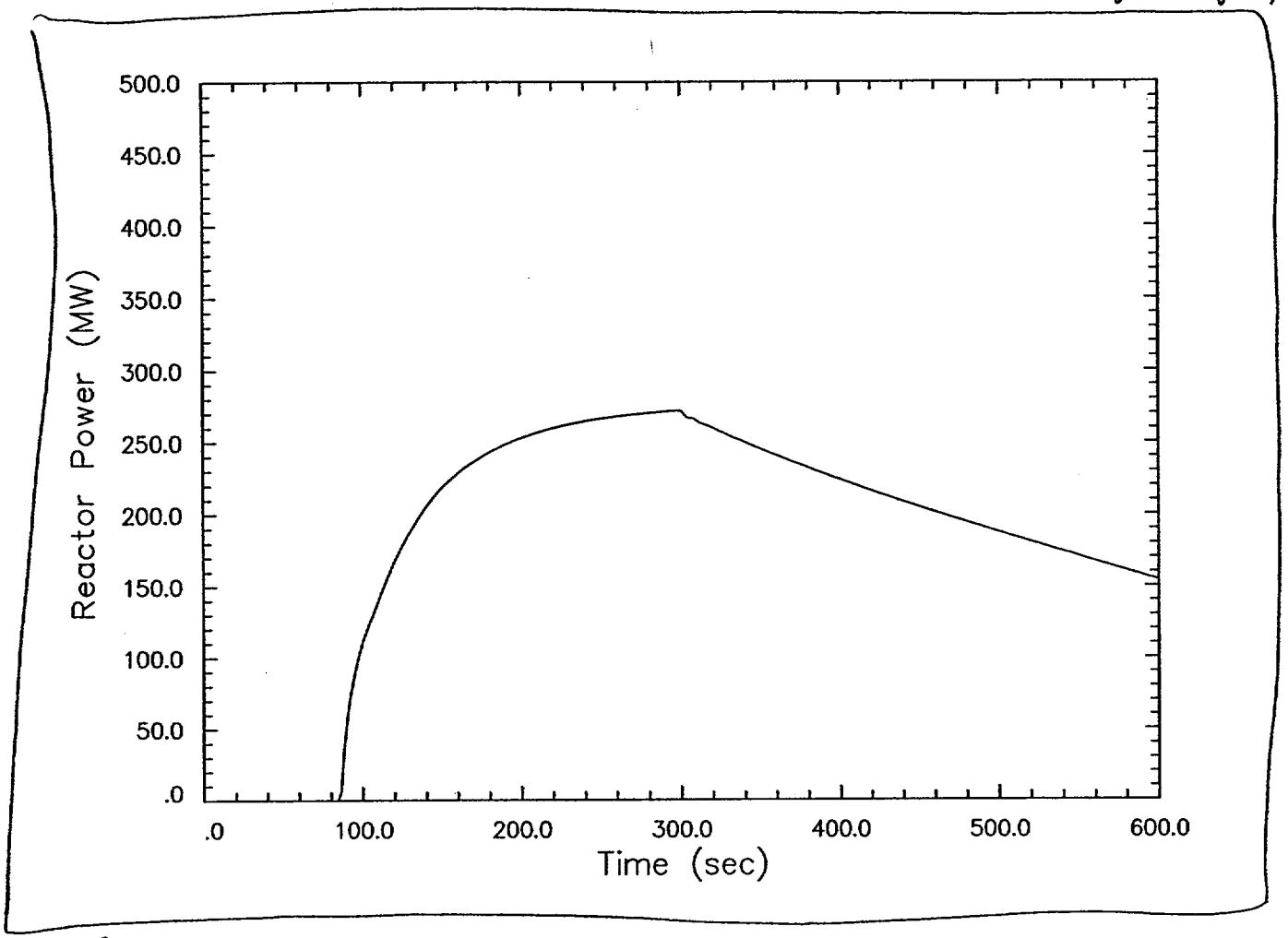

~~**Figure 14.1.5.2-9 HZP Offsite Power Available (Reactor Power)**~~

Figure 9

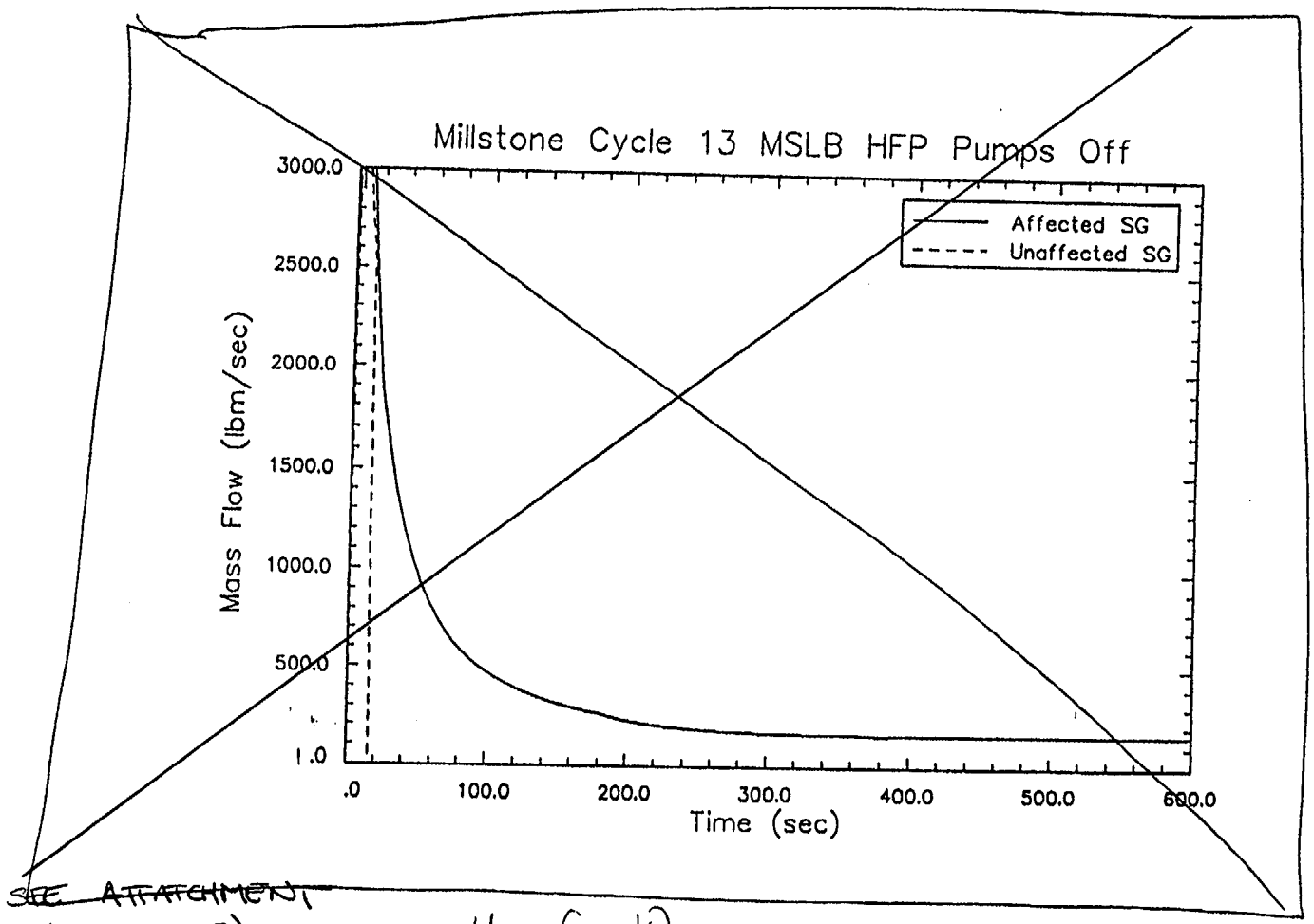

~~SEE ATTACHMENT~~ (NEXT PAGE) Replace with fig 10

HZP FIGURE 14.1.5.2-10
STEAM GENERATOR BREAK FLOW (~~HFP~~ POST-SCRAM STEAM LINE OUTSIDE CONTAINMENT BREAK WITH LOSS OF OFFSITE POWER)

FSARCR 00-MP2-23
ATTACHMENT 2
Page 91 of 104

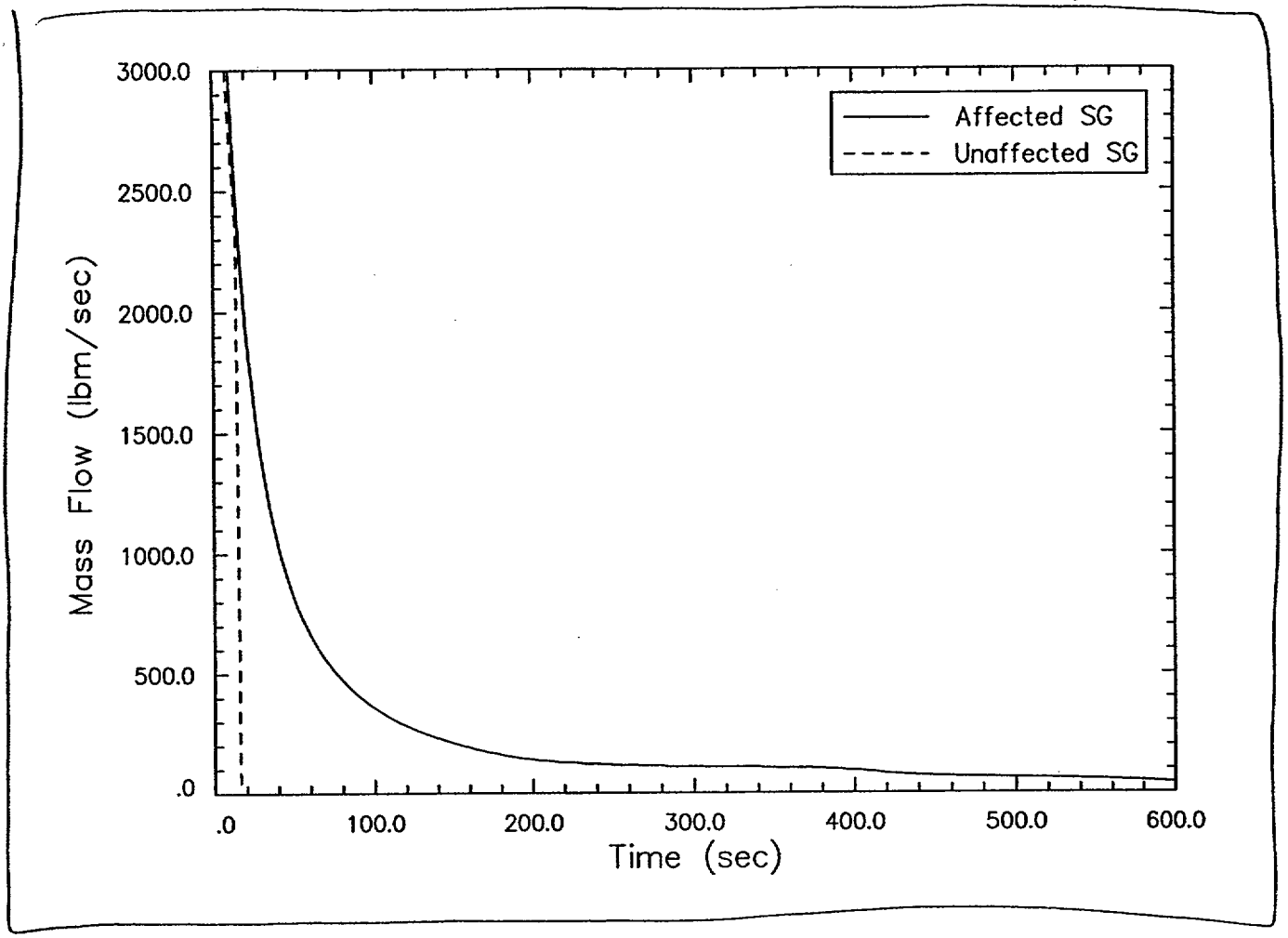

~~Figure 14.1.5.2-10 HZP Loss of Offsite Power (Break Flows)~~

Figure 10

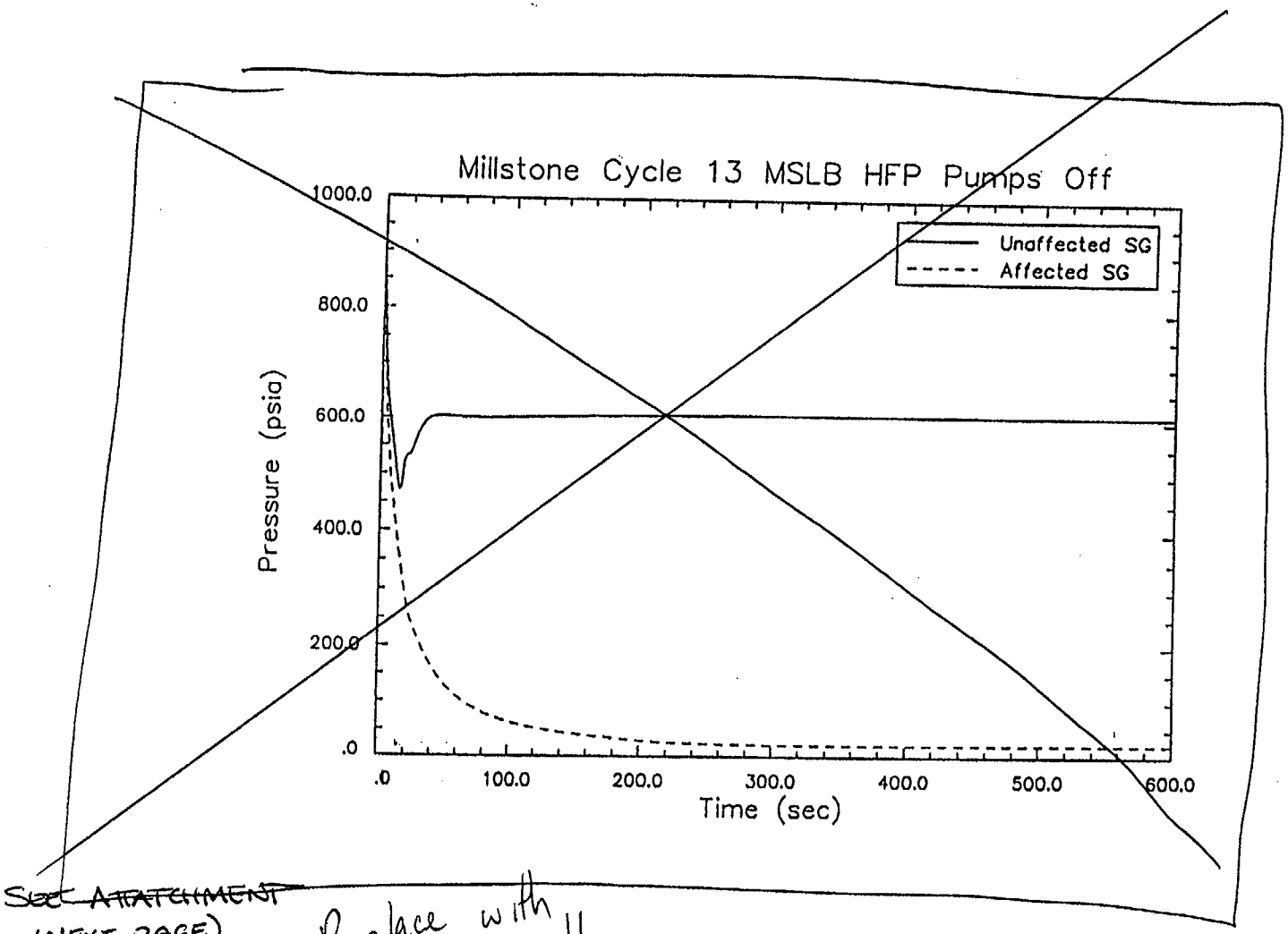

See ~~ATTATCHMENT~~ (NEXT PAGE)

Replace with Figure 11

FSARCR 00-MP2-23

ATTACHMENT 2
Page 93 of 104

FIGURE 14.1.5.2-11 HZP

STEAM GENERATORS' SECONDARY PRESSURES (~~HFP~~ POST-SCRAM STEAM LINE OUTSIDE CONTAINMENT BREAK WITH LOSS OF OFFSITE POWER)

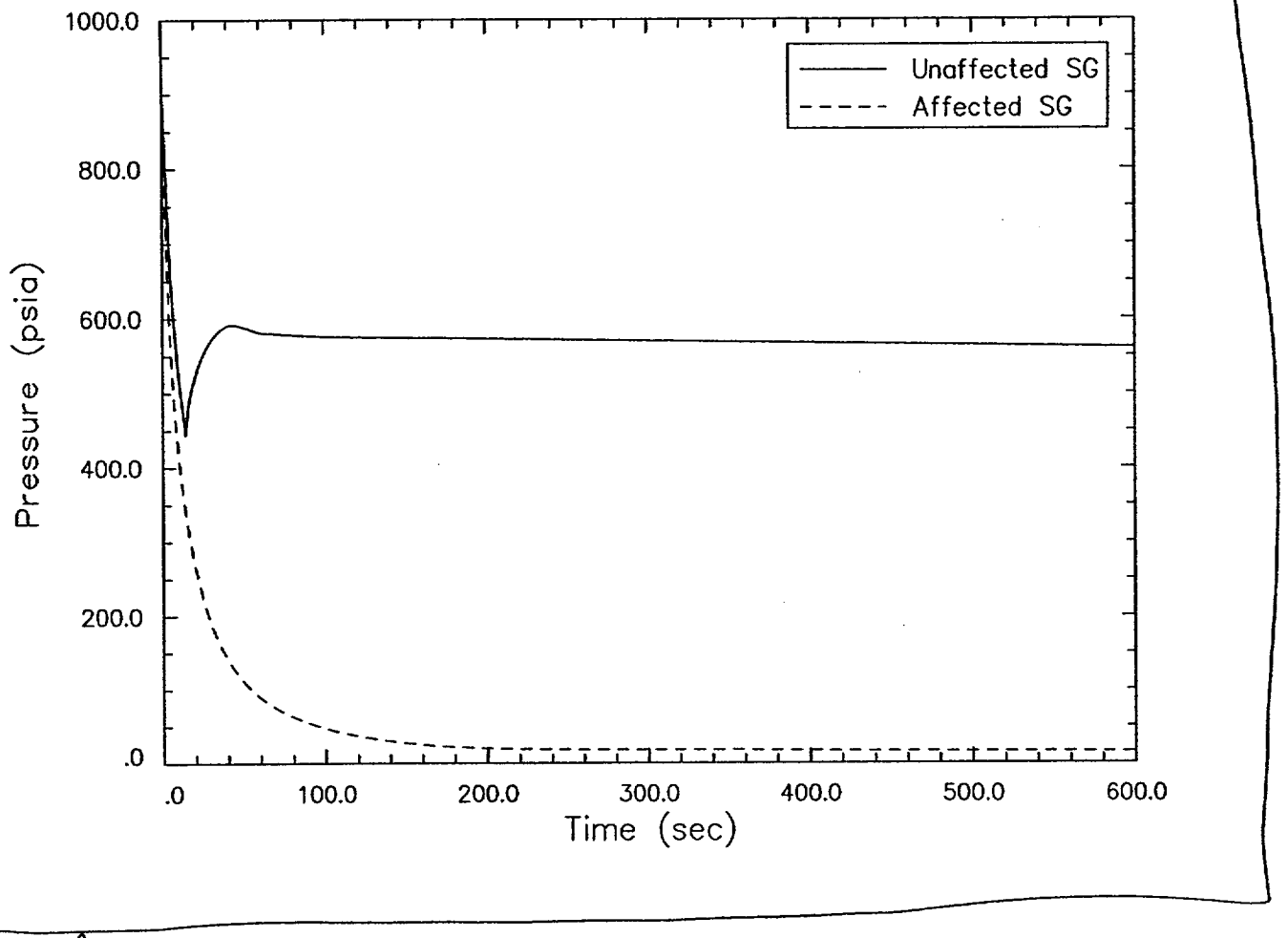

~~**Figure 14.1.5.2-11 HZP Loss of Offsite Power (Steam Generators' Secondary Pressures)**~~

Figure 11

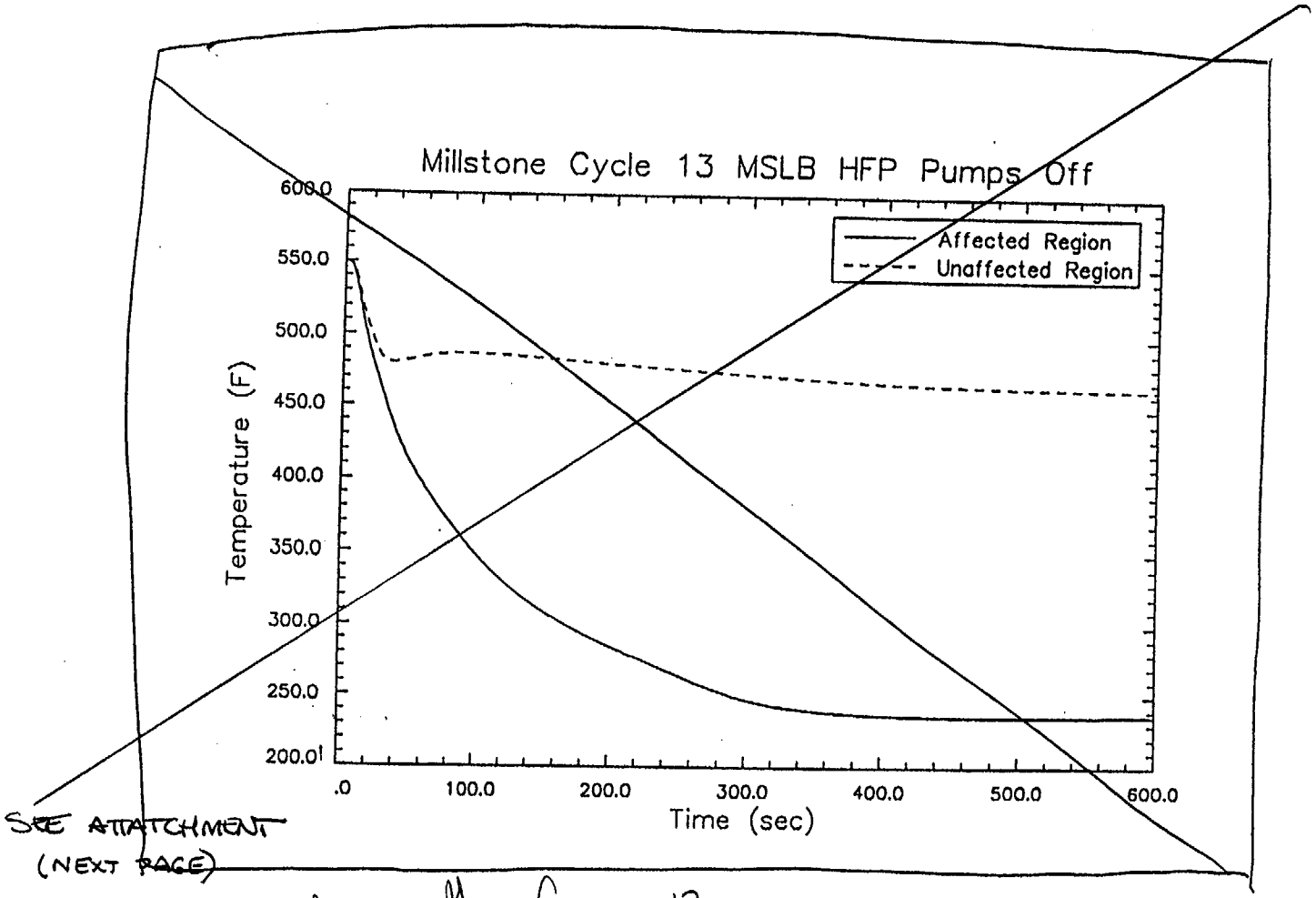

SEE ATTACHMENT (NEXT PAGE)

Replace with figure 12

HZP FIGURE 14.1.5.2-12
CORE INLET TEMPERATURES (~~HFP~~ POST-SCRAM STEAM LINE OUTSIDE CONTAINMENT BREAK WITH LOSS OF OFFSITE POWER)

MARCH 1999

FSAR CR 00-MP2-23

ATTACHMENT 2
Page 95 of 104

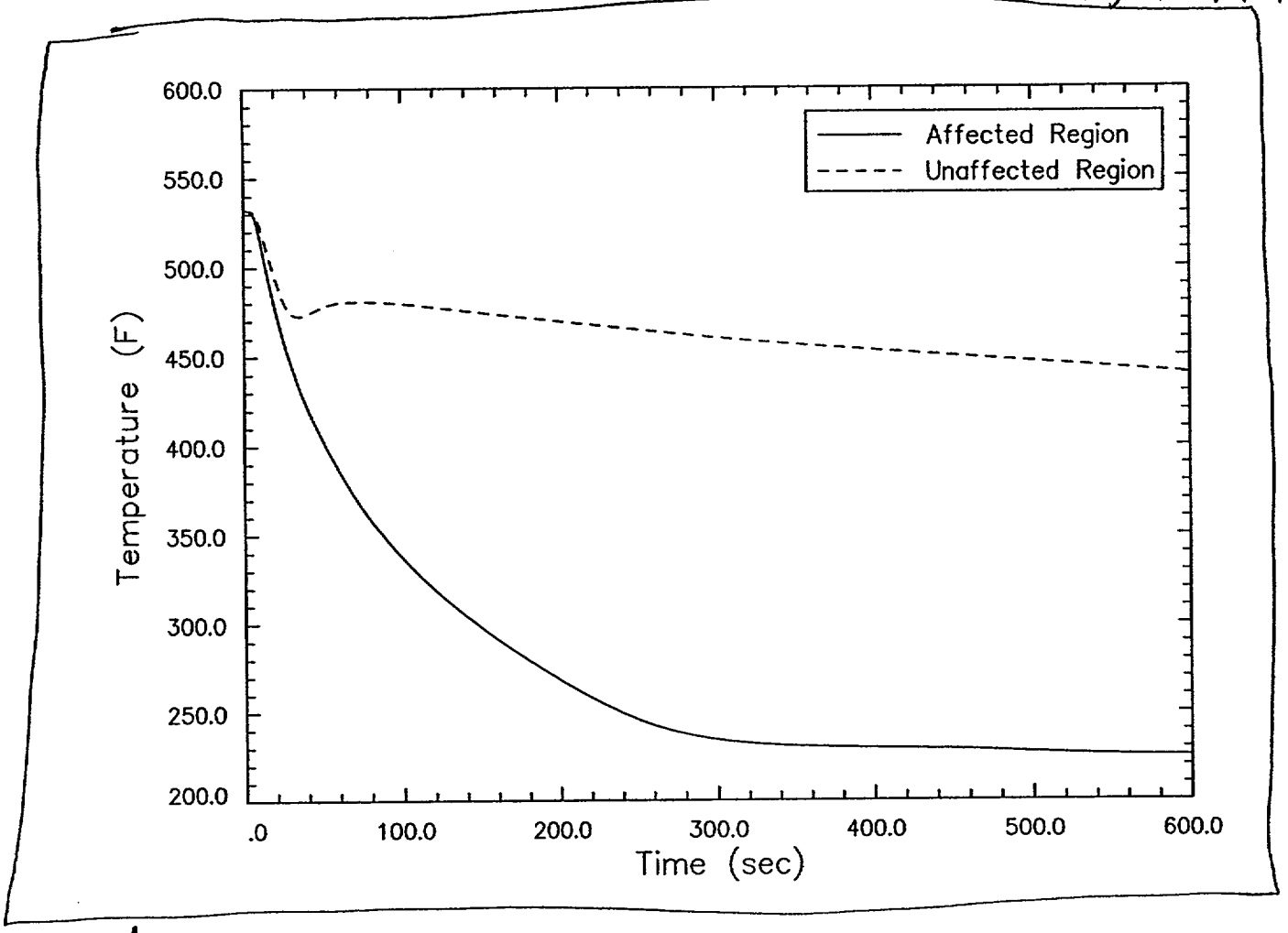

~~Figure 14.1.5.2-12 HZP Loss of Offsite Power (Core Inlet Temperatures)~~

Figure 12

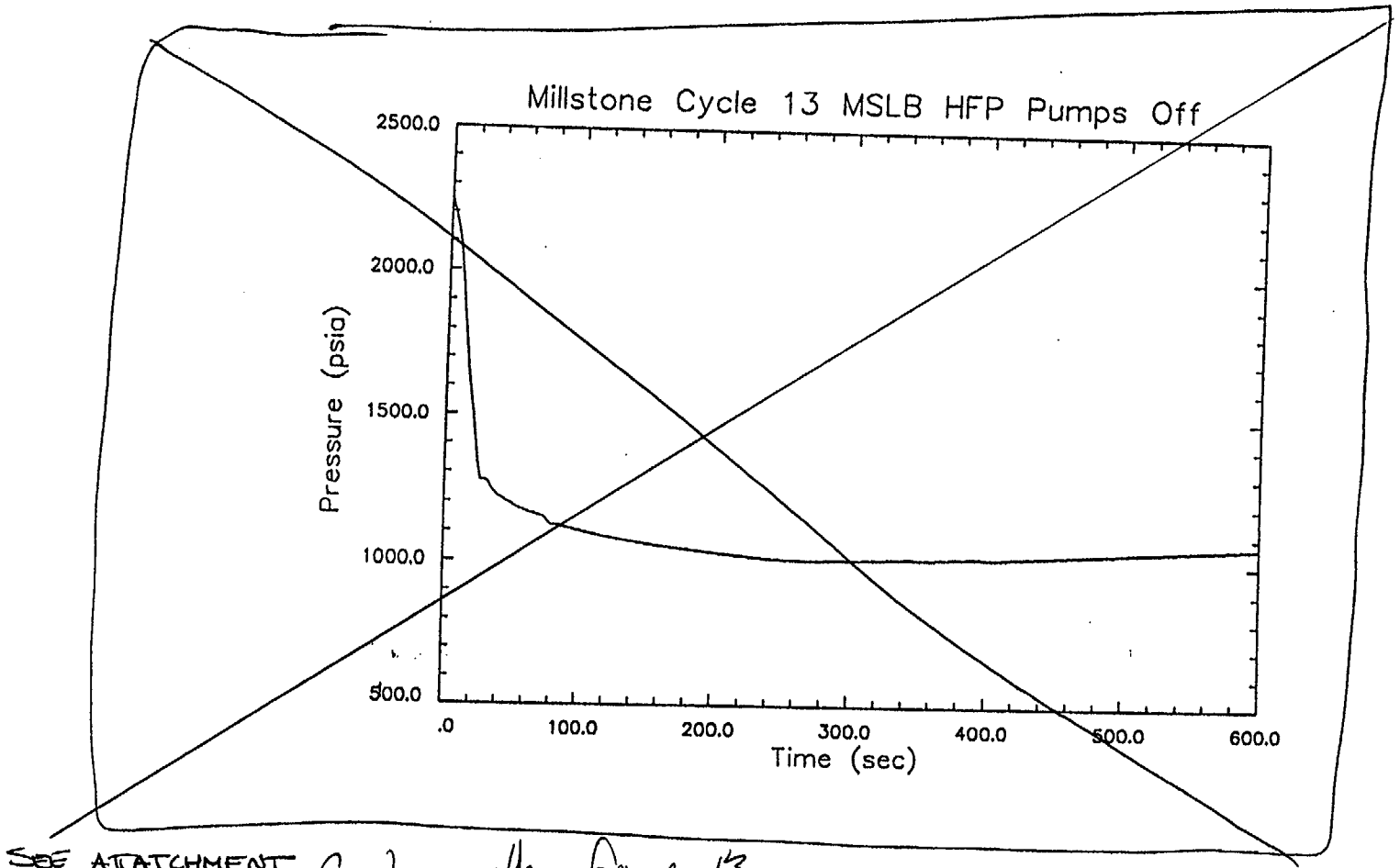

SEE ATTATCHMENT (NEXT PAGE) Replace with figure 13

HZP **FIGURE 14.1.5.2-13**
PRESSURIZER PRESSURE (~~HFP~~ POST-SCRAM STEAM LINE OUTSIDE CONTAINMENT BREAK WITH LOSS OF OFFSITE POWER)

MARCH 1999

FSAR CR 00-MP2-23

ATTACHMENT 2
Page 97 of 104

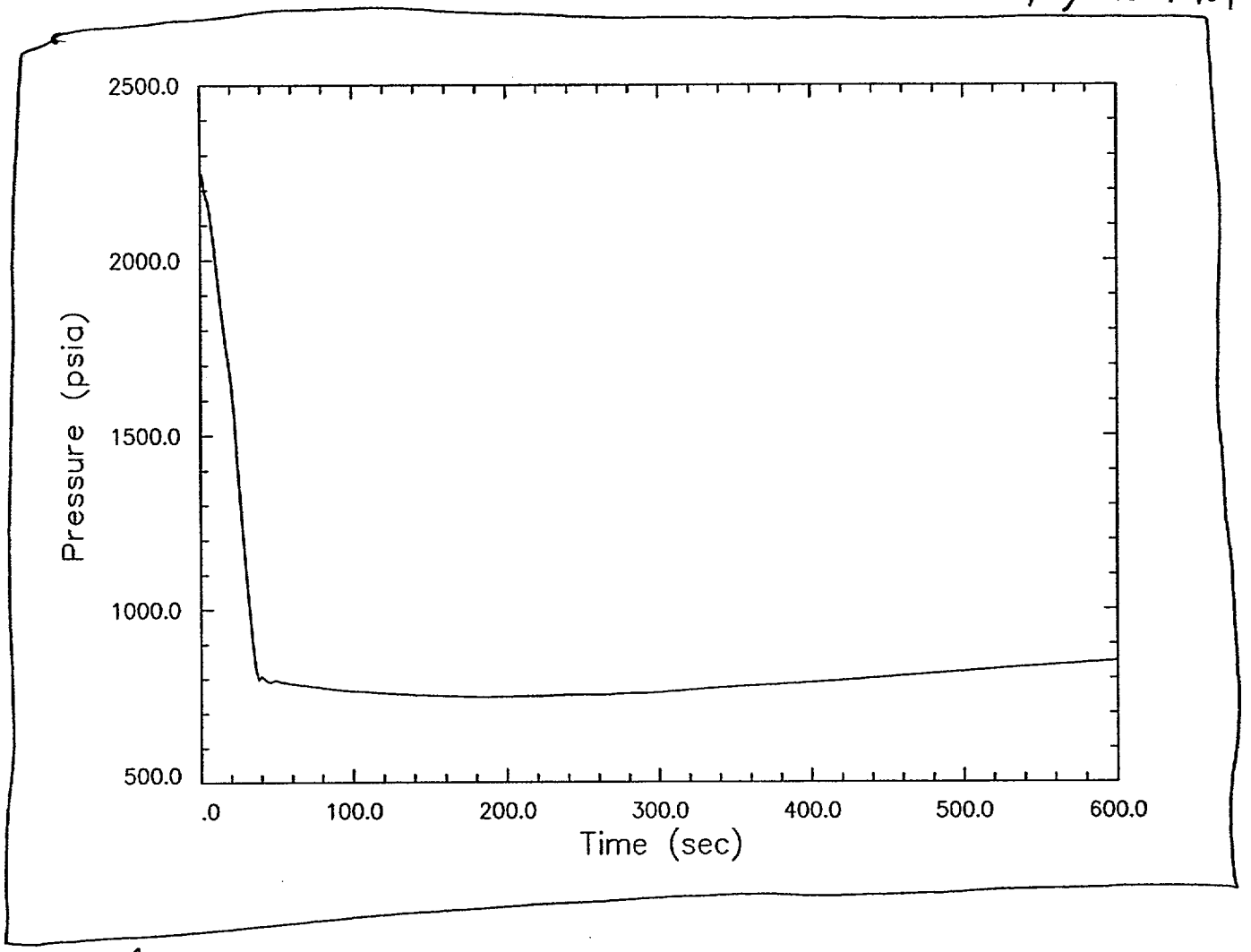

~~Figure 14.1.5.2-13 HZP Loss of Offsite Power (Pressurizer Pressure)~~

figure 13

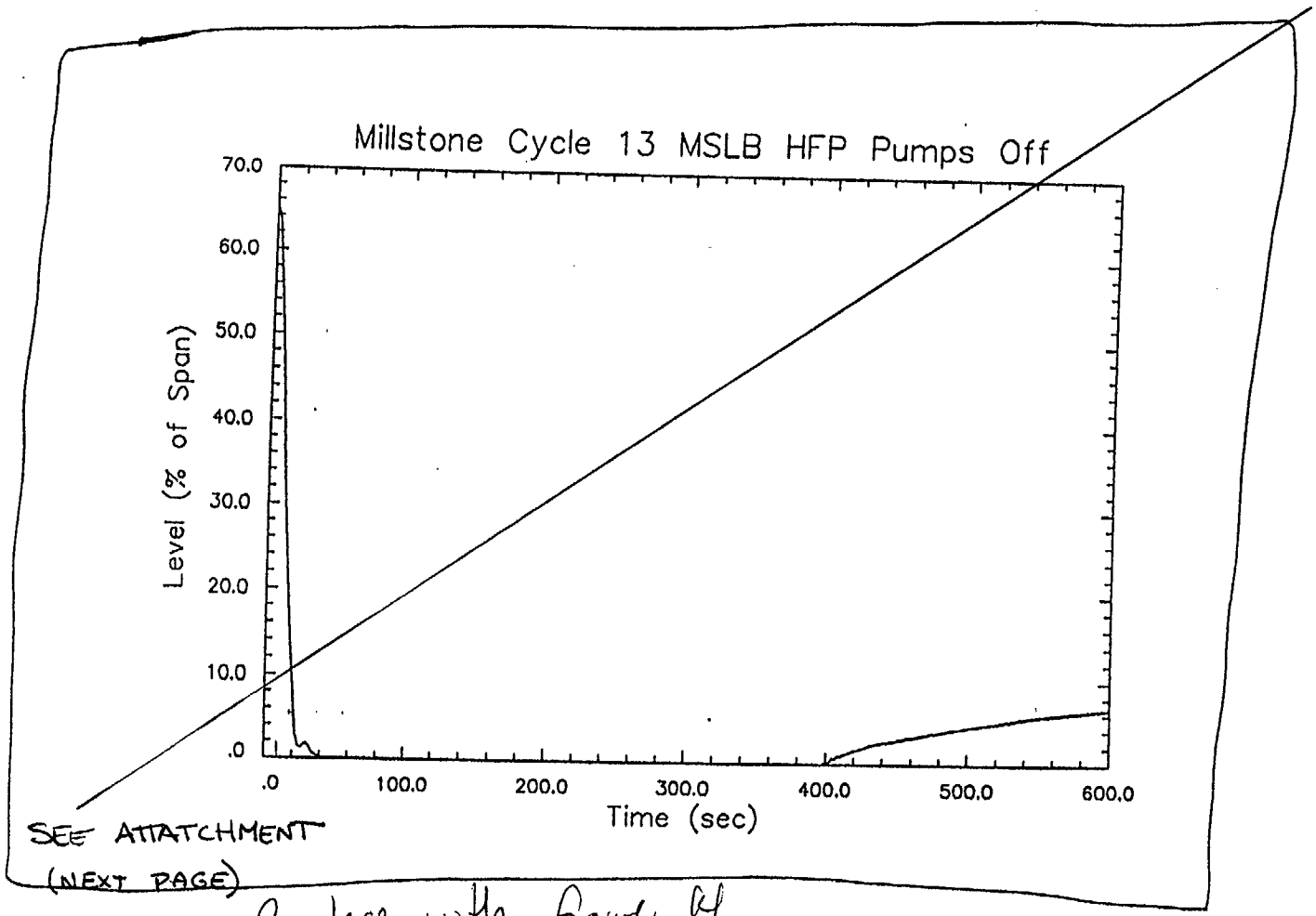

SEE ATTATCHMENT (NEXT PAGE)

Replace with figure 4

HZP FIGURE 14.1.5.2-14
PRESSURIZER LEVEL (~~HFP~~ POST-SCRAM STEAM LINE OUTSIDE CONTAINMENT BREAK WITH LOSS OF OFFSITE POWER)

FSARCR 00-MP2-23

ATTACHMENT 2
Page 99 of 104

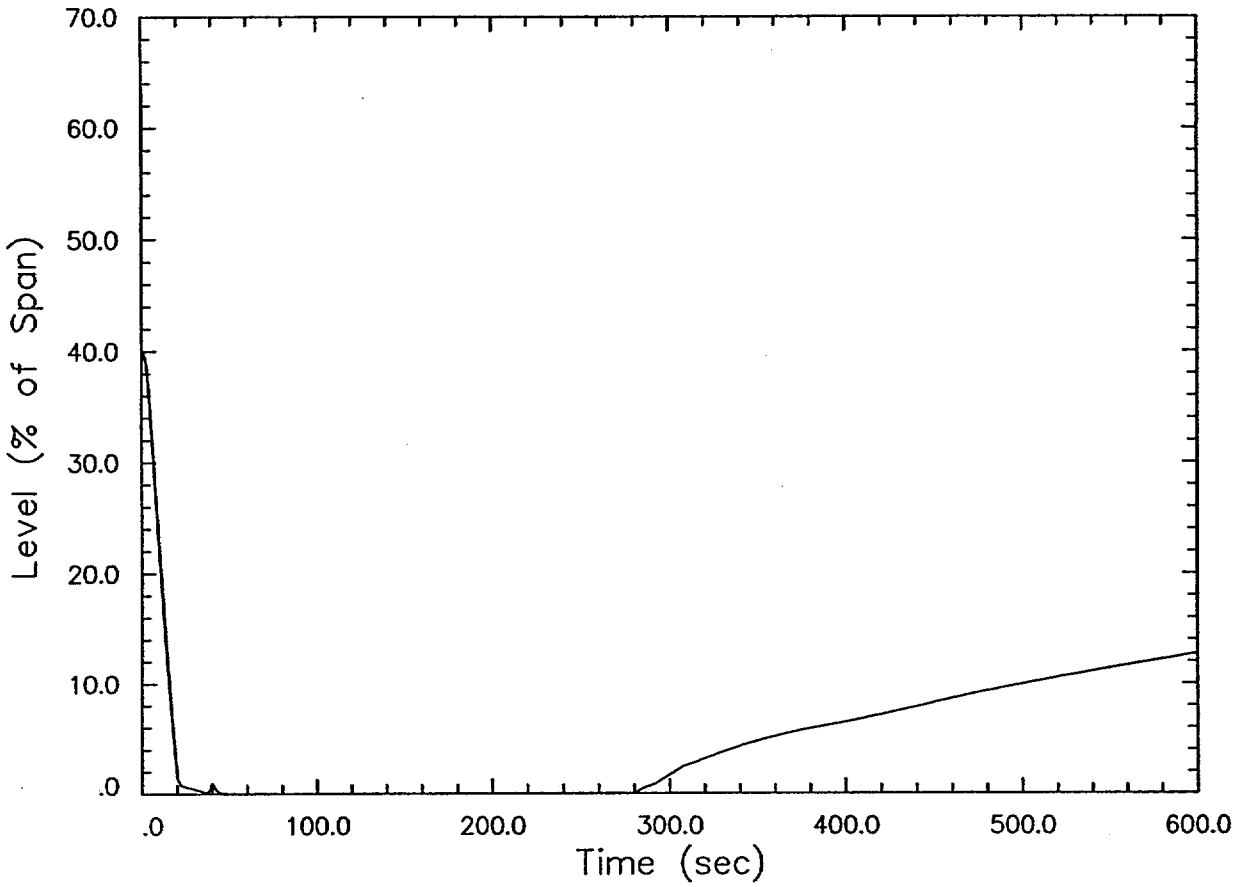

~~Figure 14.1.5.2-14 HZP Loss of Offsite Power (Pressurizer Level)~~

figure 14

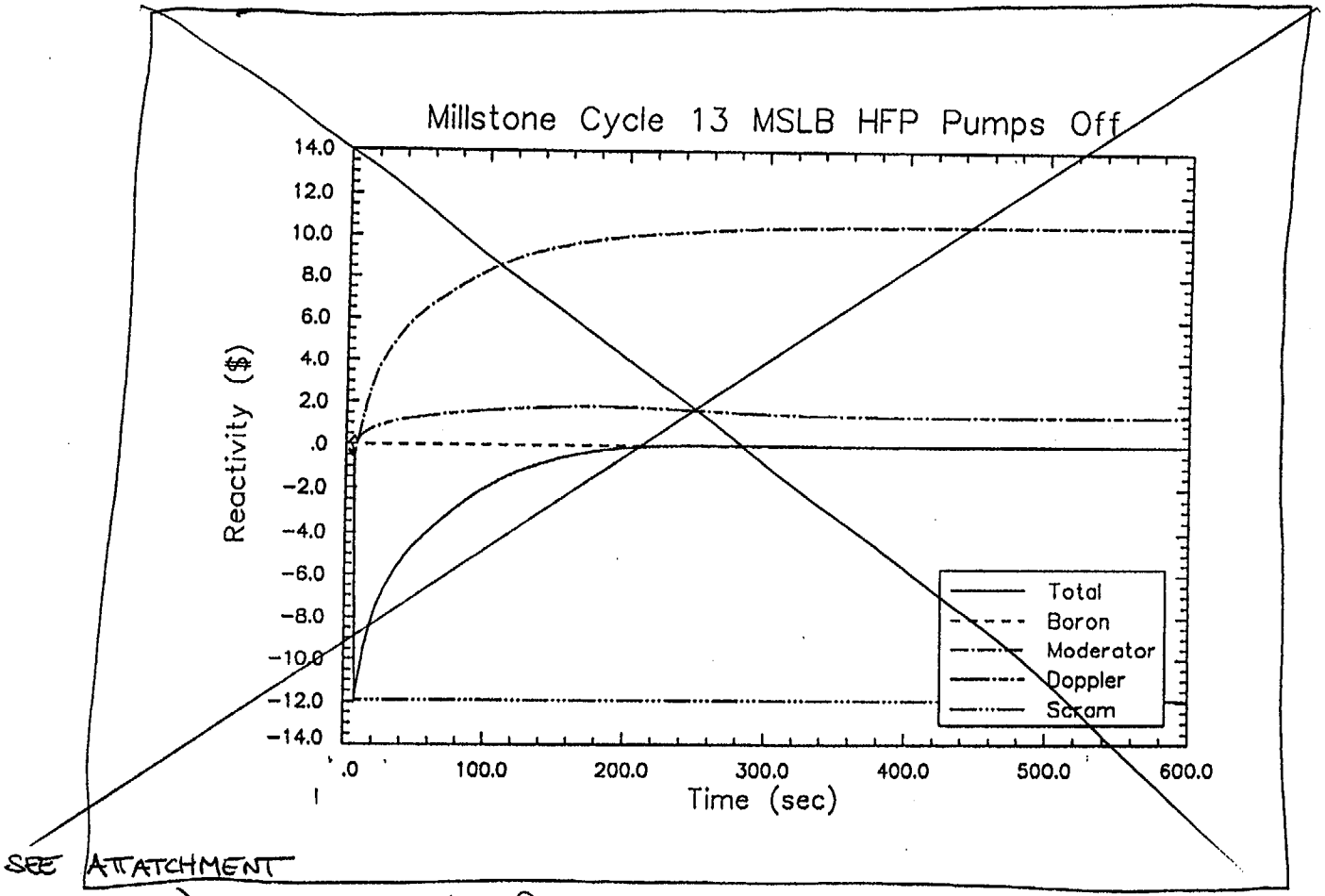

SEE ATTACHMENT (NEXT PAGE)

Replace with figure 15

HZP FIGURE 14.1.5.2-15
REACTIVITY COMPONENTS (~~HFP~~ POST-SCRAM STEAM LINE OUTSIDE CONTAINMENT BREAK WITH LOSS OF OFFSITE POWER)

MARCH 1999

FSAR CR 00-MP2-23

ATTACHMENT 2
Page 101 of 104

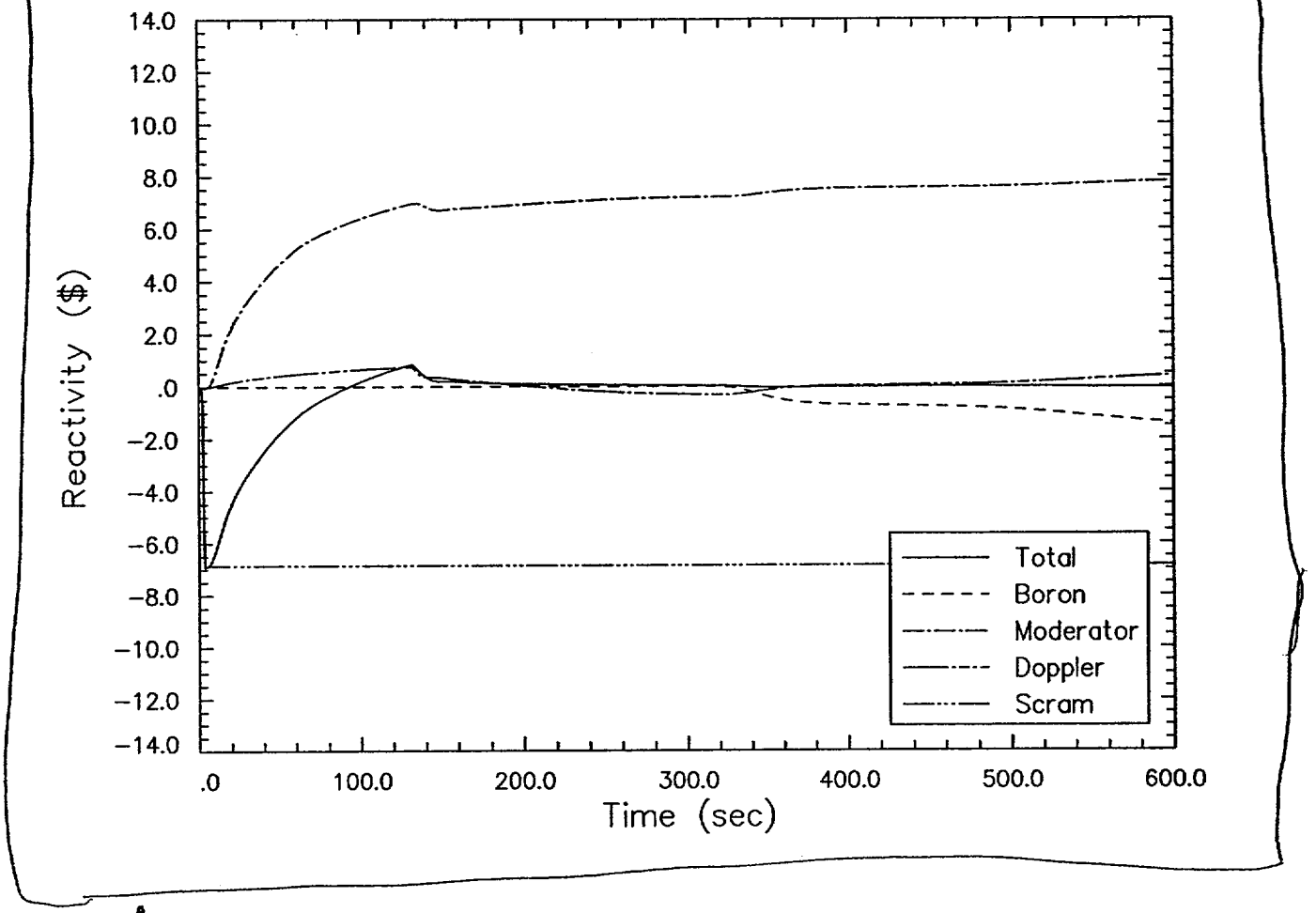

~~Figure 14.1.5.2-15 HZP Loss of Offsite Power (Reactivity Components)~~

Figure 15

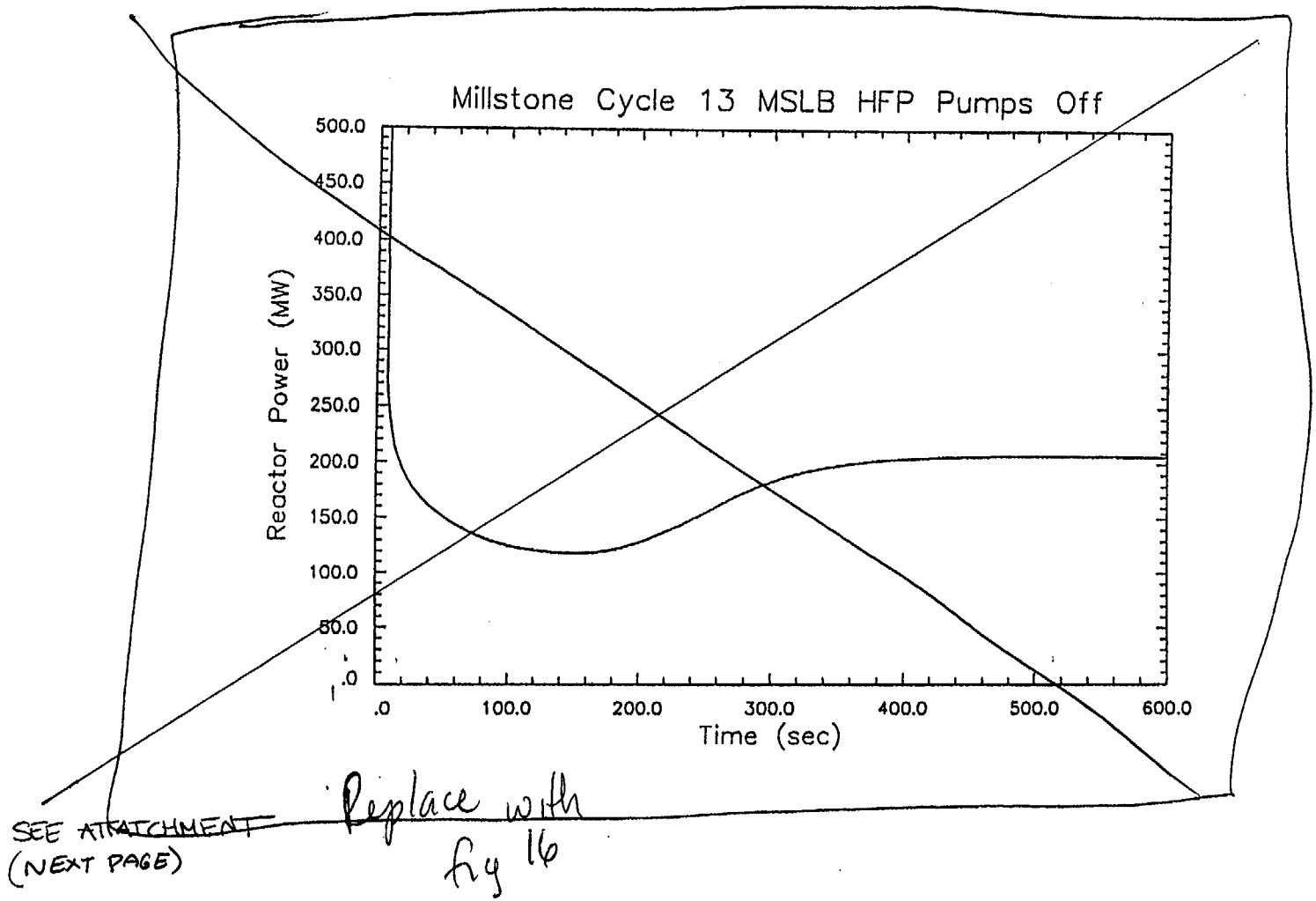

SEE ATTACHMENT (NEXT PAGE)

Replace with fig 16

~~HZP~~ FIGURE 14.1.5.2-16
REACTOR POWER (~~HFP~~ POST-SCRAM STEAM LINE OUTSIDE CONTAINMENT BREAK WITH LOSS OF OFFSITE POWER)

FSARCR 00-MP2-23

ATTACHMENT 3
Page 103 of 104

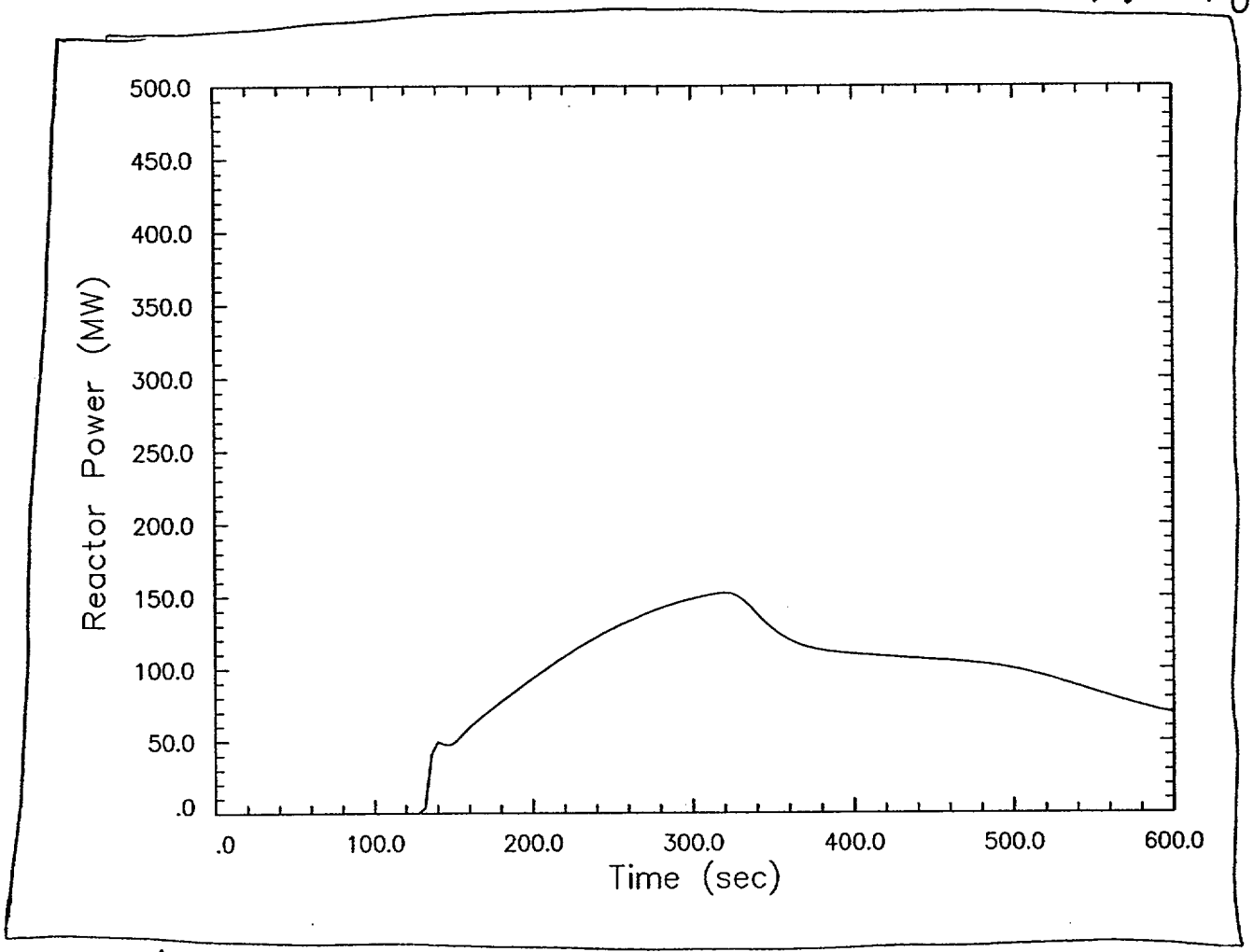

~~Figure 14.1.5.2-16 HZP Loss of Offsite Power (Reactor Power)~~

Figure 16

Docket No. 50-336
B18294

Attachment 3

Millstone Nuclear Power Station, Unit No. 2

Proposed Revision to Final Safety Analysis Report
Fuel Centerline Melt Linear Heat Rate Limit (PLAR 2-00-2)

Typed Version of the Text and Tables Contained in Attachment 2

14.1 INCREASE IN HEAT REMOVAL BY THE SECONDARY SYSTEM

14.1.1 Decrease in Feedwater Temperature

14.1.1.1 Event Initiator

A decrease in feedwater temperature may be caused by loss of one or more feedwater heaters. The loss could be due to the interruption of steam extraction flow or to an accidental opening of a feedwater heater bypass line. The worst loss of feedwater heaters incident would occur if all of the low pressure heaters were bypassed. The effects of any decrease in the feedwater temperature due to flow increases (Main or Auxiliary Feedwater (AF)) are discussed in Section 14.1.2.

14.1.1.2 Event Description

Due to a malfunction in the feedwater heater system, the enthalpy of the feedwater being injected into the steam generators is reduced. The increased subcooling of the feedwater reduces the secondary system average fluid enthalpy and increases the energy removal rate from the primary system. The increase in primary to secondary heat transfer causes the reactor coolant temperature at the outlet of the steam generator to decrease. This causes a corresponding decrease in the core inlet coolant temperature. With a negative moderator temperature coefficient (MTC), the reactor core power will begin to increase as the cooler moderator fluid reaches the core.

14.1.1.3 Reactor Protection

Reactor protection is provided by the variable overpower, thermal margin/low pressure (TM/LP), local power density (LPD), and low steam generator pressure trips. Reactor protection for the decrease in feedwater temperature event is summarized in Table 14.1.1-1.

14.1.1.4 Disposition and Justification

For operating Modes 1-3, the response of the nuclear steam supply system (NSSS) is governed by the magnitude of the overcooling introduced by the initiating event. There is no extraction to the feedwater heaters for operating Modes 4-6. As such, there is not a credible event for these reactor operating conditions.

The most limiting case for Mode 1 is from rated power conditions because the feedwater flow rate and heater duty decrease with load. Also, at rated power conditions, the initial Departure from Nucleate Boiling Ratio (DNBR) margin is minimized. The consequences of the event in Modes 2 and 3 are bounded by those of Mode 1 because the magnitude of the initiating event in Modes 2 or 3 is much smaller than in Mode 1.

This cooldown rate due to bypassing the feedwater heaters is bounded by that of the maximum cooldown event postulated in Section 14.1.3. As such, the consequences of the Increase in Steam Flow (Event 14.1.3) bound the consequences for the Decrease in Feedwater Temperature event discussed in this section. The disposition of events for the Decrease in Feedwater Temperature event is summarized in Table 14.1.1-2.

14.1.2 Increase in Feedwater Flow

14.1.2.1 Event Initiator

This event is initiated by a failure in the feedwater system which causes an increase in the feedwater flow to the steam generators. The initiators considered are complete opening of the feedwater control valves, overspeed of the feedwater pumps, inadvertent start of a second feedwater pump at low power, startup of the auxiliary feedwater system (AFWS), and inadvertent opening of the feedwater control valve bypass lines.

14.1.2.2 Event Description

The increased flow to the steam generators causes an increase in the energy removal capability of the steam generators by reducing the average fluid enthalpy in the steam generators. The increased energy removal from the primary system causes the reactor coolant temperature at the outlet of the steam generator to decrease. The core inlet temperature will correspondingly be reduced, which will cause the core power to increase if the moderator temperature coefficient (MTC) is negative.

Because this event is characterized as a primary system overcooling event, the primary system pressure initially decreases along with the core inlet temperature. There is also a possibility for a core power increase in the presence of a negative moderator reactivity feedback coefficient. Increased reactor power reduces the core Departure from Nucleate Boiling (DNB) margin. A potential exists that the net effect of these three factors will represent a challenge to the core DNB margin.

14.1.2.3 Reactor Protection

Reactor protection for the rated power and power operation conditions (Mode 1) is provided by the variable overpower trip, LPD trip, TM/LP trip, low steam generator pressure trip and by the safety injection actuation signal (SIAS) on low pressurizer pressure. Additional protection is provided by the control-grade reactor trip on turbine trip due to high steam generator water level.

For Modes 2 and 3, protection is provided by the low steam generator pressure trip, safety injection actuation signal (SIAS), and the variable overpower trip. Reactor protection for the Increase in Feedwater Flow event is summarized in Table 14.1.2-1.

14.1.2.4 Disposition and Justification

The event consequences at rated power operating conditions will bound the consequences from all other power operating conditions. At rated power operating conditions, the initial thermal margin (DNBR) is minimized. Maximizing the increase in feedwater flow maximizes the load demand. This results in the maximum rate of moderator cooldown which, in the presence of a negative MTC, results in the maximum challenge to the specified acceptable fuel design limits (SAFDLs). Therefore, the limiting consequences of the increase in feedwater flow will occur at the full load rated power conditions and will bound all other power operating conditions due to the initial steam generator inventory and initial margin to DNB. The greatest cooldown which can be postulated due to feedwater addition at full power is the inadvertent startup of all three AF pumps. This

cooldown is larger than that due to the full opening of both feedwater control valves but less than that calculated for Event 14.1.3, Increased Steam Flow.

The main feedwater system is off-line in Modes 4-6 but may be on-line in Mode 3. For Mode 3 operating conditions, the potential cooldown in conjunction with a negative MTC may result in a return to power at reduced primary pressure, elevated all-rods-in peaking, and less than four reactor coolant pump (RCP) conditions. This case may pose a greater challenge to the SAFDLs than the full power case, and would bound zero power operation in Mode 2 if the cooldown provides sufficient reactivity insertion to overcome the shutdown margin. This is due to the potential for prompt criticality in Mode 3. The greatest increase in feed flow would result from the startup of an idle pump with both control valves full open. The cooldown rate is less than the rate computed for Event 14.1.3 in Mode 3, and consequently Event 14.1.2 in Modes 2 and 3 is bounded by Event 14.1.3 initiated from Mode 3.

In Modes 4-6, the only increased feed flow event initiator is inadvertent startup of one or more AF pumps since the main feedwater system is off-line. The startup of all three AF pumps results in an increased energy removal rate, less than the maximum possible for the Increase in Steam Flow (Event 14.1.3) for Modes 4-6.

The disposition of events for the Increase in Feedwater Flow event is summarized in Table 14.1.2-2.

14.1.3 Increase in Steam Flow

14.1.3.1 Event Initiator

This event is initiated by a failure or misoperation in the main steam system which results in an increase in steam flow from the steam generators. This event could be caused by the rapid opening of the turbine control valves (TCVs), the atmospheric steam dump valves (ADVs), the turbine bypass valves (TBVs), the steam dump to condenser valves (SDVs), a safety relief valve (SRV), or the turbine feed pump control valves.

14.1.3.2 Event Description

The increased steam flow resulting from the failure creates a mismatch between the heat being generated in the core and that being extracted by the steam generators. As a result of this power mismatch, the primary-to-secondary heat transfer increases and the primary system cools down. If the MTC is negative, the cooldown of the primary system coolant would cause an insertion of positive reactivity and the potential erosion of thermal margin.

14.1.3.3 Reactor Protection

The main steam system is designed to accommodate a 10% increase in load (step increase). Reactor protection against a main steam flow increase greater than a 10% step is provided by the following trip signals: variable overpower trip, TM/LP trip, LPD trip, low steam generator water level trip, and low secondary pressure trip. In Modes 1, 2, and 3, protection is also provided by the Safety Injection Actuation Signal (SIAS) on low pressurizer pressure. Reactor protection for the Increase in Steam Flow event is summarized in Table 14.1.3-1.

14.1.3.4 Disposition and Justification

This event is predominantly a cooldown event characterized by a primary pressure and temperature drop with a power rise. Therefore, the most limiting event for power operation is one which results in the highest power, the highest core inlet temperature, and the lowest primary pressure. Core flow remains essentially unchanged. The magnitude of the pressure drop for a given increase in steam flow is about the same regardless of the initial power level. The core inlet temperature will be maximized at HFP. The margin to DNB is the smallest at full power since the product of reactor power and peaking factor decreases as power drops. Additionally, the Variable Overpower trip setpoint will decrease as power decreases, thus providing greater margin to the SAFDLs at lower powers. Therefore, for Mode 1 and for nonzero power operation in Mode 2, the bounding event is one initiated from HFP.

The maximum possible steam release results from the simultaneous opening of the steam dump to condenser valves and the turbine bypass valves. Furthermore, simulating the turbine control valves as operating in the "automatic" mode, rather than the "manual" mode, is limiting. Therefore, a spectrum of HFP cases, with steam releases ranging up to that for the steam dump to condenser valves and turbine bypass valves fully open with the turbine control valves operating in the "automatic" mode, were analyzed. The effects of power decalibration were also included in the analysis.

The ADVs are sized to accommodate 15% of steam flow at 2700 MWt. The SDVs and the TBV are sized to accommodate 40.5% of steam flow at 2700 MWt. Each SRV will pass 6.75% of steam flow at 2700 MWt. The TCVs are sized to accommodate 111.3% of steam flow at 2700 MWt. The capacities of the control valves for the main feedwater and AF pump turbines are significantly less.

To bound the allowable plant operation with the TCVs in automatic control mode, the TCVs were opened fully, simultaneous with the SDVs and the TBV opening. This scenario results in an increased load as great as 51.8% of the steam flow above the rated power operating condition of 2700 MWt. This energy removal rate bounds those of the rated power operating conditions for Events 14.1.1 to 14.1.2, and 14.1.4. Therefore, this event is analyzed as part of the plant transient analysis for Millstone Unit 2. The consequences of this event for all other operating conditions are bounded by the rated power operating condition due to the increased margin to DNB at the other power operating conditions.

The disposition of events for the Increase in Steam Flow event is summarized in Table 14.1.3-2.

14.1.3.5 Definition of Events Analyzed

A spectrum of HFP cases were analyzed, with steam flows ranging from 11.3% excess steam flow (turbine control valves fully open) to 51.8% excess steam flow (steam dump to condenser valves, turbine bypass valve, and turbine control valves fully open). The effects of power decalibration were also included in the analysis.

The end-of-cycle (EOC) Doppler feedback coefficient was selected to maximize the

challenge to the specified fuel design limits. The consequences of this event are bounded at EOC conditions when the MTC is at its maximum negative value. Therefore, the technical specification most negative MTC limit (-28 pcm/°F) was used.

Only full-power cooldown and low-power events which credit power-dependent reactor trips have the potential to be adversely affected by power decalibration. Power decalibration is caused by density-induced changes in the reactor vessel downcomer shadowing the power-range ex-core detectors during heatup or cooldown transients. The nuclear power levels indicated by those instruments are lower than the actual reactor power levels when the coolant entering the reactor vessel is cooler than the normal temperature for full-power operation. The Variable Overpower trip, the TM/LP trip function, and the LPD trip all depend on the indicated nuclear power level. The power decalibration effect was included in the modeling of any power-dependent reactor trips credited in this analysis.

The initial conditions for the Increase in Steam Flow event is summarized in Table 14.1.3-3.

14.1.3.6 Analysis Results

The transient for the limiting case (51.8% excess steam flow) is initiated by a failure which causes the steam dump to bypass valves and the turbine bypass valves to open fully. The turbine control valves are also modeled as opening fully at initiation. The increased steam flow (see Figure 14.1.3-7) creates a mismatch between the core heat generation rate and the steam generator heat removal rate. This power mismatch causes the primary-to-secondary heat transfer rate to increase, which in turn causes the primary system to cool down (see Figure 14.1.3-3). With a negative MTC (see Figure 14.1.3-2), the primary system cooldown causes the reactor power level to increase (see Figure 14.1.3-1. However, due to power decalibration, the indicated nuclear power level does not increase along with the reactor power level. Eventually, the indicated thermal power level reaches the Variable Overpower reactor trip ceiling, and the reactor is tripped. This terminates the power excursion.

The minimum DNBR for the limiting Increase in Steam Flow case (with 51.8% excess steam flow) is calculated to be 1.36, which is well above the 95/95 DNBR safety limit. The maximum linear heat generation rate was not calculated for this event because it is not a limiting moderate frequency event with respect to challenging the fuel centerline melt criterion of 21 kW/ft. Because the limiting moderate frequency events do not violate the fuel centerline melt criteria, it is concluded that this event will not violate the fuel centerline melt criterion. These results demonstrate that fuel failures do not occur for the Increase in Steam Flow event and that the event acceptance criteria are satisfied. 00-23

The responses of key system variables are given in Figures 14.1.3-1 to 14.1.3-7. The sequence of events is given in Table 14.1.3-4. The MDNBR and the peak reactor power level calculated for each of the Increase in Steam Flow cases analyzed are listed in Table 14.1.3-5.

14.1.3.7 Conclusion

The results of the analysis demonstrate that the event acceptance criteria are met since

the minimum DNBR predicted for the full power case is greater than the safety limit. The correlation limit assures that with 95% probability and 95% confidence, DNB is not expected to occur; therefore, no fuel is expected to fail. The fuel centerline melt threshold of 21 kW/ft is not violated during this event.

14.1.4 Inadvertent Opening of a Steam Generator Relief or Safety Valve

14.1.4.1 Event Initiator

This event is initiated by an increase in steam flow caused by the inadvertent opening of a secondary side safety or relief valve.

14.1.4.2 Event Description

The resulting mismatch in energy generation and removal rates results in an overcooling of the primary system. If the MTC is negative, the reactor power will increase.

14.1.4.3 Reactor Protection

Reactor protection is provided by the variable overpower trip, LPD trip, TM/LP trip, low secondary pressure trip, and low steam generator water level trip. In Modes 1, 2, and 3, protection is also provided by the safety injection actuation signal (SIAS) on low pressurizer pressure. Reactor protection for the Inadvertent Opening of a Steam Generator Relief or Safety Valve event is summarized in Table 14.1.4-1.

14.1.4.4 Disposition and Justification

The inadvertent opening of a steam generator safety valve would result in an increased steam flow of approximately 6.75% of full rated steam flow. Each dump (relief) valve is sized for approximately 7.50% steam flow with the reactor at full rated power. As such, the consequences of any of these occurrences will be bounded by the events in Section 14.1.3. The disposition of events for the Inadvertent Opening of a Steam Generator Relief or Safety Valve event is summarized in Table 14.1.4-2.

14.1.5 Steam System Piping Failures Inside and Outside of Containment

00-23 | Two separate analyses have been performed for the Steam Line Break (SLB) event. Section 14.1.5.1 describes the pre-scram analysis performed to determine Departure from Nucleate Boiling Ratio (DNBR) and Linear Heat Generation Rate (LHGR) up to and including reactor trip. This time period represents the highest reactor power condition and the assumptions have been selected to minimize DNBR and maximize LHGR during this time frame. Section 14.1.5.2 describes the post-scram analyses performed to determine MDNBR and LHGR during the return to power caused by the overcooling. A different set of assumptions and single failure were determined to minimize MDNBR and maximize LHGR for the return to power time frame.

14.1.5.1 Pre-Scram Analysis

14.1.5.1.1 Event Initiator

The pre-scram SLB analysis is initiated by a rupture in the main steam piping which results in an uncontrolled steam release from the secondary system.

14.1.5.1.2 Event Description

The increase in energy removal through the secondary system results in a severe overcooling of the primary system. With a negative MTC, the primary system cooldown causes the reactor power level to increase. If the break is not large enough to trip the reactor on a Low Steam Generator Pressure signal, the cooldown will continue until the reactor is tripped on a Variable Overpower or TM/LP signal (for breaks outside containment) or a High Containment Pressure signal (for breaks inside containment) or until the reactor reaches a new steady-state condition at an elevated power level.

Although the SLB calculation is typically a cooldown event, for the pre-scram analysis the cooldown event is not significant for the limiting pre-scram case. The case with a loss of offsite power, also known as a "pumps off" case, credits the low reactor coolant flow trip for harsh conditions. In this case, the Reactor Coolant Pumps (RCPs) are tripped shortly after the initiation of the transient. The sharp reduction in reactor coolant flow causes the pre-scram pumps off calculation to become a heat up transient very similar to a Loss of Coolant Flow (LOCF). Therefore, the conditions for this case are biased as if it were a LOCF (i.e. BOC neutronics). This case becomes a combination of an MSLB and an LOCF event.

14.1.5.1.3 Reactor Protection

Reactor protection is provided by the low steam generator pressure and water level trips, variable overpower trip, LPD trip, TM/LP trip, high containment pressure trip, low reactor coolant flow, and SIAS. Reactor protection for the Steam System Piping Failures Inside and Outside of Containment event is summarized in Table 14.1.5.1-1.

14.1.5.1.4 Disposition and Justification

HFP initial conditions are limiting for the pre-scram SLB cases since this is the highest power condition.

The outside containment breaks do not cause harsh conditions inside containment, and therefore, do not cause the Low Reactor Coolant Flow trip to be degraded. If a loss of offsite power were concurrent with an outside containment break, the primary coolant flow rate would coastdown similar to an LOCF event, without the Low Reactor Coolant Flow trip being degraded. The outside containment break case with loss of offsite power is therefore bounded by the LOCF event.

The inside containment breaks do cause harsh conditions inside containment, and therefore, an increased allowance for instrument uncertainty was applied for the Low Reactor Coolant Flow trip. Therefore, only the inside containment breaks will be analyzed with a loss of offsite power.

The following pre-scram HFP Steam Line Break cases for break sizes ranging up to a double-ended guillotine break in a main steam line were analyzed, with the effects of power decalibration and harsh containment conditions (where applicable) included in the analysis:

1. Breaks outside containment and downstream of the check valves (symmetric cases)

2. Breaks outside containment and upstream of a check valve (asymmetric cases)

3. Breaks inside containment with RCPs on (asymmetric cases)

4. Breaks inside containment with RCPs off (asymmetric cases)

The event is analyzed to support the technical specification EOC MTC limit. This event must be analyzed both with and without a coincident loss-of-offsite power.

The single failure assumed in this analysis is the loss of one channel of Nuclear Instrumentation (NI) which provides power indication to the RPS. If one channel is out of service, the three remaining NI safety channels will be in a 2-out-of-3 coincidence mode. With the assumption of a failure in one of these channels, both of the remaining channels are required for a trip, relying on the lowest power indication for the safety function.

The disposition of events for the Steam System Piping Failures Inside and Outside of Containment event is summarized in Table 14.1.5.1-2.

14.1.5.1.5 Definition of Events Analyzed

The pre-scram SLB event is initiated by a rupture in the main steam piping. The break location is downstream of the steam generator integral flow restrictor and either :

1. outside containment and upstream of the main steam line check valves (asymmetric break), or

2. outside containment and downstream of the main steam line check valves (symmetric break), or

3. inside containment and upstream of the main steam check valves (asymmetric break).

Steam released through a break located downstream of the main steam line check valves flows to the break from both steam generators and, therefore, results in a symmetric transient. However, steam released through a break located upstream of one of the check valves flows to the break from the upstream steam generator only (because the check valve precludes backflow to the break from the other steam generator) and, therefore, results in an asymmetric transient.

Power decalibration is caused by density-induced changes in the reactor vessel downcomer shadowing of the power-range ex-core detectors during heatup or cooldown

transients. The nuclear power levels indicated by those instruments are lower than the actual reactor power levels when the coolant entering the reactor vessel is cooler than the normal temperature for full-power operation (and higher when the vessel inlet coolant is warmer than the normal full-power temperature). This effect is included in the modeling of any power-dependent reactor trips credited in the analysis of full-power cooldown events and low-power events. The Variable Overpower trip, the Thermal Margin/Low Pressure (TM/LP) trip function, and the Local Power Density (LPD) trip all depend on the indicated nuclear power level.

Harsh containment conditions can be caused by the release of steam within the reactor containment. Under such conditions, only those trips which have been qualified for harsh environments are credited, and increased uncertainties are included in the setpoints of all environmentally qualified trips which are credited.

As outlined in Reference 14.1-1, three computerized calculations are required prior to the final calculation of the Minimum Departure From Nucleate Boiling Ratio (MDNBR) values and the maximum Linear Heat Generation Rate (LHGR) values utilized in the determination of fuel failure. The NSSS response is computed using the Siemens Power Corporation (SPC) ANF-RELAP code (Reference 14.1-2), the detailed core and hot assembly power distributions and the reactivity at the time of peak post-scram power are calculated using the SPC PRISM code (Reference 14.1-3), and the detailed core and hot assembly flow and enthalpy distributions are calculated using the SPC XCOBRA-IIIC code (Reference 14.1-4). The SPC XNB correlation was utilized to calculate MDNBR. 00-23

14.1.5.1.5.1 Analysis of Results

The ANF-RELAP analysis provides the NSSS boundary conditions for the PRISM and the XCOBRA-IIIC calculations. This section presents a description of the treatment of factors which can have a significant impact on NSSS response and resultant MDNBR and LHGR values. The plant specific parameters used in this analysis are listed in Tables 14.1.5.1-3 to 14.1.5.1-5. Conservatisms are included in parameters or factors known to have significant effects on the NSSS performance and resulting MDNBR and LHGR values. 00-23

14.1.5.1.5.1.1 Break Location, Size, and Flow Model

The pre-scram SLB event analyzes breaks outside containment both downstream (symmetric cases) and upstream (asymmetric cases) of the main steam line check valves and breaks inside containment (asymmetric cases). A full range of break sizes, up to the double-ended guillotine break of a main steam line, were considered.

The ANF-RELAP break mass flow rate is computed using the Moody critical flow model modified such that only steam flows out the break.

14.1.5.1.5.1.2 Power Decalibration

Power decalibration is caused by density-induced changes in the reactor vessel downcomer shadowing of the power-range ex-core detectors during heatup or cooldown transients. The nuclear power levels indicated by those instruments are lower than the actual reactor power levels when the coolant entering the reactor vessel is cooler than the normal temperature for full-power operation (and higher when the vessel inlet coolant is

warmer than the normal full-power temperature). This effect is included in the modeling of any power-dependent reactor trips credited in the analysis of full-power cooldown events and low-power events. The Variable Overpower trip, the Thermal Margin/Low Pressure (TM/LP) trip function, and the Local Power Density (LPD) trip all depend on the indicated nuclear power level.

14.1.5.1.5.1.3 Harsh Containment Conditions

Harsh containment conditions can be caused by the release of steam within the reactor containment. Under such conditions, only those trips which have been qualified for harsh environments are credited, and increased uncertainties are included in the setpoints of all environmentally qualified trips which are credited.

14.1.5.1.5.1.4 Boron Injection

Boron injection into the primary system acts to mitigate the return to power. Injection of boron is modeled from the HPSI system. The HPSI system is conservatively modeled to take suction from the Refueling Water Storage Tank (RWST) at 35°F with a boron concentration of 1720 ppm. Initially, the line volume between the check valves isolating the system pumps and the cold leg injection location is assumed to be filled with unborated water. The time required to flush this unborated water from the safety injection lines is included as an integral part of the ANF-RELAP NSSS calculation. In the pre-scram SLB event, the analysis is terminated shortly after reactor trip, therefore injection of borated water is not a factor in the analysis.

14.1.5.1.5.1.5 Single Failure Assumption

In order to simulate the asymmetric thermal-hydraulic and reactivity feedback effects that occur during the pre-scram SLB event, the core is divided into an affected sector (1/2 of the core) and an unaffected sector (1/2 of the core). The single failure assumed in this analysis is the loss of one channel of Nuclear Instrumentation (NI) which provides power indication to the Reactor Protection System (RPS). If one channel is out of service, the three remaining NI safety channels will be in a 2-out-of-3 coincidence mode to cause a reactor trip. The excore detectors are placed around the reactor vessel in positions that result in one detector seeing the flux only from the affected region, one seeing the flux only from the unaffected region, and two detectors seeing nearly equal flux from both regions. If one of these latter two is out of service, and the other is assumed to be a single failure, the remaining two channels will be required to cause an RPS trip (high power or TM/LP). Since the power in the affected region will always be higher than in the unaffected region, it is sufficient to model the NI channel reading the unaffected region only.

14.1.5.1.5.1.6 Feedwater

Normal MFW flow is assumed to be delivered to both SGs. The MFW flow increases as the secondary pressure decreases at the lowest possible fluid temperature until the feedwater regulator valve closes. Fluid temperature is determined by assuming heating of the feedwater ceases at the same time the break is initiated. The MFW flow is terminated 14 seconds after receiving the isolation signal.

14.1.5.1.5.1.7 Trips and Delays

Actuation signals and delays are given in Table 14.1.5.1-4. Biases to account for uncertainties are included in the trip setpoints as shown. In the pre-scram SLB event, the analysis is terminated shortly after reactor trip, therefore injection of borated water is not a factor in the analysis.

14.1.5.1.5.1.8 Neutronics

The core kinetics input for this calculation consisted of the minimum required control rod shutdown worth at EOC, and EOC values associated with the reactivity feedback curves, delayed neutron fraction, delayed neutron fraction distribution and related time constants, and prompt neutron generation time. The ANF-RELAP default fission product and actinide decay constants were utilized for this calculation.

The core reactivity is derived from input of several functions. These include effects from control rod worth, moderator density changes, boron concentration, and Doppler effects. The reactivity is weighted between the core sectors. The ANF-RELAP analyses for cases with offsite power available were performed with an MTC of -28 pcm/°F. The ANF-RELAP analyses for cases with a loss of offsite power were performed with an MTC of +4.0 pcm/°F. A summary of the nuclear input and assumptions is given in Table 14.1.5.1-5.

14.1.5.1.5.1.9 Decay Heat 00-39

The presence of radioisotope decay heat at the initiation of the SLB event will reduce the rate and the extent of cooldown of the primary system. The initial decay heat is calculated on the basis of infinite irradiation time at a power of 2754 MW prior to transient initiation. This treatment of decay heat serves to maximize the stored energy and provide limiting stored energy conditions for the SLB cases.

14.1.5.1.5.1.10 Nodalization

The NSSS transient calculations presented in this report utilized the nodalization model described in Reference 14.1-1. The nodalization treats all major NSSS components and subcomponents as discrete elements, with the exception of the secondary side of the steam generators. In addition, all components with long axial dimensions are divided into subcells adequate to minimize numerical diffusion and smearing of gradients.

In order to simulate the asymmetric thermal-hydraulic and reactivity feedback effects that occur during the pre-scram SLB event, the core is divided into an affected sector (1/2 of the core) and an unaffected sector (1/2 of the core).

14.1.5.1.5.1.11 Interloop Mixing

During an actual SLB transient, some mixing between the parallel channels within the reactor pressure vessel will occur in the downcomer, the lower plenum, the core, and the upper plenum due to lateral momentum imbalances, and turbulence or eddy mixing. The mixing will act to reduce the positive reactivity feedback effects due to a reduced rate and magnitude of cooldown of the affected loop and associated core sector.

In this analysis, no credit is taken for turbulent or eddy mixing of coolant between loops or the parallel flow channels within the reactor pressure vessel. However, interloop mixing is calculated to occur due to flow in interloop junctions in the upper and lower plenums. Mixing in the lower plenum was effectively reduced to zero by using an extremely high loss coefficient between the affected and intact sectors.

14.1.5.1.5.2 Minimum Departure From Nucleate Boiling and Linear Heat Generation Rate Analysis

00-23 | The PRISM (Reference 14.1-3) core neutronics code is used to calculate the core radial power distributions for XCOBRA-IIIC (Reference 14.1-4) during the asymmetric transients
00-23 | with offsite power available only. The PRISM model is a three-dimensional representation of the entire core, with four radial nodes and 24 axial nodes for each fuel assembly.

Based on the overall core conditions calculated by ANF-RELAP for the symmetric cases (or
00-23 | ANF-RELAP and PRISM for the asymmetric cases with offsite power available) at the peak heat flux time-point, the XCOBRA-IIIC fuel assembly thermal-hydraulic code is used to calculate the flow and enthalpy distributions for the entire core and the DNB performance for the DNB-limiting assembly. The XCOBRA-IIIC model consists of a thermal-hydraulic model of the core (representing each assembly by a single "channel") linked to a detailed thermal-hydraulic model of the limiting assembly (representing each subchannel by a single "channel"). The limiting assembly DNBR calculations are performed using the XNB DNB correlation (Reference 14.1-4).

For the asymmetric transients, the radial power peaking is augmented above the Technical Specification limit to account for the increase in radial power peaking which occurs during
00-23 | the transient. The increase in peaking is determined by PRISM.

14.1.5.1.6 Analysis Results

A summary of calculated results important to this analysis is presented in Table 14.1.5.1-6 for the limiting MDNBR and LHGR cases. The MDNBR values are listed together with the corresponding core power values at the time of MDNBR which corresponds to the maximum power level. For cases where offsite power was available for operation of the primary coolant system pumps, the MDNBR and the maximum LHGR occurred at the time of the maximum power condition. For cases where offsite power is lost and the primary system pumps coast down, the maximum LHGR and the MDNBR occur when the worst combination of core power, flow, inlet temperature, and pressure are present. These conditions occurred at the time of peak power in this analysis.

The scenario which resulted in the highest power level and the largest LHGR is the HFP 3.50 ft^2 symmetric break outside containment with offsite power available for operation of the primary coolant pumps. This case is presented in detail.

The scenario which resulted in the limiting MDNBR is the HFP case with a loss of offsite power and is also presented in detail.

14.1.5.1.6.1 Hot Full Power 3.50 ft^2 Break Outside Containment and Downstream of a Check Valve with Offsite Power Available

The ANF-RELAP simulation of the NSSS during the HFP symmetric break transient with offsite power available is illustrated in Figures 14.1.5.1-1 through 14.1.5.1-6. A tabulation of the sequence of events is presented in Table 14.1.5.1-7. The ANF-RELAP computation was terminated 60 seconds after break initiation. This is well beyond the

time of MDNBR or peak LHGR. The general response of the reactor was the same for all the symmetric break sizes but the occurrence of events was delayed as the break size decreased.

14.1.5.1.6.1.1 Secondary System Parameters

Upon break initiation the break flow increased sharply and then began to decline in response to falling secondary side pressure. When the turbine trip occurred, the break flow increased due to a local pressure increase. The main steam line flow rate from each generator initially increased (see Figure 14.1.5.1-6) in response to the break and the assumed instantaneous full opening of the turbine control valves. The increased steam flow creates a mismatch between the core heat generation rate and the steam generator heat removal rate. This power mismatch causes the primary-to-secondary heat transfer rate to increase, which in turn causes the primary system to cool down (see Figure 14.1.5.1-2). When the reactor scram occurred, the turbine valves closed and steam flow declined sharply. At this point, the MFW flow may exceed the steam flow as the control system attempts to restore steam generator mass. Both steam flow and MFW flow were terminated when the main steam isolation valves closed.

14.1.5.1.6.1.2 Primary System Parameters

Approximately five seconds after the break occurred, the core inlet temperature began to decline. With a negative MTC (see Figure 14.1.5.1-3), the primary system cooldown caused the reactor power level to increase. The core power continues to increase until reactor scram on low steam generator pressure occurs. This terminated the power excursion. The pressurizer pressure and level began to decline as the volume of water in the primary system shrank. The core inlet mass flow rate increased due to the increasing density of the primary system fluid while the reactor coolant pumps' speed remained constant.

14.1.5.1.6.1.3 Departure From Nucleate Boiling Ratio and Linear Heat Generation Rate Results

The MDNBR value for this scenario was calculated to be 1.299 which is above the 95/95 XNB correlation limit. Therefore, no fuel rods would be expected to fail during this transient scenario from an MDNBR stand point. 00-39

The peak LHR for the LHR-limiting case (3.50 ft^2 break outside containment and downstream of a check valve) is calculated to be 20.8 kW/ft. Comparing this LHGR value with the FCMLHR limit, it is apparent that centerline melt is not predicted to occur. Thus, no fuel failures are predicted to occur due to violation of the centerline melt criteria. 00-39 00-38

14.1.5.1.6.2 Hot Full Power 3.51 ft^2 Inside Containment Asymmetric Break Concurrent with a Loss of Offsite Power

The ANF-RELAP NSSS simulation of the most limiting pre-scram SLB scenario from an MDNBR standpoint (i.e., HFP 3.51 ft^2 inside containment asymmetric break concurrent with a loss of offsite power) is illustrated in Figures 14.1.5.1-7 through 14.1.5.1-11. A tabulation of the sequence of events is presented in Table 14.1.5.1-8. The ANF-RELAP computation was terminated 60 seconds after break initiation. This is well beyond the time of MDNBR or peak LHGR.

The transient is initiated by the opening of the break. The RCPs tripped shortly after transient initiation. The sharp reduction in the reactor coolant flow causes this pre-trip pumps off calculation to become a heat up transient very similar to a Loss of Coolant Flow event. Typically, the Steam Line Break calculation is a cooldown event. Because this case is a heat up event the most positive BOC neutronics conditions are used, and the maximum inside containment asymmetric break size is used. The maximum break size causes the biggest decrease in primary pressure. Maximizing the primary system pressure decrease causes the maximum decrease in moderator density and the maximum positive moderator feedback. The RCP trip causes the RCS flow to decrease rapidly throughout this transient. The decreasing RCS flow causes the transient time of the fluid in the core to increase and the fluid temperature begins to rise. The increasing fluid temperature causes positive moderator feedback, which in turn causes an increase in core power. However, the decreasing RCS flow causes the heat transfer to the fluid to decrease. The increase in core power is offset by the decrease in heat transfer from the fuel rods, such that, the fuel rod heat flux decreases slightly until reactor scram. The reactor scrams on the low reactor coolant flow trip signal.

00-39 | 14.1.5.1.6.2.1 Departure From Nucleate Boiling Ratio and Linear Heat Generation Rate Results

The MDNBR value for the pre-scram 3.51 ft^2 asymmetric break inside containment with a loss of offsite power was calculated to be 0.88 which is below the 95/95 XNB correlation limit. The number of failed assemblies is determined by comparing the core power distribution to the assembly power where DNB occurs. This results in a predicted failure of 3.7% of the fuel rods in the core.

The peak LHR for this case is bounded by the 3.50 ft^2 outside containment symmetric
00-38 | break. Therefore, the LHGR for this case is below the FCMLHR limit and no fuel failures are predicted to occur due to violation of the centerline melt criteria.

14.1.5.1.7 Conclusions

The HFP 3.50 ft^2 break outside containment and downstream of a check valve (symmetric break) with offsite power available was determined to be the most limiting in this analysis
00-39 | from an LHGR standpoint (20.8 kW/ft). In no scenario evaluated, however, was fuel
00-38 | failure calculated to occur as a result of violating the FCMLHR limit.

The HFP 3.51 ft^2 asymmetric break inside containment coincident with a loss of offsite power was determined to be the most limiting in this analysis from the standpoint of MDNBR. The MDNBR was calculated to be 0.88 which is below the 95/95 XNB correlation limit. This results in a predicted failure of 3.7% of the fuel rods in the core.

14.1.5.2 Post-Scram Analysis

14.1.5.2.1 Event Initiator

This event is initiated by a rupture in the main steam piping downstream of the integral steam generator flow restrictors and upstream of the MSIVs which results in an uncontrolled steam release from the secondary system.

14.1.5.2.2 Event Description

The increase in energy removal through the secondary system results in a severe overcooling of the primary system. In the presence of a negative MTC, this cooldown causes a decrease in the shutdown margin (following reactor scram) such that a return to power might be possible following a steam line rupture. This is a potential problem because of the high power peaking factors which exist, assuming the most reactive control rod to be stuck in its fully withdrawn position.

14.1.5.2.3 Reactor Protection

Reactor protection is provided by the low steam generator pressure and water level trips, LPD trip, TM/LP trip, high containment pressure trip, and SIAS. Reactor protection for the Steam System Piping Failures Inside and Outside of Containment event is summarized in Table 14.1.5.2-1. 00-23

14.1.5.2.4 Disposition and Justification

At rated power conditions, the stored energy in the primary coolant is maximized, the available thermal margin is minimized, and the pre-trip power level is maximized. These conditions result in the greatest potential for cooldown and provide the greatest challenge to the SAFDLS. Initiating this event from rated power also results in the highest post-trip power since it maximizes the concentration of delayed neutrons providing for the greatest power rise for a given positive reactivity insertion. Thus, this event initiated from rated power conditions will bound all other cases initiated from at power operation modes. 00-23

For the zero power and subcritical plant states (Modes 2-6), there is a potential for a return-to-power at reduced pressure conditions. The most limiting steam line break (SLB) event at zero power is one which is initiated at the highest temperature, thereby providing the greatest capacity for cooldown. This occurs in Modes 2 and 3. Thus, the event initiated from Modes 2 and 3 will bound those initiated from Modes 4-6. Further, the limiting initial conditions will occur when the core is just critical. These conditions will maximize the available positive reactivity and produce the quickest and largest return to power. Thus, the SLB initiated from critical conditions in Mode 2 will bound the results of the event initiated form subcritical Mode 3 conditions.

The technical specifications only require a minimum of one RCP to be operating in Mode 3. One pump operation provides the limiting minimum initial core flow case. Minimizing core flow minimizes the clad to coolant heat transfer coefficient and degrades the ability to remove heat generated within the fuel pins. Conversely, however, a maximum loop flow will maximize the primary to secondary heat transfer coefficient, thus providing for the greatest cooldown. Higher loop flow will sweep the cooler fluid into the core faster, maximizing the rate of positive reactivity addition and the peak power level.

The worst combination of conditions is achieved for the four pump loss of offsite power case. In this situation, the initial loop flow is maximized resulting in the greatest initial cooldown, while the final loop flow is minimized providing the greatest challenge to the DNB SAFDL. Since the natural circulation flow which is established at the end of the transient will be the same regardless of whether one or four pumps were initially operating

the results of the four pump loss of offsite power case will bound those of the one pump case. Thus, only four pump operation need be analyzed for the Mode 2 case.

The event is analyzed to support the technical specification EOC MTC limit. This event must be analyzed both with and without a coincident loss-of-offsite power. Typically there are two single failures which are considered for the offsite power available case. The first is failure of a High Pressure Safety Injection (HPSI) pump to start. The second is failure of an MSIV to close, resulting in a continued uncontrolled cooldown. However, Millstone 2 has combination MSIV/swing disc check valves. A double valve failure would thus be required for steam from the intact steam generator to reach the break. This is not deemed credible. Thus, the single failure to be considered with offsite power available is failure of a HPSI pump to start. For the loss-of-offsite power case, the limiting single failure is the failure of a diesel generator to start. This is assumed to result in the loss of one HPSI pump. The disposition of events for the Steam System Piping Failures Inside and Outside of Containment event is summarized in Table 14.1.5.2-2.

14.1.5.2.5 Definition of Events Analyzed

The post-scram SLB is initiated by a rupture in the main steam piping downstream of the integral steam generator flow restrictors and upstream of the MSIVs which results in an uncontrolled steam release from the secondary system. The effects of harsh containment conditions (where applicable) are included in the following analyses:

1. HFP and HZP breaks outside containment with offsite power available

2. HFP and HZP breaks outside containment with a loss of offsite power

3. HFP and HZP breaks inside containment with offsite power available

4. HFP and HZP breaks inside containment with a loss of offsite power

The event is analyzed to support the technical specification EOC MTC limit. This event must be analyzed both with and without a coincident loss-of-offsite power.

The single failure assumed in this analysis results in the disabling of one of the two HPSI pumps required to be in service during normal operation. In addition to the single failure, there is no credit taken for the charging pump system. This assumption results in an additional delay in the time required for boron to reach the core. The delay is amplified when combined with the assumption of a stagnant upper head which serves to maintain the primary system pressure due to flashing of the hot fluid in the upper head.

The increase in energy removal through the secondary system results in a severe overcooling of the primary system. In the presence of a negative MTC, this cooldown results in a large decrease in the shutdown margin and a return to power. This return to power is exacerbated because of the high power peaking factors which exist, with the most reactive control rod stuck in its full withdrawn position.

As outlined in Reference 14.1-1, three computerized calculations are required prior to the final calculation of the Minimum Departure From Nucleate Boiling Ratio (MDNBR) values and the maximum Linear Heat Generation Rate (LHGR) values utilized in the determination

of fuel failure. The NSSS response is computed using the Siemens Power Corporation (SPC) ANF-RELAP code (Reference 14.1-2), the detailed core and hot assembly power distributions and the reactivity at the time of peak post-scram power are calculated using the SPC PRISM code (Reference 14.1-3), and the detailed core and hot assembly flow and enthalpy distributions are calculated using the SPC XCOBRA-IIIC code (Reference 14.1-4). The modified Barnett correlation was utilized to calculate MDNBR due to the reduced pressures occurring during the SLB event. 00-23

14.1.5.2.5.1 Analysis of Results

The ANF-RELAP analysis provides the NSSS boundary conditions for the PRISM and the XCOBRA-IIIC calculations. This section presents a description of the treatment of factors which can have a significant impact on NSSS response and resultant MDNBR and LHGR values. The plant specific parameters used in this analysis are listed in Tables 14.1.5.2-3 to 14.1.5.2-5. Conservatisms are included in parameters or factors known to have significant effects on the NSSS performance and resulting MDNBR and LHGR values. 00-23

14.1.5.2.5.1.1 Break Location, Size, and Flow Model

The post-scram SLB event is initiated by a double ended guillotine break of a main steam line downstream of the integral steam generator flow restrictors and upstream of the MSIVs. The flow is choked at the integral steam generator flow restrictor, which has an area of 3.51 ft^2. On the steam generator side of the break, steam flows out of the break throughout the entire transient. On the MSIV side of the break, break flow terminates after the MSIVs are fully closed. As an added conservatism, the main steam check valves are not credited in the analysis. The event occurs concurrent with the most reactive control rod stuck out of the core. The break flow areas for the affected and intact steam generators are listed in Table 14.1.5.2-3. 00-23

The ANF-RELAP break mass flow rate is computed using the Moody critical flow model modified such that only steam flows out the break.

14.1.5.2.5.1.2 Boron Injection

Boron injection into the primary system acts to mitigate the return to power. Injection of boron is modeled from the HPSI system. The HPSI system is conservatively modeled to take suction from the Refueling Water Storage Tank (RWST) at 35°F with a boron concentration of 1720 ppm. Initially, the line volume between the check valves isolating the system pumps and the cold leg injection location is assumed to be filled with unborated water. The time required to flush this unborated water from the safety injection lines is included as an integral part of the ANF-RELAP NSSS calculation. The characteristics of the HPSI system are listed in Table 14.1.5.2-3. The delivery curve for the HPSI system used in this analysis is given in Figure 14.1.5.2-1.

14.1.5.2.5.1.3 Single Failure Assumption

The single failure assumed in the engineered safeguards system results in the disabling of one of the two HPSI pumps required to be in service during normal operation. In addition to the single failure, there is no credit taken for the charging pump system. This assumption results in an additional delay in the time required for boron to reach the

reactor core. The delay is further amplified when combined with the assumption of a stagnant upper head which serves to maintain the primary system pressure due to flashing of the hot fluid in the upper head.

14.1.5.2.5.1.4 Feedwater

00-23 For the HFP scenarios, normal MFW flow is assumed to be delivered to both steam generators. The MFW flow increases as the secondary pressure decreases at the lowest possible fluid temperature until the feedwater regulating valve closes. Fluid temperature is determined by assuming heating of the feedwater ceases at the same time the break is initiated. The MFW flow is terminated 14 seconds after receiving the isolation signal.

For the HFP scenarios, the AFW flow is assumed to be zero at break initiation. After 180 seconds, AFW is delivered at the maximum capacity of the AFW system with flow restrictors installed on the AFW delivery lines. For the HZP scenarios, the AFW flow is increased to the maximum capacity immediately at break initiation. For all scenarios, all of the AFW flow is directed to the affected steam generator to maximize the cooldown rate. The operator is assumed to terminate the AFW flow to the affected steam generator at 600 seconds.

14.1.5.2.5.1.5 Trips and Delays

Trips for the HPSI, main feedwater valves, and MSIVs are given in Table 14.1.5.2-4. Biases to account for uncertainties are included in the trip setpoints as shown. For the steam and feedwater valves, the delay times given are between the time the trip setpoint is reached and the time full valve closure is reached. For the HPSI system, the delay time given is from the time the setpoint is reached until the pumps have accelerated to rated speed. Additional delay time required to sweep the lines of unborated water is accounted for by setting the boron concentration of the injected flow to zero until the volume of the injection lines has been cleared.

14.1.5.2.5.1.6 Neutronics

The core kinetics input for this calculation consisted of the minimum required control rod shutdown worth at the EOC, and EOC values associated with the reactivity feedback curves, delayed neutron fraction, delayed neutron fraction distribution and related time constants, and prompt neutron generation time. The ANF-RELAP default fission product and actinide decay constants were utilized for this calculation.

The core reactivity is derived from input of several functions. These include effects from control rod worth, moderator density changes, boron concentration, and Doppler effects. The reactivity is weighted between the core sectors. Different reactivity functions were utilized where necessary for the HZP and the HFP cases. The ANF-RELAP analyses were performed with an MTC of -28 pcm/°F. A summary of the nuclear input and assumptions is given in Table 14.1.5.2-5.

14.1.5.2.5.1.7 Decay Heat

The presence of radioisotope decay heat at the initiation of the SLB event will reduce the rate and the extent of cooldown of the primary system. For the HFP scenarios, the initial decay heat is calculated on the basis of infinite irradiation time at a power of 2700 MW prior to transient initiation. For the HZP scenarios, the initial decay heat is calculated on the basis of infinite irradiation time at a power of 1 W prior to transient initiation. For both scenarios, decay heat generated from return to power is calculated. This treatment of decay heat serves to maximize the stored energy in the HFP cases and to minimize it in the HZP cases. This treatment provides limiting stored energy conditions for the SLB cases.

14.1.5.2.5.1.8 Nodalization

The NSSS transient calculations utilized the nodalization model described in Reference 14.1-1. The nodalization treats all major NSSS components and subcomponents as discrete elements, with the exception of the secondary side of the steam generators. In addition, all components with long axial dimensions are divided into subcells adequate to minimize numerical diffusion and smearing of gradients.

In order to simulate the asymmetric thermal hydraulic and reactivity feedback effects that occur during an SLB transient, the core is nodalized into three radial sectors. One sector corresponds to the region immediately surrounding the assembly where the most reactive control rod is assumed stuck out of the core. This sector is termed the 'stuck rod' sector. The remainder of the region of the core which is directly affected by the loop containing the break is the second sector and is termed the 'affected' sector. The remainder of the core and the other loop is termed either the 'unaffected' or the 'intact' sector or loop.

14.1.5.2.5.1.9 Interloop Mixing

During an actual SLB transient, some mixing between the parallel channels within the reactor pressure vessel will occur in the downcomer, the lower plenum, the core, and the upper plenum due to lateral momentum imbalances, and turbulence or eddy mixing. The mixing will act to reduce the positive reactivity feedback effects due to a reduced rate and magnitude of cooldown of the affected loop and associated core sector.

In this analysis, no credit is taken for turbulent or eddy mixing of coolant between loops or the parallel flow channels within the reactor pressure vessel (RPV). However, interloop mixing is calculated to occur due to flow in interloop junctions in the upper and lower plenums. Mixing in the lower plenum was reduced to a minimum by using an extremely high loss coefficient between the affected and intact sectors.

14.1.5.2.5.1.10 Harsh Containment Conditions

Harsh containment conditions can be caused by the release of steam within the reactor containment. Under such conditions, only those trips which have been qualified for harsh environments are credited, and increased uncertainties are included in the setpoints of all environmentally qualified trips which are credited.

14.1.5.2.5.2 Minimum Departure From Nucleate Boiling and Linear Heat Generation Rate Analysis

MDNBR calculations require determination of the power, enthalpy, and flow distributions within the highest power assembly of the stuck rod core sector. Similarly, determination of the maximum LHGR also requires characterization of the power distribution. The power distribution within the core, including the highest powered assembly within the stuck rod
00-23 | core sector, is calculated with PRISM (Reference 14.1-3). Flow and enthalpy distributions within the core, including the highest powered assembly within the stuck rod core sector, are calculated with XCOBRA-IIIC (Reference 14.1-4). In order to obtain compatible flows, moderator densities, and powers within the high power assemblies, iteration between
00-23 | PRISM and XCOBRA-IIIC is conducted.

For this calculation, the modified Barnett correlation was found to be suitable for the MDNBR calculation. The modified Barnett correlation is based upon closed channels and primarily uniform power distribution data. The correlation is based on assembly inlet (or upstream) fluid conditions rather than on local fluid conditions as is the case with
00-23 | subchannel based correlations.

14.1.5.2.6 Analysis Results

A summary of calculated results important to this analysis is presented in Table 14.1.5.2-6 for the limiting MDNBR and LHGR scenarios. The MDNBR values are listed together with the corresponding core power values at the time of MDNBR which corresponds to the maximum post-scram power level. The outside containment cases, regardless of whether or not offsite power was or was not available, were found to be the most limiting. For cases where offsite power was available for operation of the primary coolant system pumps, the MDNBR and the maximum LHGR occurred at the time of the maximum power condition. For cases where offsite power is lost and the primary system pumps coast down, the maximum LHGR and the MDNBR occur when the worst combination of core power, flow, inlet temperature, and pressure are present. These conditions occurred at the time of peak power in this analysis.

The scenario which resulted in the highest post-scram power level and the largest LHGR is
00-23 | that initiated from HZP with the break occurring outside containment and with offsite power available for operation of the primary coolant pumps. This case is presented in detail.

The NSSS responses for the scenarios with loss of offsite power for operation of the primary system coolant pumps are different from those scenarios where offsite power is
00-23 | available throughout the transient due to the pump coastdown and subsequent natural circulation of the primary coolant. Post-scram maximum power levels attained during the transient are significantly lower. Lower power levels result from lower positive moderator feedback. The positive moderator feedback is reduced due to the coolant density reductions that occur axially upwards in the core at low core flow rates, even for low core power levels. Lower power levels cause MDNBR values to increase, but lowering flow rates cause MDNBR values to decrease. Overall, the combination of factors results in lower MDNBR values for the reduced flow condition than for the full flow condition.

00-23 | Of the two loss of offsite power scenarios analyzed, the HZP break occurring outside

containment case resulted in lower MDNBR values. The general response of the HFP and HZP cases with loss of offsite power is comparable. Because the two scenarios are quite similar in terms of their general response, only the limiting MDNBR case (i.e., HZP break outside containment and without offsite power) is presented in detail. 00-23

14.1.5.2.6.1 Hot Zero Power Outside Containment with Offsite Power Available 00-23

The ANF-RELAP simulation of the NSSS during the HZP transient with offsite power available is illustrated in Figures 14.1.5.2-2 through 14.1.5.2-9. A tabulation of the sequence of events is presented in Table 14.1.5.2-7. The ANF-RELAP computation was terminated 600 seconds after break initiation. This is well beyond the time of MDNBR or peak LHGR. 00-23 00-23

14.1.5.2.6.1.1 Secondary System Thermal Hydraulic Parameters

Steam flow out the break is the source of the NSSS cooldown. Break flow for the steam generators is plotted in Figure 14.1.5.2-2. Secondary pressure for the steam generators is plotted in Figure 14.1.5.2-3. After break initiation, the pressure in the affected steam generator decreased immediately and then stabilized around 180 seconds. The mass inventory in the affected steam generator decreased throughout the first 450 seconds of the transient and began increasing slowly thereafter. With the exception of a slight decrease at the beginning of the transient, the unaffected steam generator mass inventory remained essentially constant throughout the transient. 00-23

The intact steam generator blows down for a short period until the MSIVs completely close approximately 15 seconds after the break is initiated. The pressure recovers as the intact steam generator equilibrates with the primary system. 00-23

14.1.5.2.6.1.2 Primary System Thermal Hydraulic Parameters

The primary system coolant temperature and pressurizer pressure and level responses resulting from the break flow are illustrated in Figures 14.1.5.2-4 through 14.1.5.2-6. 00-23
The primary system pressure decays rapidly as the coolant contracts due to cooldown and the pressurizer empties. The MSIVs close at 15 seconds, ending the blowdown of the intact steam generators and reducing the rate of energy removal from the primary fluid. 00-23
The pressurizer emptied at approximately 40 seconds and system pressure (which increased slowly for the duration of the transient) was thereafter established by the saturation temperature of the primary coolant in the upper head of the reactor vessel. 00-23

14.1.5.2.6.1.3 Reactivity and Core Power

The reactivity transient calculated by ANF-RELAP is illustrated in Figure 14.1.5.2-8. Initially, the core is assumed to be at zero power. All control rods, except the most reactive one, are assumed to be inserted into the core following the reactor trip signal. 00-23
The reactivity transient then proceeds. The total core reactivity, initially at 0.00$, decreased initially due to reactor scram worth, then steadily increased due to moderator and Doppler feedback associated with the primary system cooldown. The reactor was approaching a quasi steady-state, with the Doppler and the moderator reactivities balancing the scram reactivity, when boron began entering the core, causing the power to decrease. 00-23

00-23 HPSI flow to the RCS began 42 seconds after break initiation and 25 seconds after the HPSI actuation signal. Twenty-five seconds was the assumed time for the HPSI pumps to reach rated speed.

Figure 14.1.5.2-9 shows the transient reactor power. The reactor power initially declined due to insertion of the control rods. The severe cooldown resulted in power increasing
00-23 after 85 seconds. A maximum power level of 272 MW or 10% of rated power occurred at 300 seconds.

00-23 14.1.5.2.6.1.4 PRISM and XCOBRA-IIIC Results

00-23 The PRISM calculation is made initially on the basis of ANF-RELAP input. Each assembly within the three channels is assumed to have a uniform flow corresponding to the sector flows calculated with ANF-RELAP. Due to high power peaking in the region of the stuck control rod, large moderator density reductions are calculated to occur in the top portions
00-23 of several assemblies in this region of the core in the PRISM calculation, and are responsible for the significant reduction in reactivity observed when PRISM is compared to ANF-RELAP. An XCOBRA-IIIC analysis is also conducted to define the flow and enthalpy distribution within the high power assembly.

00-23 A comparison of the overall change in reactivity from the event initiation to the time of maximum LHGR between ANF-RELAP and PRISM shows the ANF-RELAP power calculation is conservative.

14.1.5.2.6.1.5 Departure From Nucleate Boiling Ratio and Linear Heat Generation Rate Results

For the MDNBR portion of the calculation, the radial power distribution was modified to conservatively account for local rod power distribution affects within the hot assembly. This was done by raising the power of the hot assembly to bound the peak rod power.

On the bases of these conservative assumptions, the MDNBR value was calculated to be
00-23 2.44. This compares to a 95/95 DNBR limit of 1.135 for the modified Barnett correlation. Therefore, no fuel rods would be expected to fail during this transient scenario from an MDNBR stand point.

The analysis of the peak LHGR also comes from the PRISM and XCOBRA-IIIC analysis.
00-23 The peak LHGR is calculated from the ANF-RELAP total core power and the PRISM radial and axial peaking. The peak LHGR was calculated for the HZP outside containment break with offsite power available event. No fuel failure is predicted to occur due to the
00-38 violation of the FCMLHR limit. However, one full assembly, or 0.46% of the core, is assumed to fail when determining the radiological consequences of a main steam line break.

00-23 14.1.5.2.6.2 Hot Zero Power Outside Containment with Loss of Offsite Power

The ANF-RELAP NSSS simulation of the most limiting SLB scenario from an MDNBR
00-23 standpoint (i.e., HZP outside containment break with a loss of offsite power) is illustrated in Figures 14.1.5.2-10 through 14.1.5.2-16. A tabulation of the sequence of events is

presented in Table 14.1.5.2-8. Termination of the AFW by manual operator action was assumed to occur 600 seconds after initiation of the break. This is well beyond the time of MDNBR and maximum LHGR. 00-23

14.1.5.2.6.2.1 Secondary System Thermal Hydraulic Parameters

Steam flow out the break is the source of the NSSS cooldown. Steam flow for the affected steam generator is plotted in Figure 14.1.5.2-10. Secondary pressure for the steam generators is plotted in Figure 14.1.5.2-11. The affected steam generator blows down through the break throughout the transient. The pressure and mass flow rate dropped rapidly at first and then proceeded downward at a slower decay rate until natural circulation flow was established by approximately 220 seconds. 00-23

The intact steam generators blow down for a short period until the MSIVs completely close approximately 14 seconds after the break is initiated. The pressure recovers as the intact steam generator equilibrates with the primary system. Subsequently, the intact steam generator pressure remains essentially constant as the primary intact coolant loop approaches natural circulation conditions. 00-23

14.1.5.2.6.2.2 Primary System Thermal Hydraulic Parameters

The primary system core coolant temperature and pressurizer pressure and level responses resulting from the break flow are illustrated in Figures 14.1.5.2-12 through 14.1.5.2-14. The primary system pressure decays rapidly as the coolant contracts due to the cooldown and the pressurizer empties. Continued pressure reduction in the primary system causes the relatively hot stagnant liquid in the head of the RPV vessel to flash. The flashing in the upper head, coupled with near equilibration of other NSSS parameters, retards the pressure decay from that point forward. 00-23

A comparison of intact and affected core sector inlet temperatures throughout the transient indicates significant differences due to the limited cross flow allowed between loops. The core sector flows all show the same trend due to the coastdown of the primary coolant pumps. That is, all flows decrease rapidly until natural circulation conditions are achieved in the two flow loops.

14.1.5.2.6.2.3 Reactivity and Core Power

The reactivity transient calculated by ANF-RELAP is illustrated in Figure 14.1.5.2-15. Initially, the core is assumed to be at zero power. The total core reactivity, initially at 0.00$ decreased initially due to reactor scram worth, then steadily increased due to moderator and Doppler feedback associated with the primary system cooldown. The rise in reactor power was arrested when boron began entering the core at 320 seconds. Power then declined slowly due to an increasing boron concentration in the primary system. 00-23

The HPSI actuation signal was received at 22 seconds. After a 25 second delay, during which the HPSI pumps reached rated speed, HPSI flow to the RCS began, at 47 seconds.

The transient experienced by the core power is illustrated in Figure 14.1.5.2-16. The core power, initially at 1 Watt, increased rapidly at 130 seconds and reached a peak power 00-23

00-23 level of 5.6% of rated power (152 MW) at 320 seconds.

00-23 14.1.5.2.6.2.4 PRISM and XCOBRA-IIIC Results

00-23 The PRISM calculation is initially made on the basis of ANF-RELAP predicted core power, flow, pressure, and inlet temperatures. The PRISM calculations provide the radial and axial power distributions for use in the XCOBRA-IIIC code. Due to the high power peaking in the region of the stuck control rod, and the low core average natural circulation flow rates, large moderator density decreases are calculated in several assemblies in this region
00-23 in the PRISM calculation and are responsible for the significant reduction in reactivity observed when PRISM is compared to ANF-RELAP. An XCOBRA-IIIC analysis is also conducted to define the flow and enthalpy distribution within the high power assembly.

00-23 A comparison of the overall change in reactivity from the event initiation to the time of minimum DNBR between ANF-RELAP and PRISM shows the ANF-RELAP power calculation is conservative.

14.1.5.2.6.2.5 Departure From Nucleate Boiling Ratio and Linear Heat Generation Rate Results

00-23 The MDNBR of the hot fuel assembly is calculated to be 1.74 which is above the modified Barnett 95/95 DNBR correlation limit. Therefore, no fuel rods are expected to fail from an MDNBR standpoint.

00-23 As before, the analysis of the peak LHGR comes from the PRISM and the XCOBRA-IIIC
00-38 analysis. The peak LHGR was 16.6 kW/ft. Comparing this LHGR with the FCMLHR limit, it is apparent that centerline melt is not predicted to occur. Thus, no fuel failures are predicted to occur due to violation of the centerline melt criteria.

14.1.5.2.7 Conclusions

The HFP and HZP scenarios, with offsite power maintained for operation of the primary coolant pumps resulted in a return to higher power levels than the scenarios where offsite power is lost. However, these scenarios provide substantially greater margin to the MDNBR limit because of the higher coolant flow rate. In no scenario evaluated, however, was fuel failure calculated to occur as a result of penetration of the MDNBR safety limit.
00-23 Even though the scenarios with offsite power available have substantially greater margin to the MDNBR limit because of a higher coolant flow rate, the higher power levels in combination with the highly skewed power distribution due to the assumed stuck rod cluster resulted in them having the least margin to the fuel centerline melt limit.

00-23 The HZP outside containment break scenario concurrent with a loss of offsite power was determined to be the most limiting in this analysis from an MDNBR standpoint. The
00-23 MDNBR of the hot fuel assembly is calculated to be above the modified Barnett 95/95 DNBR correlation limit. Therefore, no fuel rods are expected to fail from an MDNBR standpoint.

00-23 The HZP outside containment break scenario with offsite power available was determined to be the most limiting in this analysis from the standpoint of centerline melt. This
00-23 scenario results in the highest return to power and highest calculated LHGR, which is

below the FCMLHR limit. 00-38

14.1.5.3 Radiological Consequences of a Main Steam Line Break

The main steam line break is postulated to occur in a main steam line outside the containment. The radiological consequences of a main steam line break inside containment is bounded by the main steam line break outside containment. The plant is assumed to be operating with Technical Specification coolant concentrations and primary to secondary leakage. A 0.035 gpm primary to secondary leak is assumed to occur in both steam generators.

Two separate main steam line break cases are analyzed. In the first case, associated with this accident is that 1 fuel assembly is assumed to experience melting and releases the melted fuel into the RCS at the onset of the accident. One fuel assembly is equivalent to 0.46% melt. The activity associated with the melt condition is therefore available for release to the atmosphere via primary to secondary leakage. In the second case a pre-accident iodine spike is assumed to occur. In this case the primary coolant iodine concentrations are 60 times the plant technical specification activity level of 1 uCi/gm DE I-131. In addition, the noble gas activity in the primary coolant is assumed to be at technical specification levels. 00-38

The noble gases and iodines in the primary coolant that leak into the faulted steam generator during the transient are released directly to the environment without holdup or decontamination. An iodine partition factor of 0.01 is used for the releases from the unaffected steam generator. Off-site power is assumed to be lost, thus making the condenser unavailable. The steam releases from the main steam line break are from the turbine building blowout panels as the atmospheric dispersion factor is greater for this release point than the enclosure building blowout panels. The steam releases from the intact steam generator are from the MSSVs/ADVs.

The radiological consequences of a main steam line break to the EAB, LPZ and Millstone 2 Control Room assuming one fuel assembly melted are reported in Tables 14.1.5.3-2 and 14.1.5.3-3. The assumptions used to perform this evaluation are summarized in Table 14.1.5.3-1. 00-38

The resulting doses to the EAB and LPZ do not exceed the limits specified in 10CFR100. The resulting doses to the Control Room do not exceed the limits specified in GDC19.

REFERENCES

14.1-1 "Steam Line Break Methodology for PWRS," EMF-84-093(P), Revision 1, Siemens Power Corporation, Richland, WA, June 1998.

14.1-2 "ANF-RELAP Methodology for Pressurized Water Reactors: Analysis of Non-LOCA Chapter 15 Events," ANF-89-151(P)(A), Advanced Nuclear Fuels Corporation, May 1992.

00-23 14.1-3 "Reactor Analysis Systems for PWRs, Volume 1 - Methodology Description, Volume 2 - Benchmarking Results," EMF-96-029(P)(A), Siemens Power Corporation, January 1997.

14.1-4 "XCOBRA-IIIC: A Computer Code to Determine the Distribution of Coolant During Steady-State and Transient Core Operation," XN-NF-75-21(A), Revision 2, Exxon Nuclear Company, January 1986.

TABLE 14.1.5.1-1

AVAILABLE REACTOR PROTECTION FOR STEAM SYSTEM PIPING FAILURES INSIDE AND OUTSIDE OF CONTAINMENT

PRE-SCRAM ANALYSIS

Reactor Operating Conditions	Reactor Protection
1	Low Steam Generator Pressure Trip
	Low Steam Generator Water Level Trip
	Low Reactor Coolant Flow
	Variable Overpower Trip
	Local Power Density Trip
	Thermal Margin/Low Pressure Trip
	High Containment Pressure Trip
	Safety Injection Actuation Signal
2	Low Steam Generator Pressure Trip
	Low Steam Generator Water Level Trip
	Low Reactor Coolant Flow
	Variable Overpower Trip
	High Containment Pressure Trip
	Safety Injection Actuation Signal
3-6	Technical Specification Requirements on Shutdown Margin, Inherent Negative Doppler Feedback

TABLE 14.1.5.1-2

DISPOSITION OF EVENTS FOR STEAM SYSTEM
PIPING FAILURES INSIDE AND OUTSIDE OF CONTAINMENT

PRE-SCRAM ANALYSIS

Reactor Operating Conditions	Disposition
1	Analyze
2	Analyze
3-6	Bounded by the above

TABLE 14.1.5.1-3

ANF-RELAP THERMAL-HYDRAULIC INPUT (PRE-SCRAM STEAM LINE BREAK)

Initial Condition Thermal-Hydraulic Input

	HFP
Reactor Power (MW)	2754
Pressurizer Pressure (psia)	2250
Pressurizer Level (%)	65
Cold Leg Coolant Temperature (°F)	549
Total Primary Flow Rate (lbm/sec)	37,640
Secondary Pressure (psia)	881
Core Bypass Flow Rate (lbm/sec) per Loop	753
Main Feedwater Temperature (°F)	432
Steam Generator Mass Inventory (lbm)	167,237

TABLE 14.1.5.1-4

ACTUATION SIGNALS AND DELAYS (PRE-SCRAM STEAM LINE BREAK)

Reactor Trip	Non-Harsh Containment Condition Setpoint	Harsh Containment Condition Setpoint	Delay
Variable Overpower (ceiling)	111.6% of rated	Not credited	0.9 s
Low Reactor Coolant Flow	Credited	85% flow	0.65 s
High Containment Pressure	Not applicable	5.83 psig	0.9 s
Low Steam Generator Pressure	658	550	0.9 s
TM/LP (floor)	1728 psia	1700 psia	0.9 s
TM/LP (function)	Evaluated from function given in Technical Specification	Not credited	0.9 s

TABLE 14.1.5.1-5

ANF-RELAP NEUTRONICS INPUT AND ASSUMPTIONS (PRE-SCRAM STEAM LINE BREAK)

Point Kinetics Input	Value
Effective Delayed Neutron Fraction	0.0054
Moderator Temperature Coefficient (pcm/°F)	
Offsite Power Available (Technical Specification most negative limit)	-28
Loss of Offsite Power (Technical Specification most positive limit above 70% RTP)	+4
HFP Scram Worth (pcm)	6628
Shutdown Margin Requirement (pcm)	3600
Doppler Coefficient	
Offsite Power Available	1.20 x most-negative value at EOC
Loss of Offsite Power	0.80 x least-negative value at BOC
Fission Product and Actinide Decay Constants	
Default values in ANF-RELAP utilized	

TABLE 14.1.5.1-6

MDNBR AND PEAK REACTOR POWER LEVEL SUMMARY (PRE-SCRAM STEAM LINE BREAK)

Location of Break	Type of Cooldown	Size of Break	MDNBR	Peak Reactor Power (% of rated)
Outside containment, downstream of check valves	Symmetric	2.40 ft^2	1.332	126.90%
		3.00 ft^2	1.310	130.01%
		3.50 ft^2	1.299	130.92%*
Outside containment, upstream of check valve	Asymmetric	1.20 ft^2	1.249	124.69%
		1.40 ft^2	1.240	126.29%
		1.60 ft^2	1.302	124.87%
		1.80 ft^2	1.334	124.92%
Inside containment, upstream of check valve	Asymmetric	0.40 ft^2	1.299	117.85%
		0.60 ft^2	1.258	121.53%
		0.80 ft^2	1.262	122.26%
		1.80 ft^2	1.318	125.51%
Inside containment, upstream of check valve with loss of offsite power	Asymmetric	3.51 ft^2	0.88**	106.86%

00-3

*The peak LHRs for all pre-scram breaks are bounded by the peak LHR for the 3.50 ft^2 break outside containment and downstream of a check valve.

**The MDNBRs for all pre-scram breaks are bounded by the MDNBR for the 3.51 ft^2 break inside containment and upstream of a check valve with the loss of offsite power.

TABLE 14.1.5.1-7

LHGR-LIMITING PRE-SCRAM STEAM LINE BREAK SEQUENCE OF EVENTS: HFP 3.50 ft^2 SYMMETRIC BREAK OUTSIDE CONTAINMENT WITH OFFSITE POWER AVAILABLE

Time (sec)	Event
0	Break downstream of main steam line check valves opens
0	Turbine control valves open fully
7	Low steam generator pressure trip setpoint reached
8	Turbine trips on reactor scram signal
9	Scram CEA insertion begins
9	Reactor power reaches maximum value
10	MDNBR occurs

TABLE 14.1.5.1-8

MDNBR-LIMITING PRE-SCRAM STEAM LINE BREAK SEQUENCE OF EVENTS: HFP 3.51 ft^2 ASYMMETRIC BREAK INSIDE CONTAINMENT WITH LOSS OF OFFSITE POWER

Time (sec)	Event
0	Break occurs
0	RCPs trip
0	Peak LHGR (kW/ft)
2	Scram signal on low flow trip
3	Scram CEA Insertion begins
3	Max Power (Fraction of RTP)
4	MDNBR

TABLE 14.1.5.2-1

AVAILABLE REACTOR PROTECTION FOR STEAM SYSTEM PIPING FAILURES INSIDE AND OUTSIDE OF CONTAINMENT

POST-SCRAM ANALYSIS

Reactor Operating Conditions	Reactor Protection	
1	Low Steam Generator Pressure Trip	
	Low Steam Generator Water Level Trip	
	Local Power Density Trip	00-23
	Thermal Margin/Low Pressure Trip	
	High Containment Pressure Trip	
	Safety Injection Actuation Signal	
2	Low Steam Generator Pressure Trip	
	Low Steam Generator Water Level Trip	
	High Containment Pressure Trip	00-23
	Safety Injection Actuation Signal	
3-6	Technical Specification Requirements on Shutdown Margin, Inherent Negative Doppler Feedback	

TABLE 14.1.5.2-2

DISPOSITION OF EVENTS FOR STEAM SYSTEM
PIPING FAILURES INSIDE AND OUTSIDE OF CONTAINMENT

POST-SCRAM ANALYSIS

Reactor Operating Conditions	Disposition
1	Analyze
2	Analyze
3-6	Bounded by the above

TABLE 14.1.5.2-3

ANF-RELAP THERMAL-HYDRAULIC INPUT (POST-SCRAM STEAM LINE BREAK)

Initial Condition Thermal-Hydraulic Input	HFP	HZP
Core Power (MW)	2700	1E-6
Primary Pressure (psia)	2250	2250
Pressurizer Level (%)	65	40
Cold Leg Temperature (°F)	549	532
Primary Flow Rate per Loop (lbm/sec)	18,820	19,241
Secondary Pressure (psia)	880	892
Steam Generator Mass Inventory (lbm)	167,237	253,989
Total Steam Flow (lbm/sec) per Steam Generator	1634	4

00-2

Break Characteristics	
Minimum Flow Area	
Affected Steam Generator (ft^2)	3.51
Unaffected Steam Generator (ft^2)	3.51
Location of Pipe Break	Downstream of steam generator integral flow restrictor and upstream of MSIV

TABLE 14.1.5.2-3

ANF-RELAP THERMAL-HYDRAULIC INPUT (POST-SCRAM STEAM LINE BREAK)

Injection Systems	HFP	HZP	
Total HPSI Pumps	3	3	
Active HPSI Pumps	2	2	
Single Failure (No credit for mounted spare)	1 HPSI pump	1 HPSI pump	
Active Charging Pumps	0	0	
Refueling Water Storage Tank Boron Concentration (ppm)	1720	1720	
HPSI Delivery Curve	Fig. 14.1.5.2-1	Fig. 14.1.5.2-1	
Feedwater			
Auxiliary			
Flow, maximum (lbm/sec)	184	184	00-2
Temperature (°F)	32	32	
Main			
Initial Flow per Steam Generator (lbm/sec)	1634	4	00-2
Initial Temperature (°F)	432	432	

TABLE 14.1.5.2-4

ACTUATION SIGNALS AND DELAYS (POST-SCRAM STEAM LINE BREAK)

Parameter Setpoints	Inside Containment	Outside Containment
1. Low Steam Generator Pressure Trip	550 psia	658 psia
2. Low Pressurizer Pressure SIAS	1500 psia	1578 psia
3. Low Steam Generator Pressure MSI	370 psia	478 psia

MSIV Closure

Required Actuation Signal
(3) Above

Delay - 6.9 seconds

HPSI Actuation

Required Actuation Signal
(2) Above

Delay - 25.0 seconds

Main Feedwater Valve Closure

Required Actuation Signal
(3) Above

Delay - 14.0 seconds

Reactor Scram

Required Actuation Signal
(1) Above

Delay - 0.9 second instrument delay
3.0 second insertion time

TABLE 14.1.5.2-5

ANF-RELAP NEUTRONICS INPUT AND ASSUMPTIONS (POST-SCRAM STEAM LINE BREAK)

Point Kinetics Input	Value	
Effective Delayed Neutron Fraction	0.00525	00-23
Moderator Temperature Coefficient (pcm/°F)	-28.0	
HFP Scram Worth (pcm)	6619.0	00-23
Shutdown Margin Requirement (pcm)	3600.0	

Stuck Rod Location

Within half-core section cooled by affected loop

Fission Product and Actinide Decay Constants

Default values in ANF-RELAP utilized

TABLE 14.1.5.2-6

POST-SCRAM STEAM LINE BREAK ANALYSIS SUMMARY

Initial Power Level	Offsite Power Available	Break Location	Maximum Post-Scram Return to Power (MW)	MDNBR	Maximum LHGR (kW/ft)	Fuel Failure (% of Core)
HFP	No	outside containment	109.3	2.62	10.3	0.0
HFP	Yes	outside containment	194.8	2.75	21.0	0.0
HZP	No	outside containment	152.1	1.74	16.6	0.0
HZP	Yes	outside containment	271.6	2.44	23.3	0.0

00-3

00-3

00-23

TABLE 14.1.5.2-7

LHGR-LIMITING SEQUENCE OF EVENTS - HZP OFFSITE POWER AVAILABLE

Time (s)	Event
0.	Reactor at HZP
0.+	Double ended guillotine break. Shutdown reactivity inserted. AFW increased to maximum flow, all directed to affected steam generator.
7.6	MSIV closure trip signal
14.5	MSIVs closed
17.1	SI signal
42.1	SI pumps at rated speed (25 s delay)
298.2	SI lines cleared. Boron begins to enter primary system
300.	Peak post-scram power reached (271.6 MW)
600.	Calculation terminated. Power decreasing.

00-23

TABLE 14.1.5.2-8

MDNBR-LIMITING POST-SCRAM STEAM LINE BREAK ANALYSIS SUMMARY

Time (s)	Event
0.	Reactor at HZP
0.+	Double ended guillotine break. Loss of offsite power. Shutdown reactivity inserted. Full AFW flow started, all directed to the affected steam generator.
7.3	MSIV closure trip signal
14.2	MSIVs closed
21.6	SI signal
46.7	SI pumps at rated speed (25 s delay)
300.5	SI lines cleared. Boron begins to enter primary system
320.	Peak post-scram power reached (152.1 MW)
600.	Calculation terminated. Power decreasing.

00-23

TABLE 14.1.5.3-1

ASSUMPTIONS USED IN MAIN STEAM LINE BREAK ANALYSIS

Core Power Level (MW_t)	2754
Primary to Secondary Leak Rate per Steam Generator	0.035 gpm
Primary Coolant Iodine Concentration	1 uCi/gpm DE I-131
Secondary Coolant Iodine Concentration	0.1 uCi/gm DE I-131
Primary Coolant Noble Gas Concentration	$100/E_{bar}$
Pre-accident Spike Iodine Concentration	60 uCi/gm DE I-131
Melted Fuel Percentage (assumed)	0.46%
Peaking Factor	1.45
Reactor Coolant Mass	430,000 lbs
Intact Steam Generator Minimum Mass	100,000 lbs
Safety Injection Signal Response	85 seconds
Site Boundary Breathing Rate (m^3/sec) 0 - 8 hr 8 - 24 hr 24 - 720 hr	 3.47E-04 1.75E-04 2.32E-04
Site Boundary Dispersion Factors (sec/m^3) EAB: 0 - 2 hr LPZ: 0 - 4 hr 4 - 8 hr 8 - 24 hr 24 - 96 hr 96 - 720 hr	 3.66E-04 4.80E-05 2.31E-05 1.60E-05 7.25E-06 2.32E-06
Control Room Breathing Rate	3.47E-04 m^3/sec
Control Room Damper Closure Time	5 seconds
Control Room Intake Prior to Isolation	800 cfm
Control Room Inleakage During Isolation	130 cfm
Control Room Emergency Filtered Recirculation Rate (t = 10 min)	2,250 cfm
Control Room Intake Dispersion Factors (sec/m^3) PORVs/ADVs: 0 - 8 hr 8 - 24 hr 24 - 96 hr 96 - 720 hr	 3.19 E-03 2.05E-03 7.61E-04 2.13E-04
Turbine Building Blowout Panels: 0 - 8 hr 8 - 24 hr 24 - 96 hr 96 - 720 hr	 4.23E-03 2.85E-03 1.12E-03 3.63E-04
Control Room Free Volume	35,650 ft^3
Control Room Filter Efficiency (all iodines)	90%
Thyroid Dose Conversion Factors	ICRP 30

00-38

TABLE 14.1.5.3-2

SUMMARY OF MILLSTONE 2 MSLB ACCIDENT DOSES
(Assuming 0.46% Melted Fuel)

00-38

Location	Thyroid (rem)	Whole Body (rem)	Beta (rem)
EAB	4.8	0.06	N/A
LPZ	2.3	0.02	N/A
Control Room	29	0.03	0.5

Attachment 2
Page 56 of 104

TABLE 14.1.5.3-3

SUMMARY OF MILLSTONE 2 MSLB ACCIDENT DOSES
(Pre-accident Iodine Spike)

Location	Thyroid (rem)	Whole Body (rem)	Beta (rem)
EAB	0.935	0.010	N/A
LPZ	0.176	0.002	N/A
Control Room	5.314	0.003	0.039

98-145

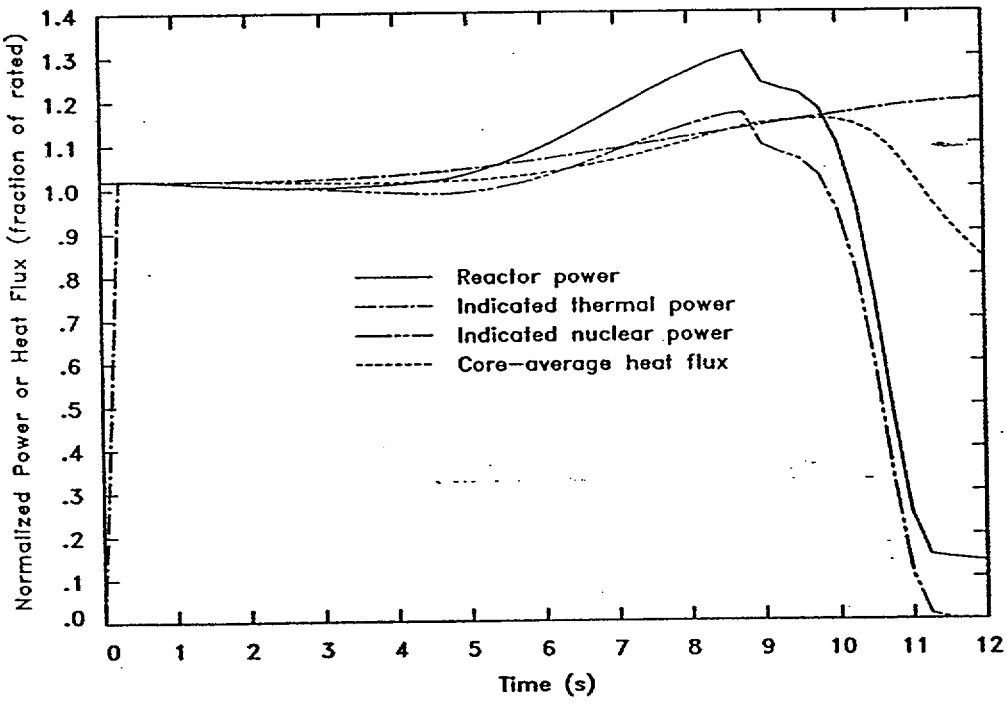

Figure 14.1.5.1-1 Normalized Core Power (Symmetric 3.50 ft^2 Break Outside Containment with Offsite Power Available)

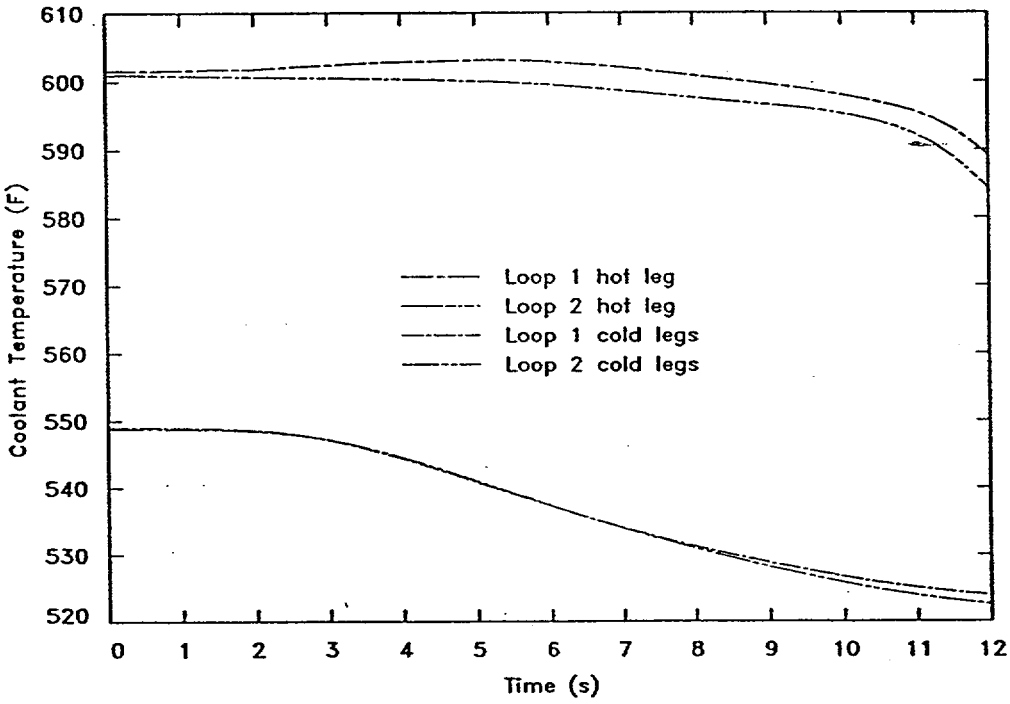

Figure 14.1.5.1-2 Core Inlet Temperatures (Symmetric 3.50 ft^2 Break Outside Containment with Offsite Power Available)

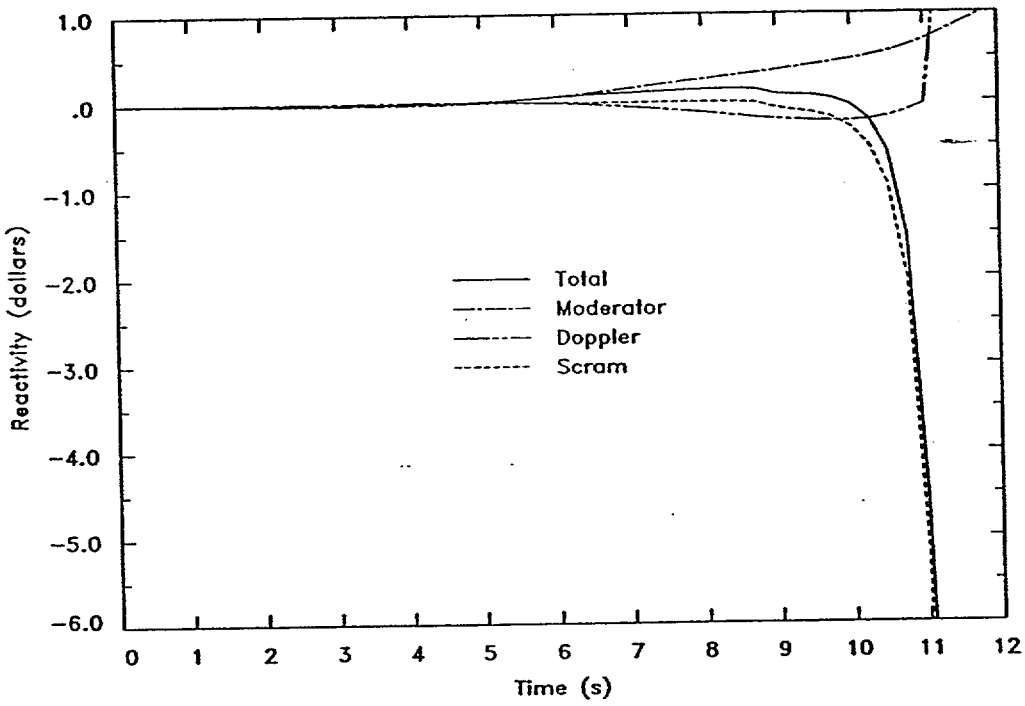

Figure 14.1.5.1-3 Reactivity Feedback (Symmetric 3.50 ft^2 Break Outside Containment with Offsite Power Available)

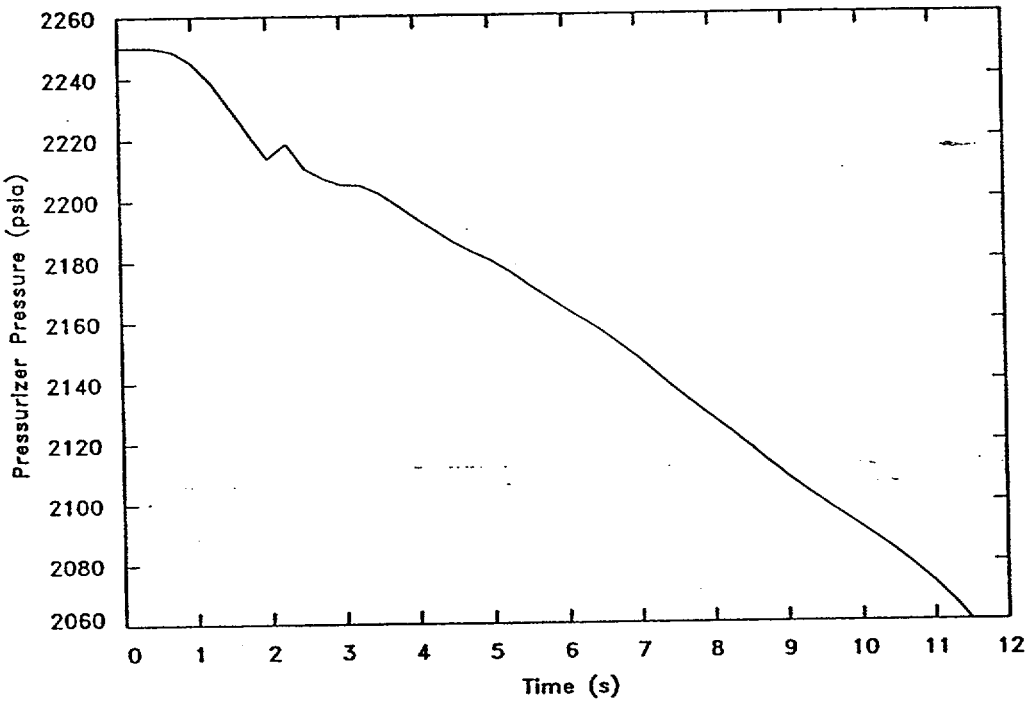

Figure 14.1.5.1-4 Pressurizer Pressure (Symmetric 3.50 ft^2 Break Outside Containment with Offsite Power Available)

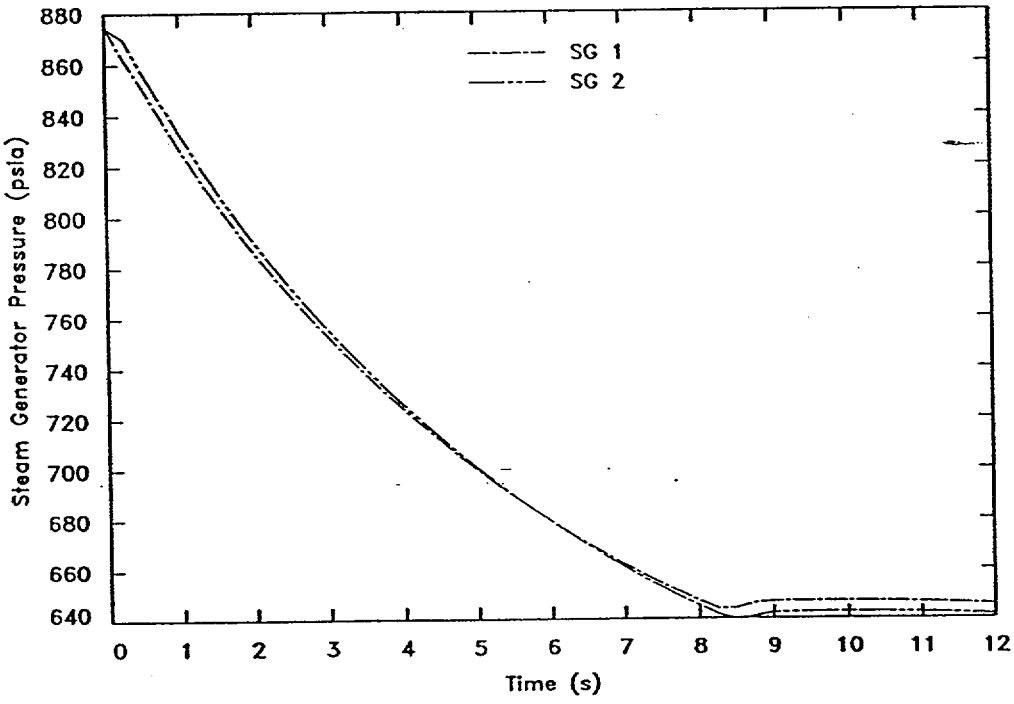

Figure 14.1.5.1-5 Steam Generator Pressures (Symmetric 3.50 ft^2 Break Outside Containment with Offsite Power Available)

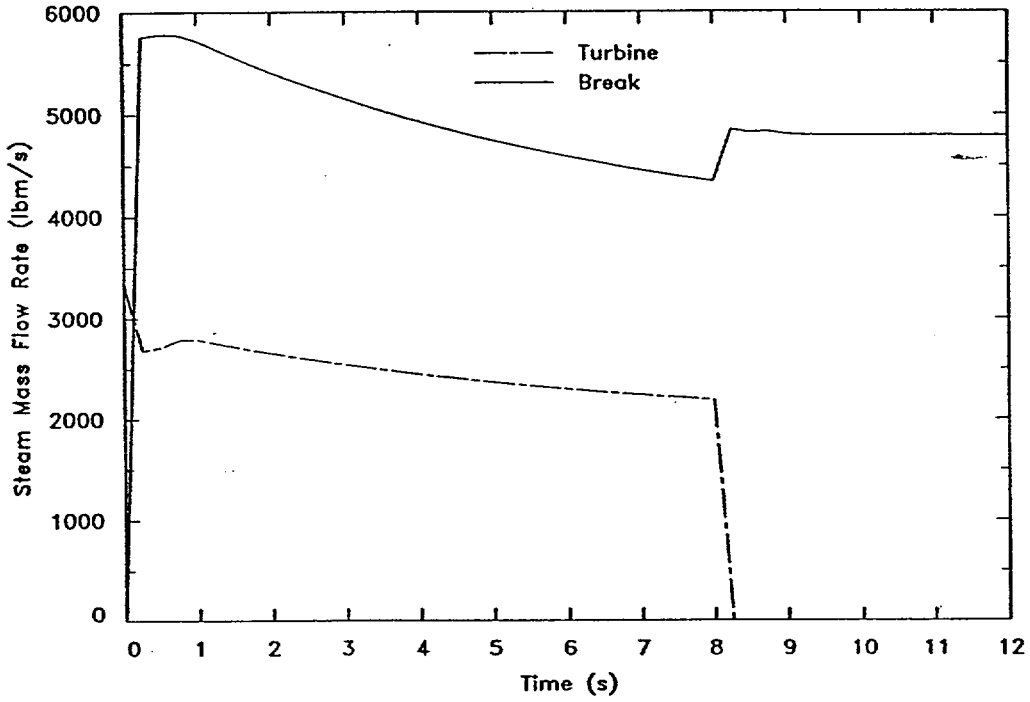

Figure 14.1.5.1-6 Main Steam Line Flow (Symmetric 3.50 ft^2 Break Outside Containment with Offsite Power Available)

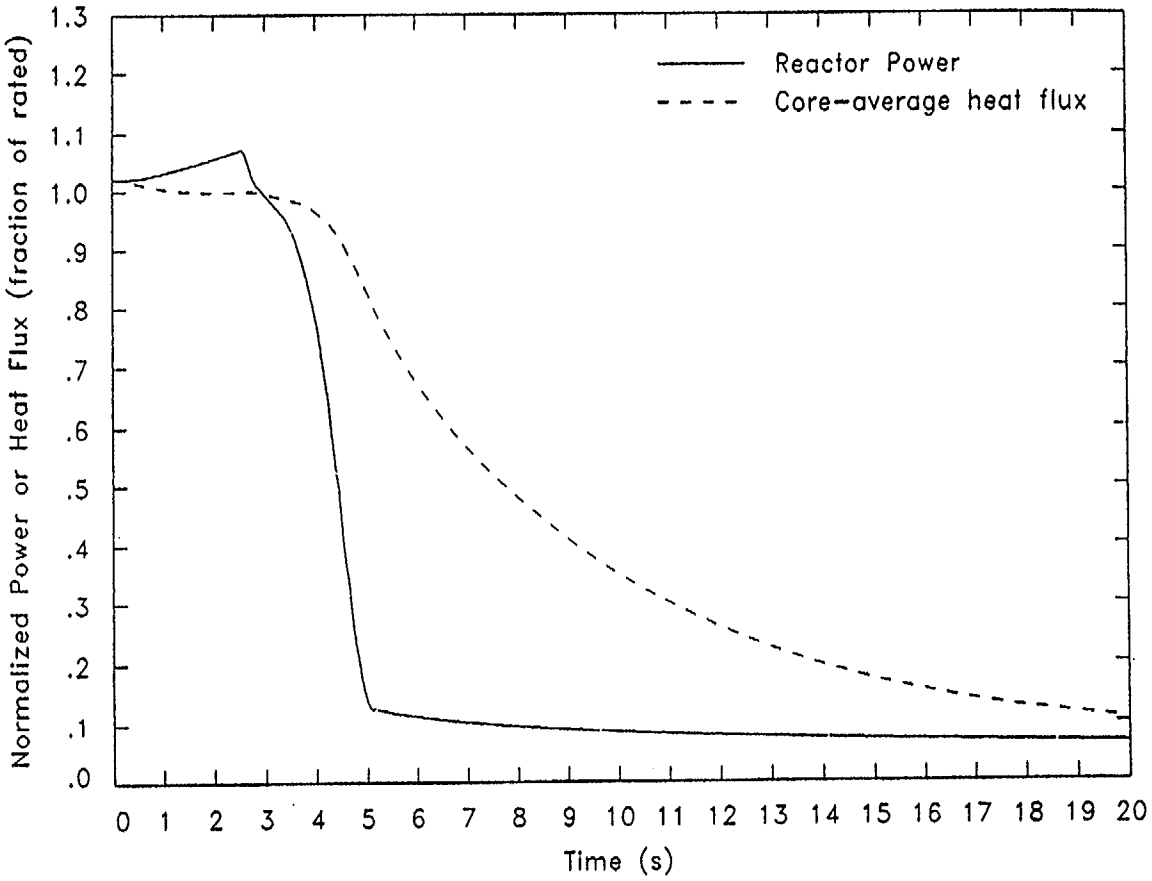

Attachment 2
Page 69 of 104

FIGURE 14.1.5.1-7
NORMALIZED POWER AND HEAT FLUX (ASYMMETRIC 3.51 FT^2 BREAK INSIDE CONTAINMENT WITH LOSS OF OFFSITE POWER)

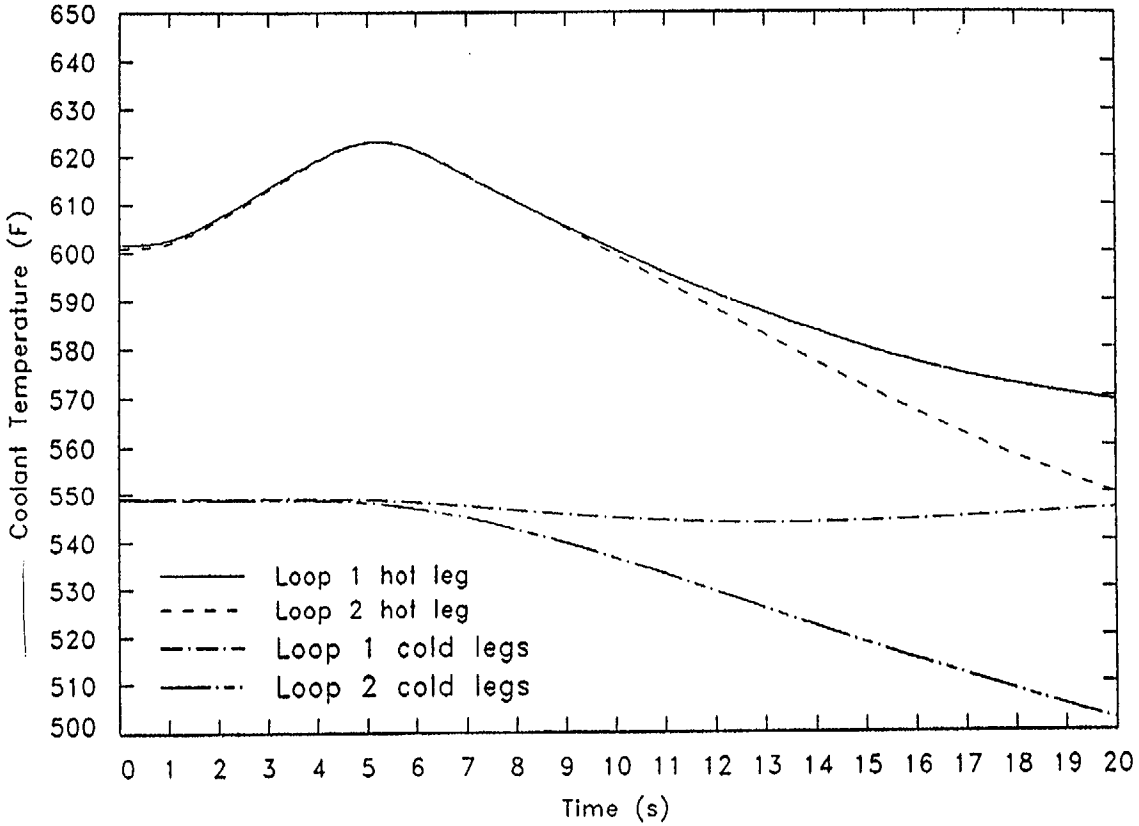

FIGURE 14.1.5.1-8
REACTOR COOLANT TEMPERATURES (ASYMMETRIC 3.51 FT² BREAK INSIDE CONTAINMENT WITH LOSS OF OFFSITE POWER)

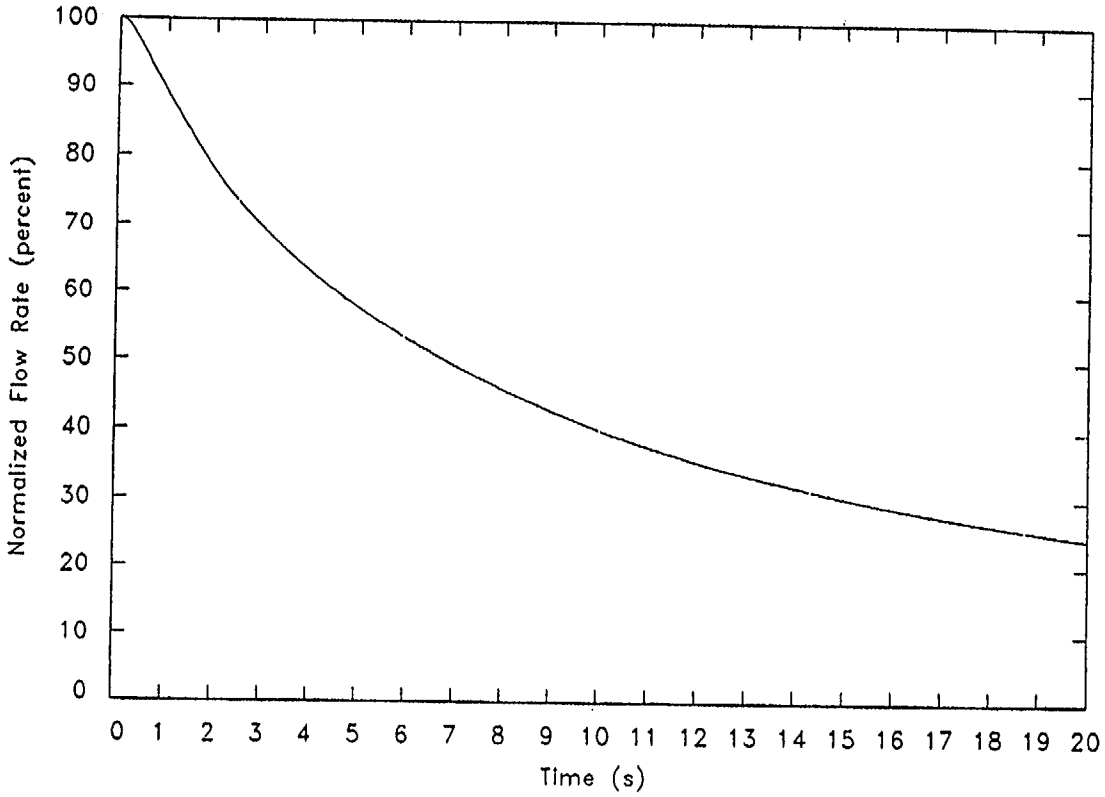

FIGURE 14.1.5.1-9
NORMALIZED REACTOR COOLANT SYSTEM FLOW RATE (ASYMMETRIC 3.51 FT^2 BREAK INSIDE CONTAINMENT WITH LOSS OF OFFSITE POWER)

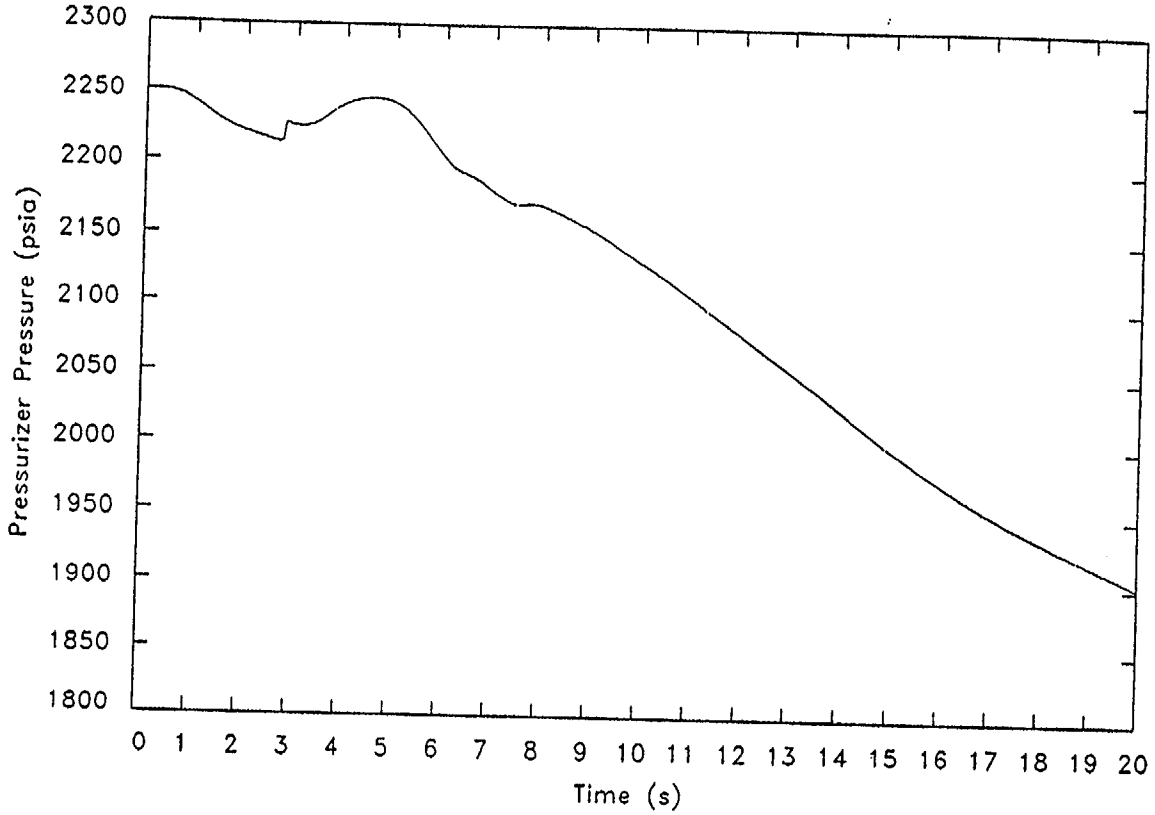

FIGURE 14.1.5.1-10
PRESSURIZER PRESSURE (ASYMMETRIC 3.51 FT^2 BREAK INSIDE CONTAINMENT WITH LOSS OF OFFSITE POWER)

MARCH 1999

ATTACHMENT 2
Page 72 of 104

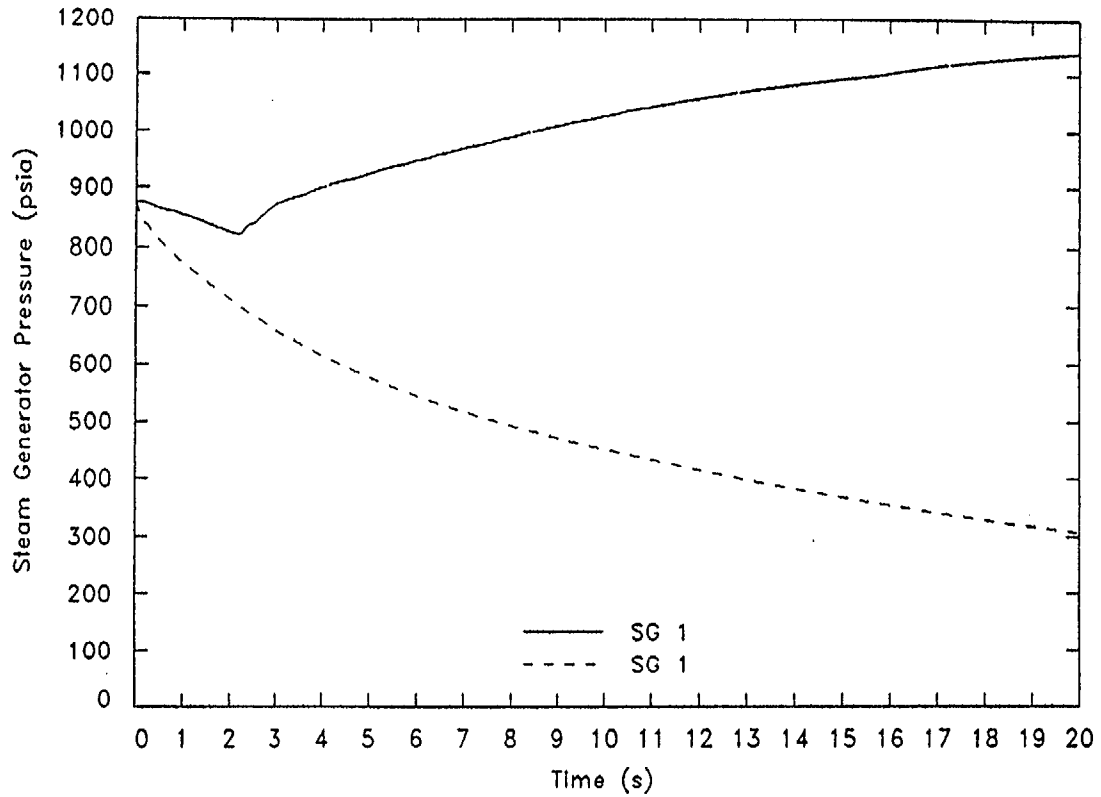

FIGURE 14.1.5.1-11
STEAM GENERATOR PRESSURES (ASYMMETRIC 3.51 FT^2 BREAK INSIDE CONTAINMENT WITH LOSS OF OFFSITE POWER)

MARCH 1999

ATTACHMENT 2
PAGE 73 OF 104

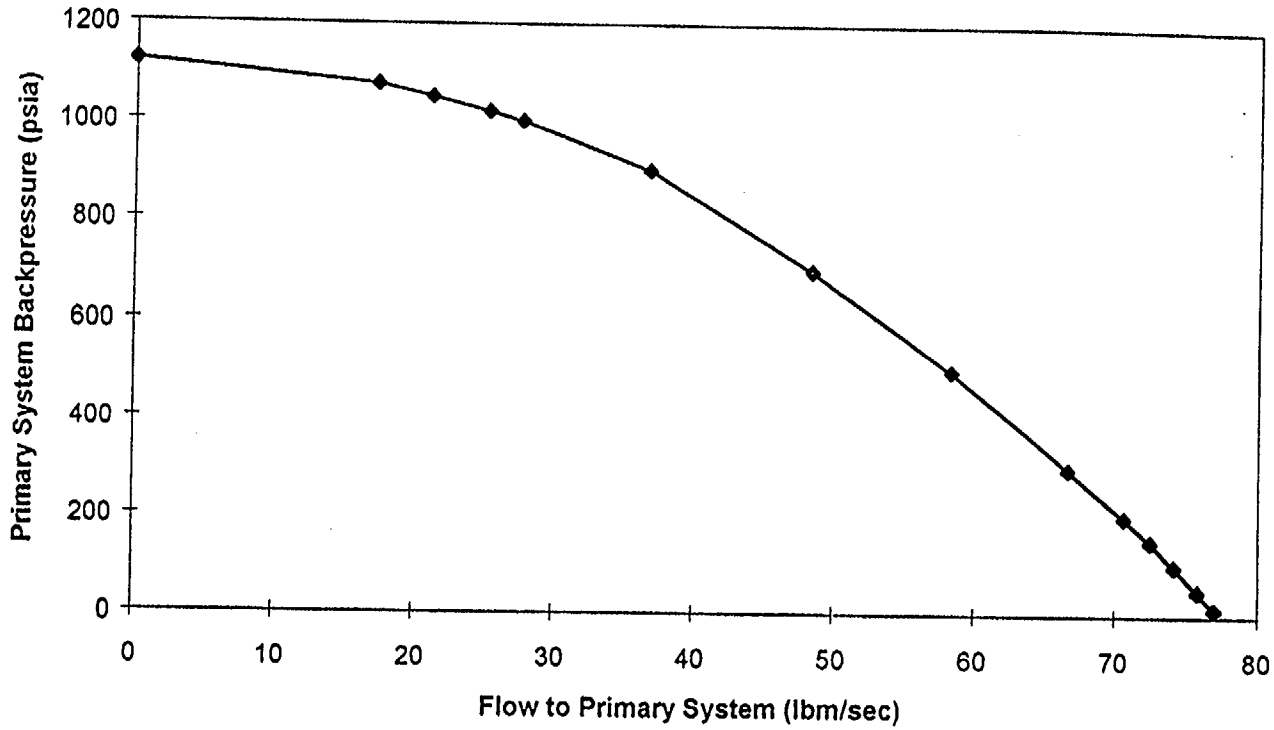

FIGURE 14.1.5.2-1
ONE PUMP HIGH PRESSURE SAFETY INJECTION SYSTEM DELIVERY VS. PRIMARY PRESSURE
(POST-SCRAM STEAM LINE BREAK)

MARCH 1999

ATTACHMENT 2
Page 74 of 104

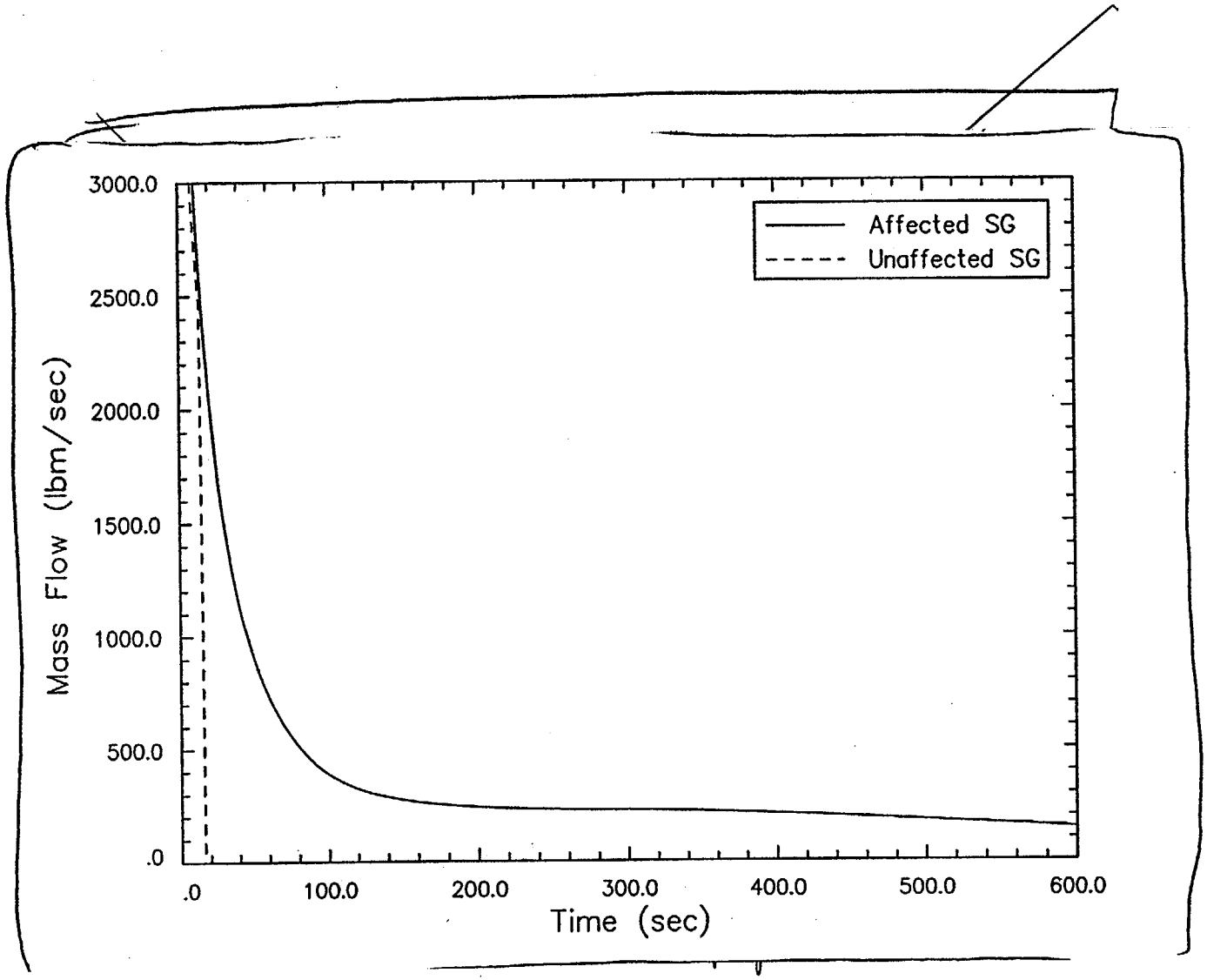

FIGURE 14.1.5.2-2
STEAM GENERATOR BREAK FLOW (HFP POST-SCRAM STEAM LINE OUTSIDE CONTAINMENT BREAK WITH OFFSITE POWER AVAILABLE)

MARCH 1999

FSARCR MP2-00-MP2-23

ATTACHMENT 2
Page 75 of 104

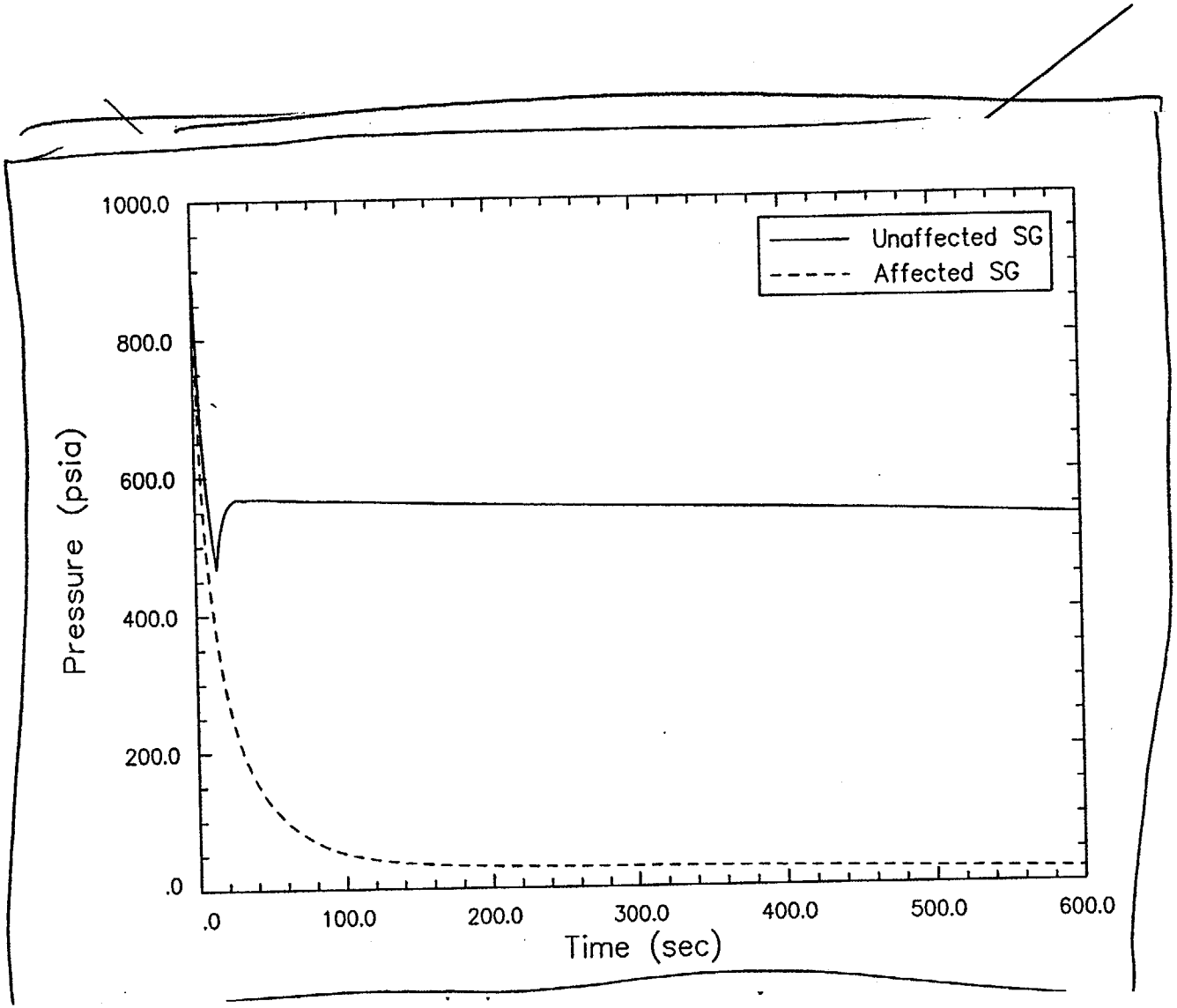

FIGURE 14.1.5.2-3
STEAM GENERATORS' SECONDARY PRESSURES (HRP POST-SCRAM STEAM LINE OUTSIDE CONTAINMENT BREAK WITH OFFSITE POWER AVAILABLE)

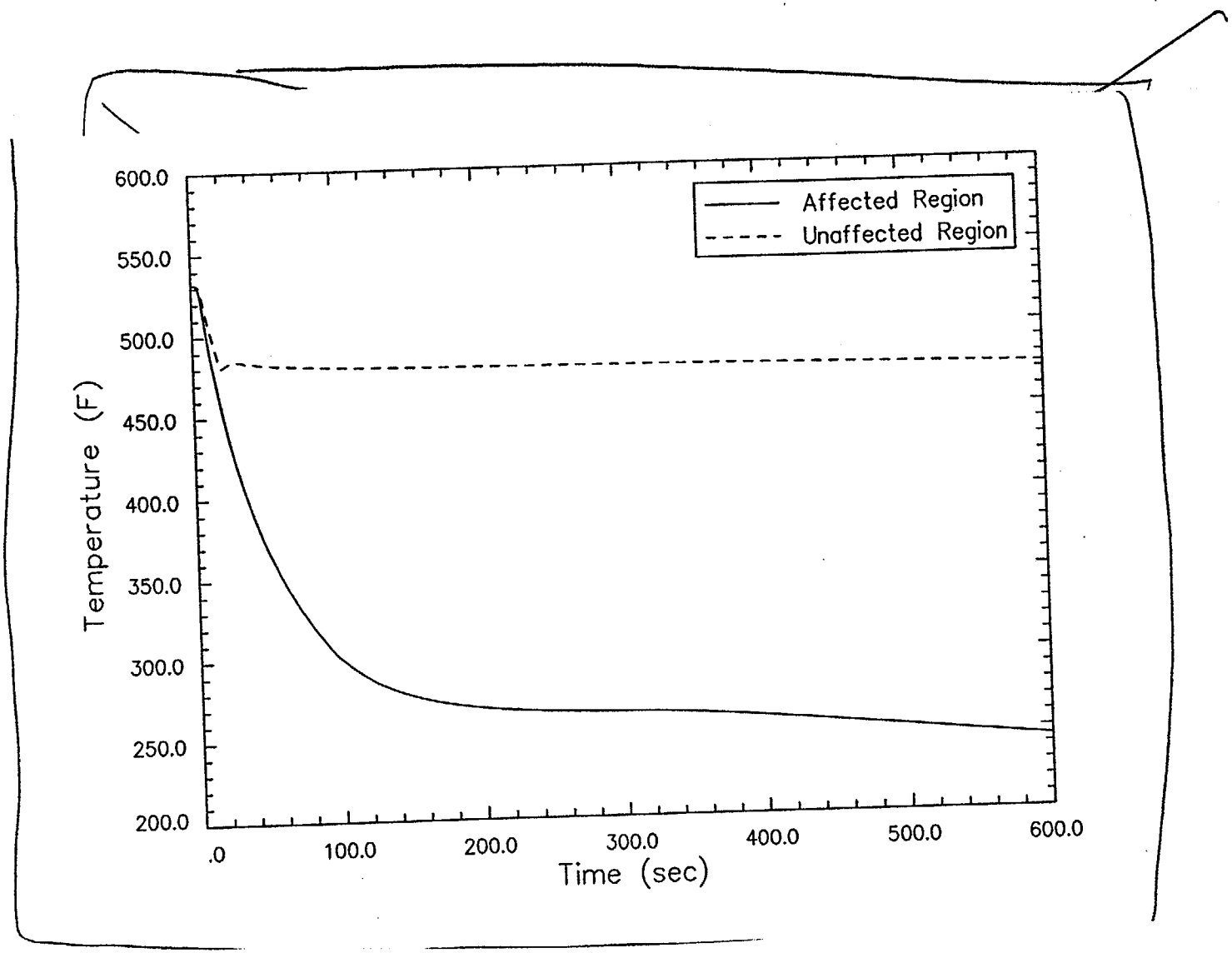

FIGURE 14.1.5.2-4
CORE INLET TEMPERATURES (HFP POST-SCRAM STEAM LINE OUTSIDE CONTAINMENT BREAK WITH OFFSITE POWER AVAILABLE)

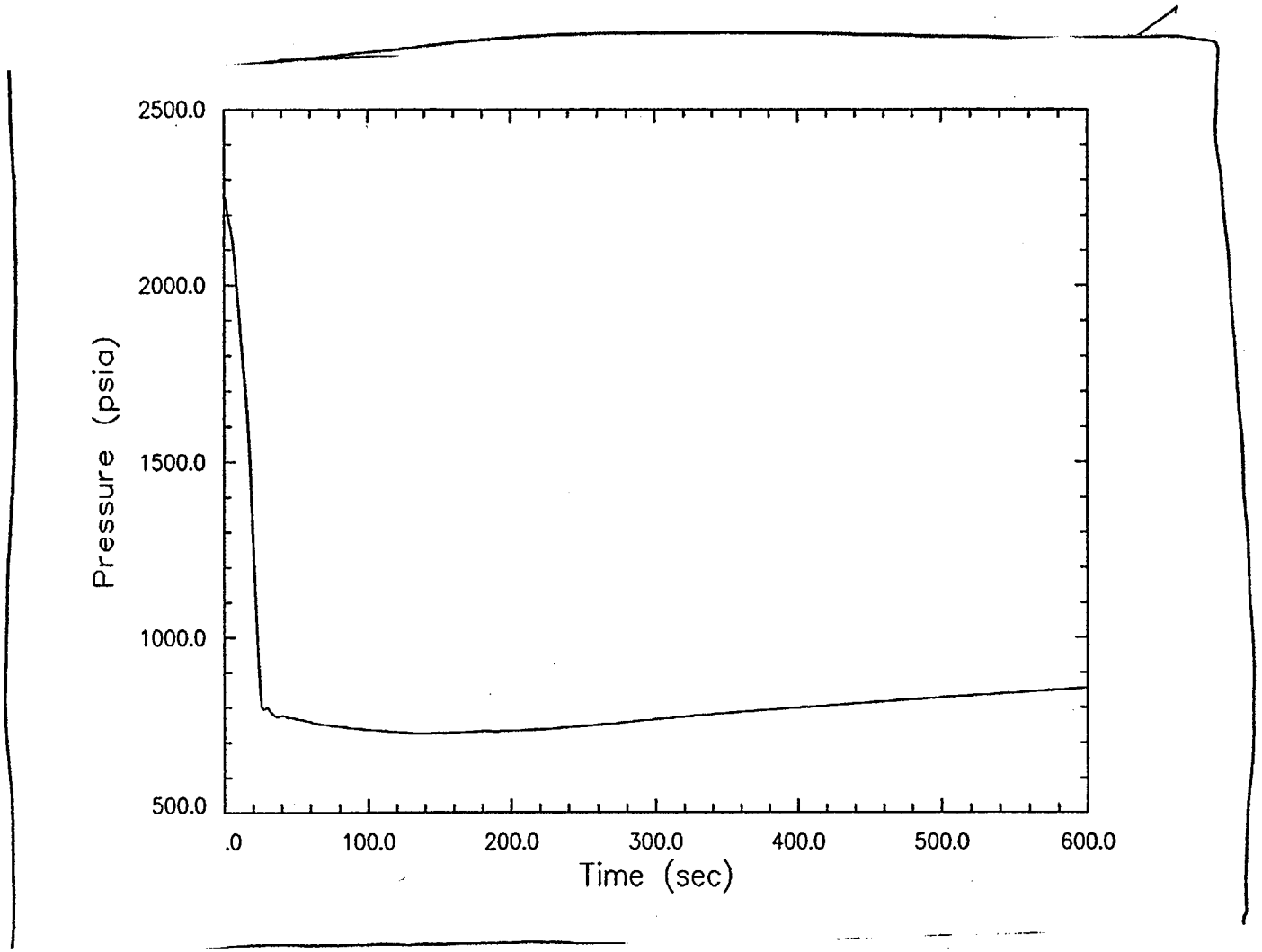

FIGURE 14.1.5.2-5
PRESSURIZER PRESSURE (HZP POST-SCRAM STEAM LINE OUTSIDE CONTAINMENT BREAK WITH OFFSITE POWER AVAILABLE)

FSARCR 00-MP2-23

ATTACHMENT 2
Page 81 of 104

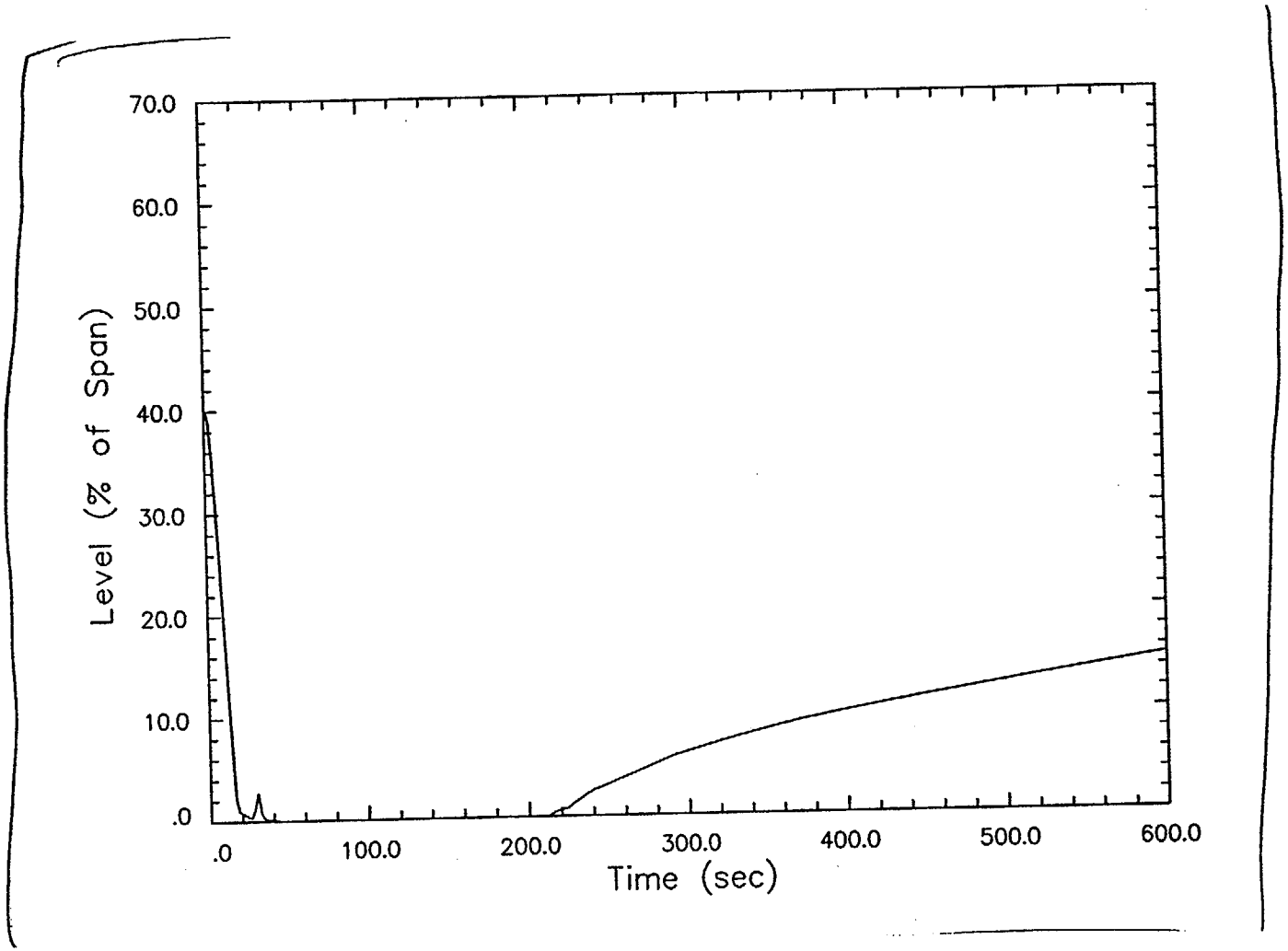

FIGURE 14.1.5.2-6
PRESSURIZER LEVEL (HEP POST-SCRAM STEAM LINE OUTSIDE CONTAINMENT BREAK WITH OFFSITE POWER AVAILABLE)

MARCH 1999

FSAR CR 00-MP2-23

ATTACHMENT 2
Page 83 of 104

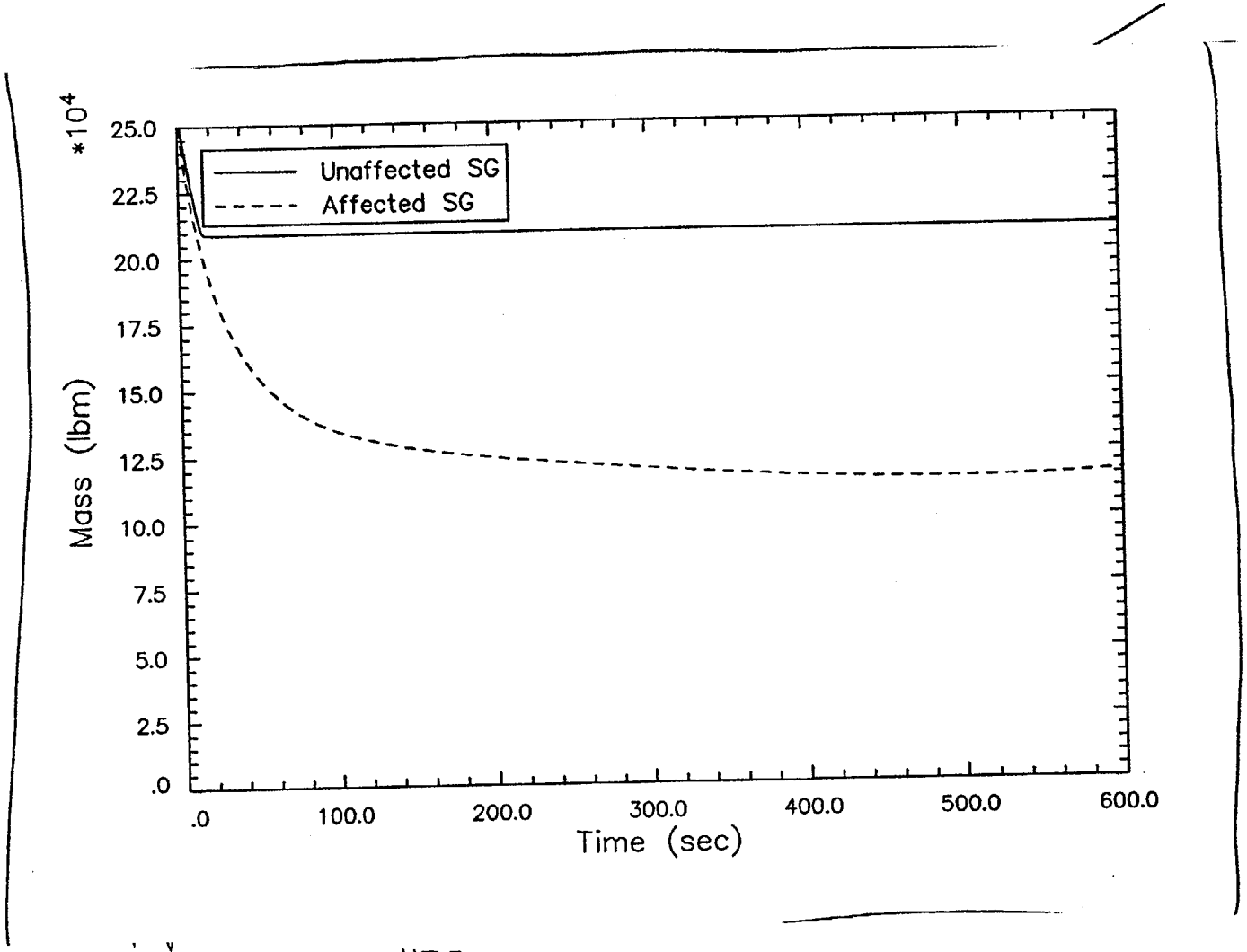

HZP

FIGURE 14.1.5.2-7

STEAM GENERATORS' SECONDARY MASS (~~HFP~~ POST-SCRAM STEAM LINE OUTSIDE CONTAINMENT BREAK WITH OFFSITE POWER AVAILABLE)

FSARCR 00-MP2-23

ATTACHMENT 2
Page 85 of 104

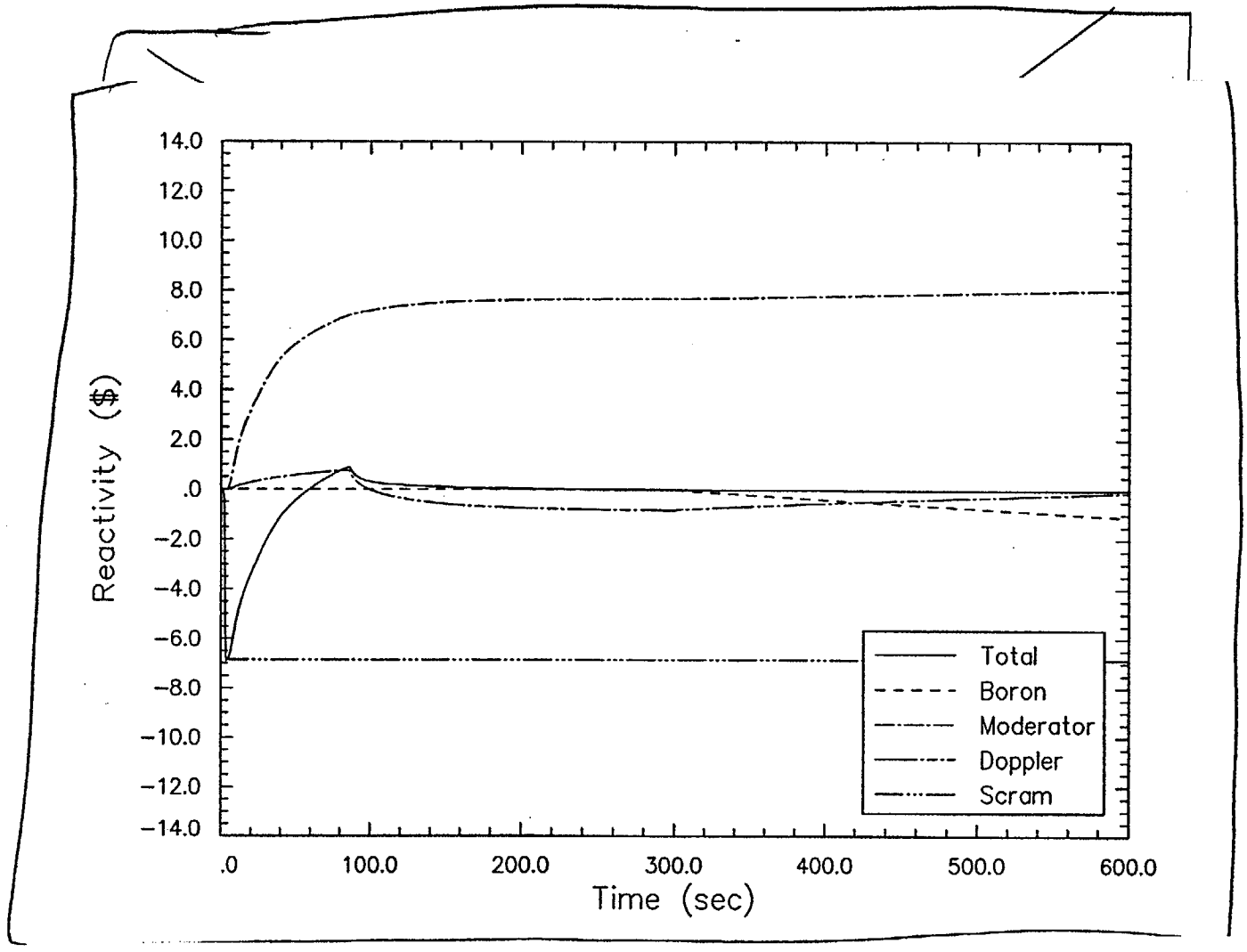

FIGURE 14.1.5.2-8
REACTIVITY COMPONENTS (HZP ~~HFP~~ POST-SCRAM STEAM LINE OUTSIDE CONTAINMENT BREAK WITH OFFSITE POWER AVAILABLE)

FSARCR 00-MP2-23

ATTACHMENT 2
Page 87 of 104

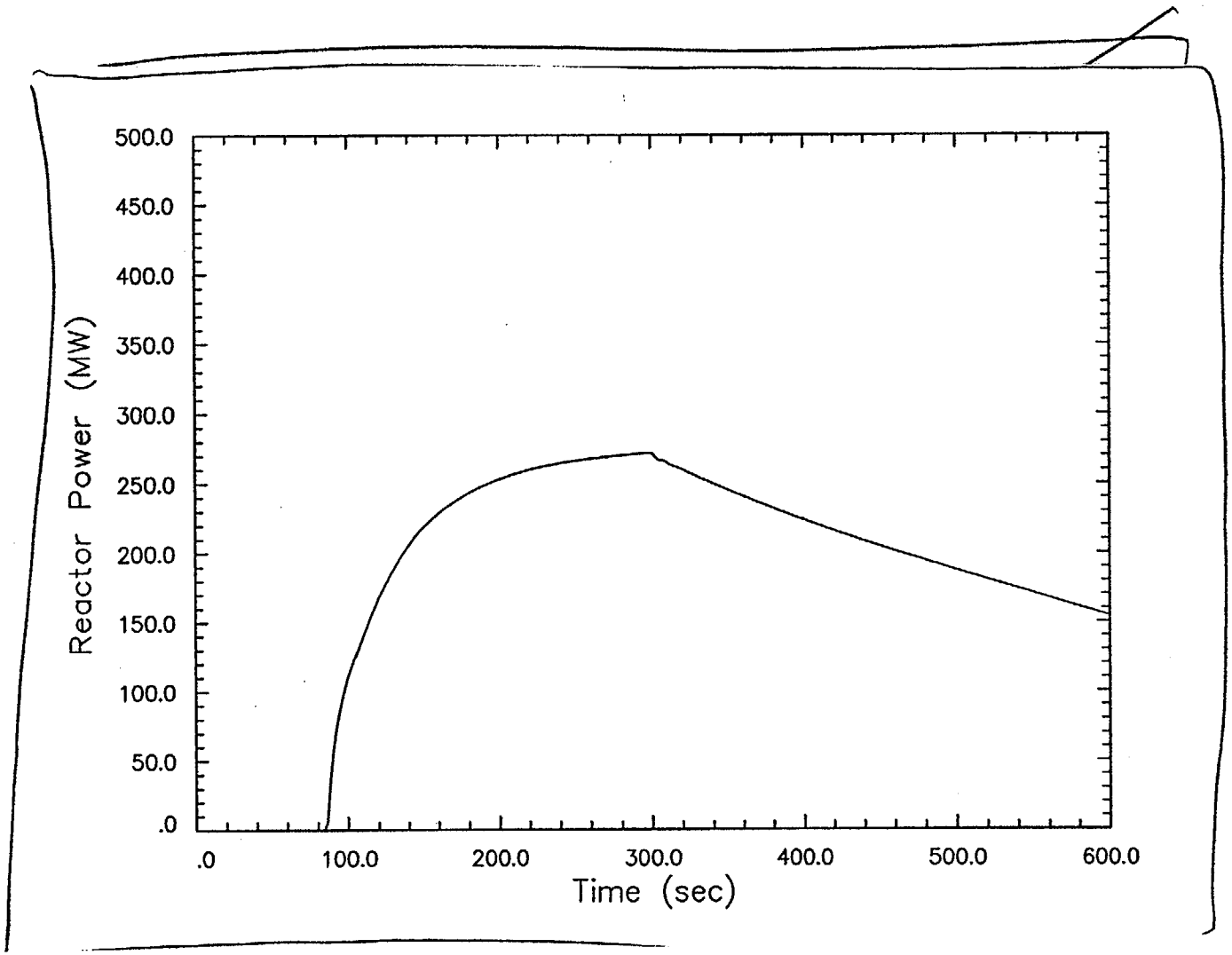

FIGURE 14.1.5.2-9
REACTOR POWER (~~HFP~~ HZP POST-SCRAM STEAM LINE OUTSIDE CONTAINMENT BREAK WITH OFFSITE POWER AVAILABLE)

FSAR CR 00-MP2-23
ATTACHMENT 2
Page 89 of 104

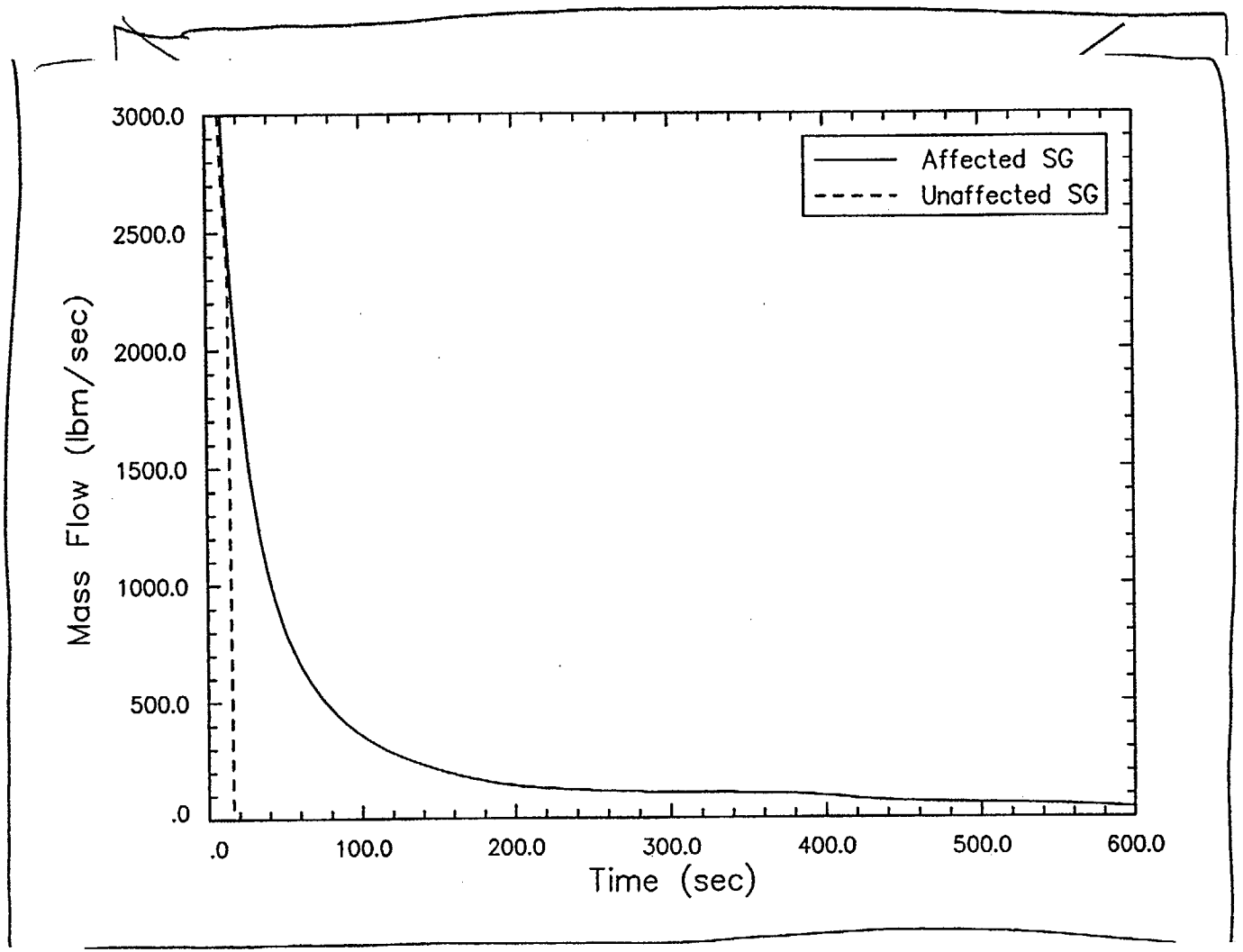

HZP FIGURE 14.1.5.2-10
STEAM GENERATOR BREAK FLOW (~~HFP~~ POST-SCRAM STEAM LINE OUTSIDE CONTAINMENT BREAK WITH LOSS OF OFFSITE POWER)

FSAR CR 00-MP2-23

ATTACHMENT 2
Page 91 of 104

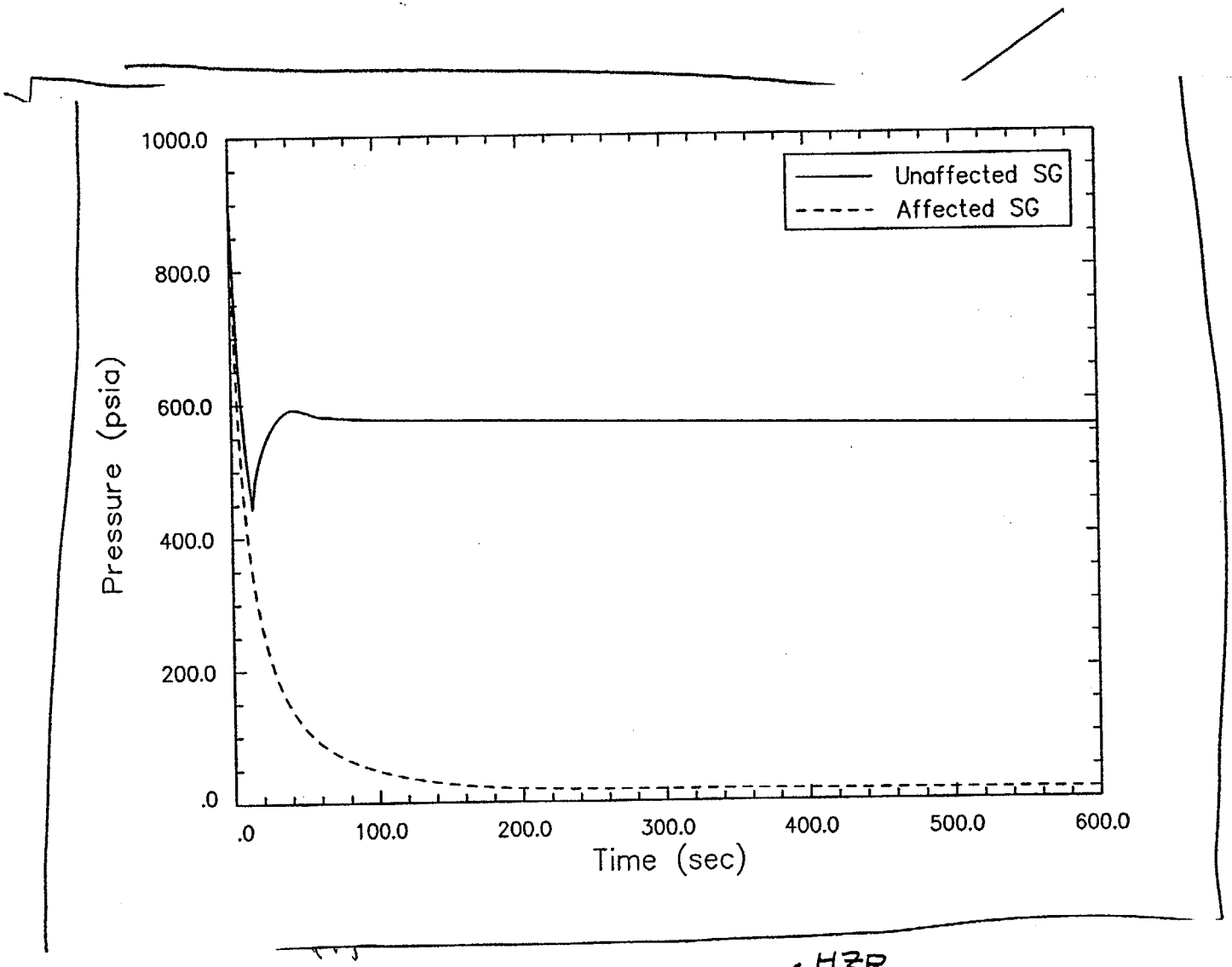

HZP

FIGURE 14.1.5.2-11

STEAM GENERATORS' SECONDARY PRESSURES (~~HFP~~ POST-SCRAM STEAM LINE OUTSIDE CONTAINMENT BREAK WITH LOSS OF OFFSITE POWER)

FSARCR 00-MP2-23

Attachment 2
Page 93 of 104

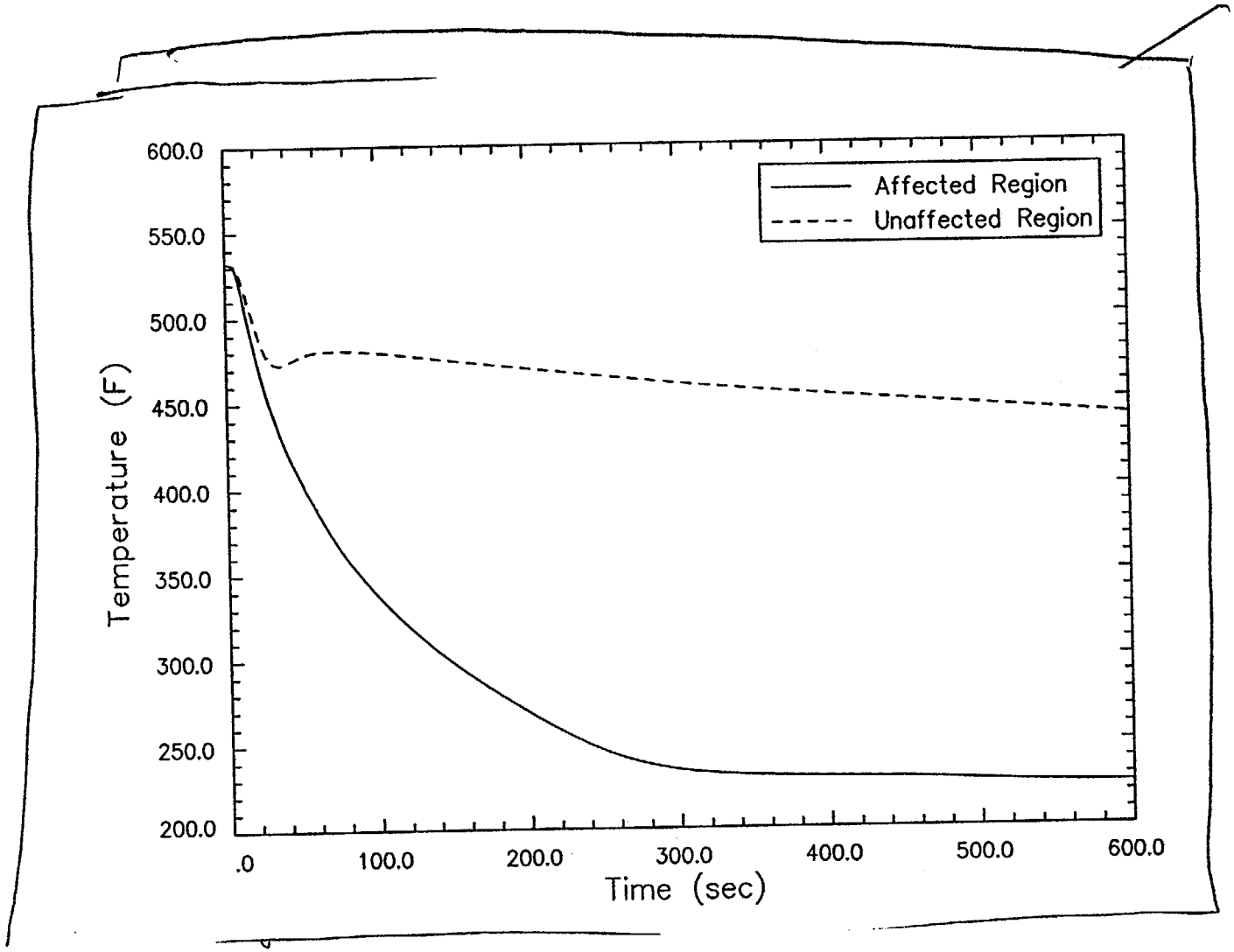

H2P FIGURE 14.1.5.2-12
CORE INLET TEMPERATURES (~~HFP~~ POST-SCRAM STEAM LINE OUTSIDE CONTAINMENT BREAK WITH LOSS OF OFFSITE POWER)

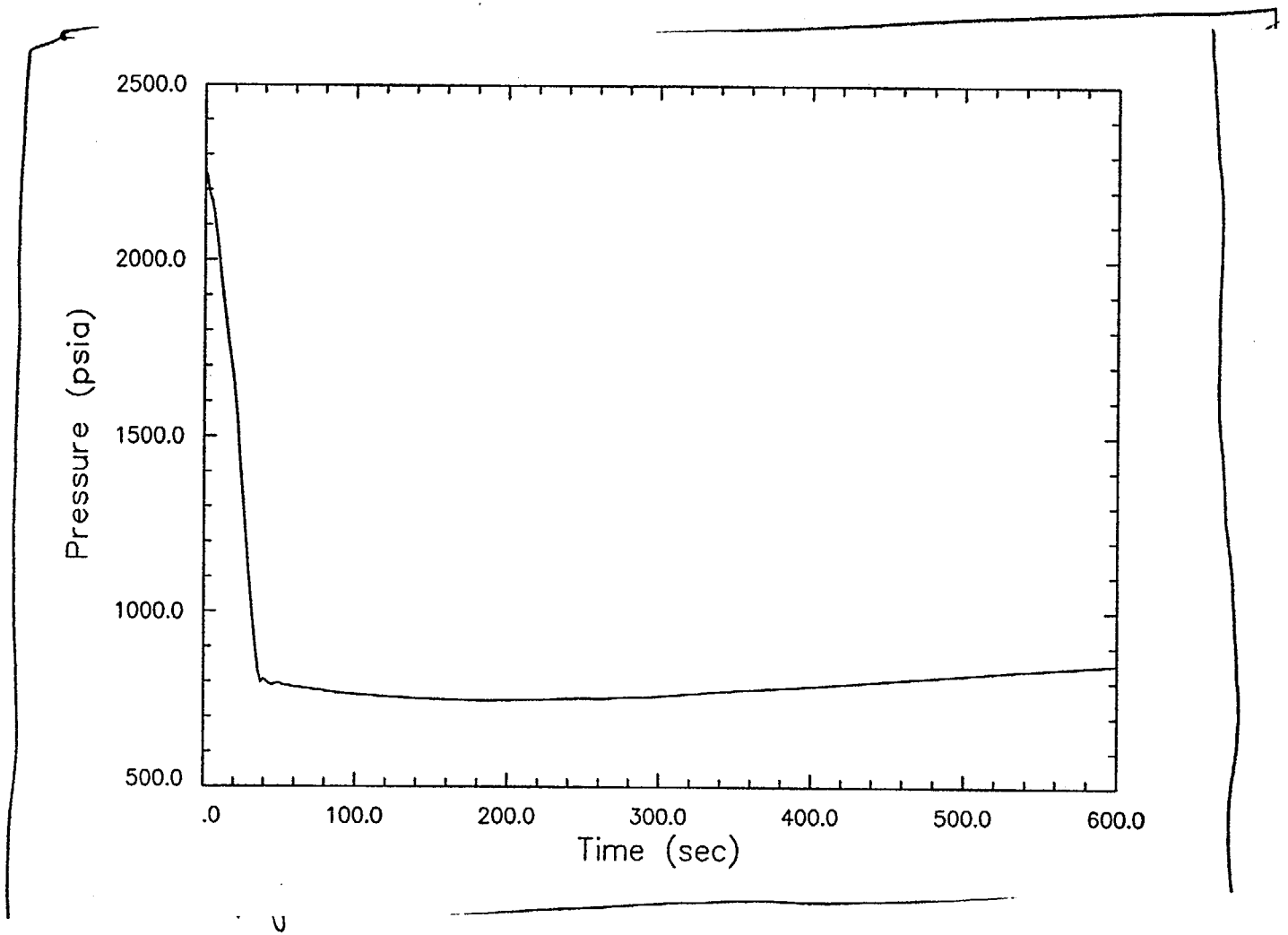

HZP FIGURE 14.1.5.2-13
PRESSURIZER PRESSURE (~~HFP~~ POST-SCRAM STEAM LINE OUTSIDE CONTAINMENT BREAK WITH LOSS OF OFFSITE POWER)

FSAR CR 00-MP2-23
ATTACHMENT 2
Page 97 of 104

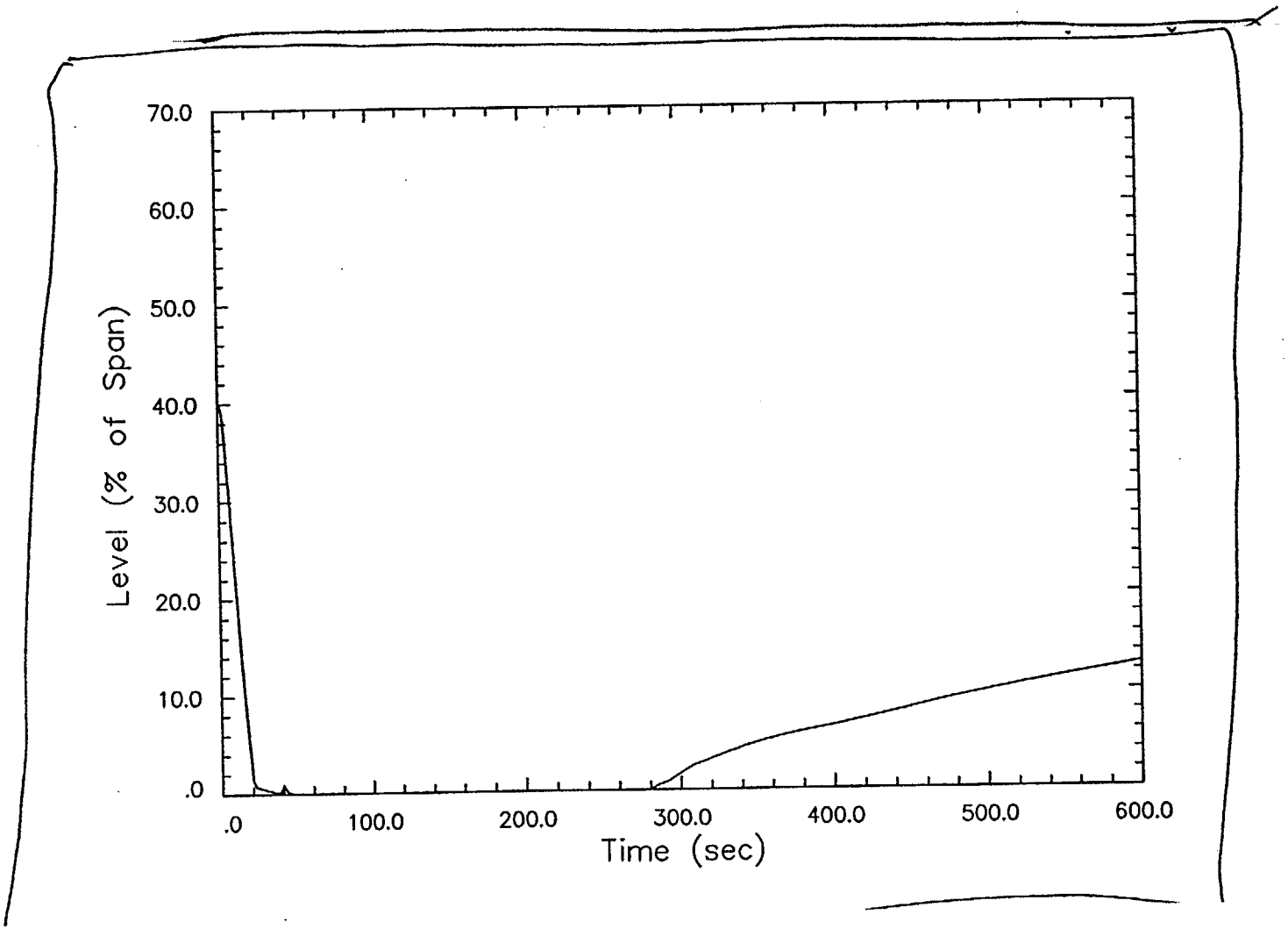

HZP
FIGURE 14.1.5.2-14
PRESSURIZER LEVEL (~~HFP~~ POST-SCRAM STEAM LINE OUTSIDE CONTAINMENT BREAK WITH LOSS OF OFFSITE POWER)

MARCH 1999

FSARCR 00-MP2-23

ATTACHMENT 2
Page 99 of 104

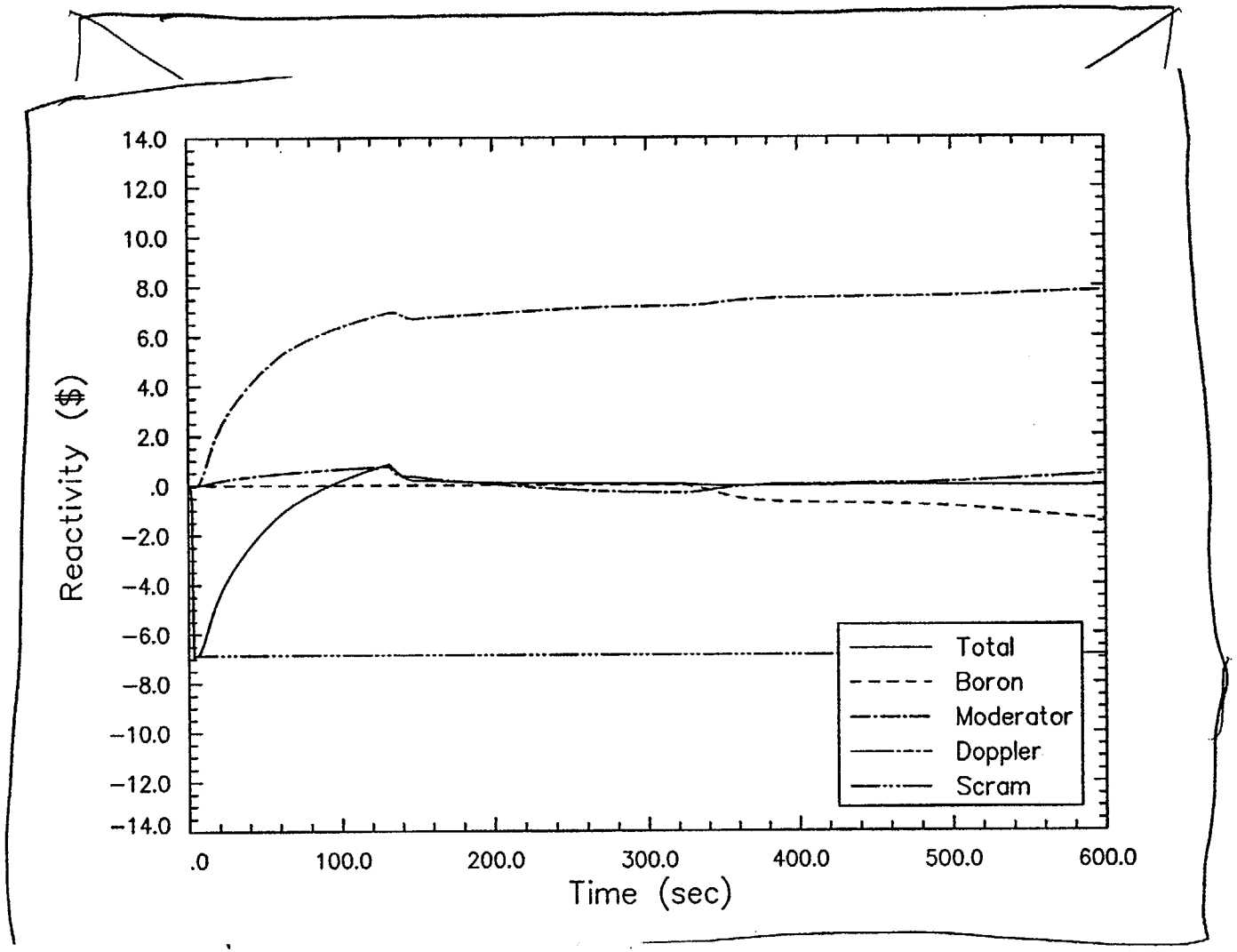

FIGURE 14.1.5.2-15
REACTIVITY COMPONENTS (~~HFP~~ HZP POST-SCRAM STEAM LINE OUTSIDE CONTAINMENT BREAK WITH LOSS OF OFFSITE POWER)

MARCH 1999

FSAR CR 00-MP2-23

ATTACHMENT 2
Page 101 of 104

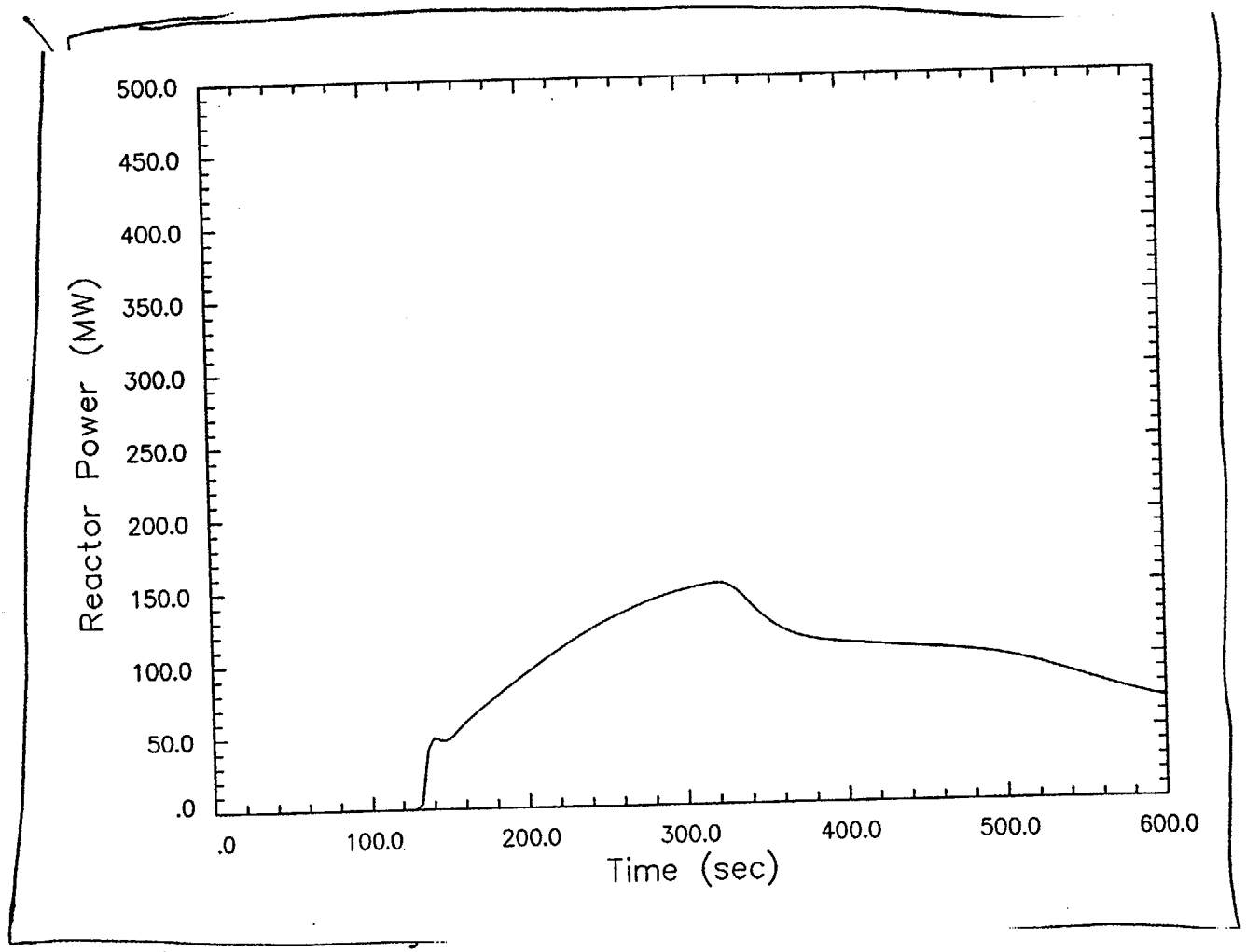

HZP
FIGURE 14.1.5.2-16
REACTOR POWER (~~HFP~~ POST-SCRAM STEAM LINE OUTSIDE CONTAINMENT BREAK WITH LOSS OF OFFSITE POWER)

FSARCR 00-MP2-23

ATTACHMENT 3
Page 103 of 104